PHOTOTHERMAL DEFLECTION TECHNIQUE

Theory and applications: the experience at "La Sapienza" in Rome

Roberto Li Voti

Dipartimento SBAI, Università di ROMA "*La Sapienza*",
Via A. Scarpa 16, 00161 ROMA - ITALY

- **PHOTOTHERMAL TECHNIQUES**
- **PRINCIPLE OF PHOTOTHERMAL DEFLECTION**
- **THE HEAT DIFFUSION**
- **MEASUREMENT OF THERMAL DIFFUSIVITY**
- **OTHER APPLICATIONS**

Thanks to
Photothermal at Roma La Sapienza
Grigore L. LEAHU, Stefano PAOLONI,
Concita SIBILIA, Mario BERTOLOTTI

PHOTOTHERMAL EFFECTS

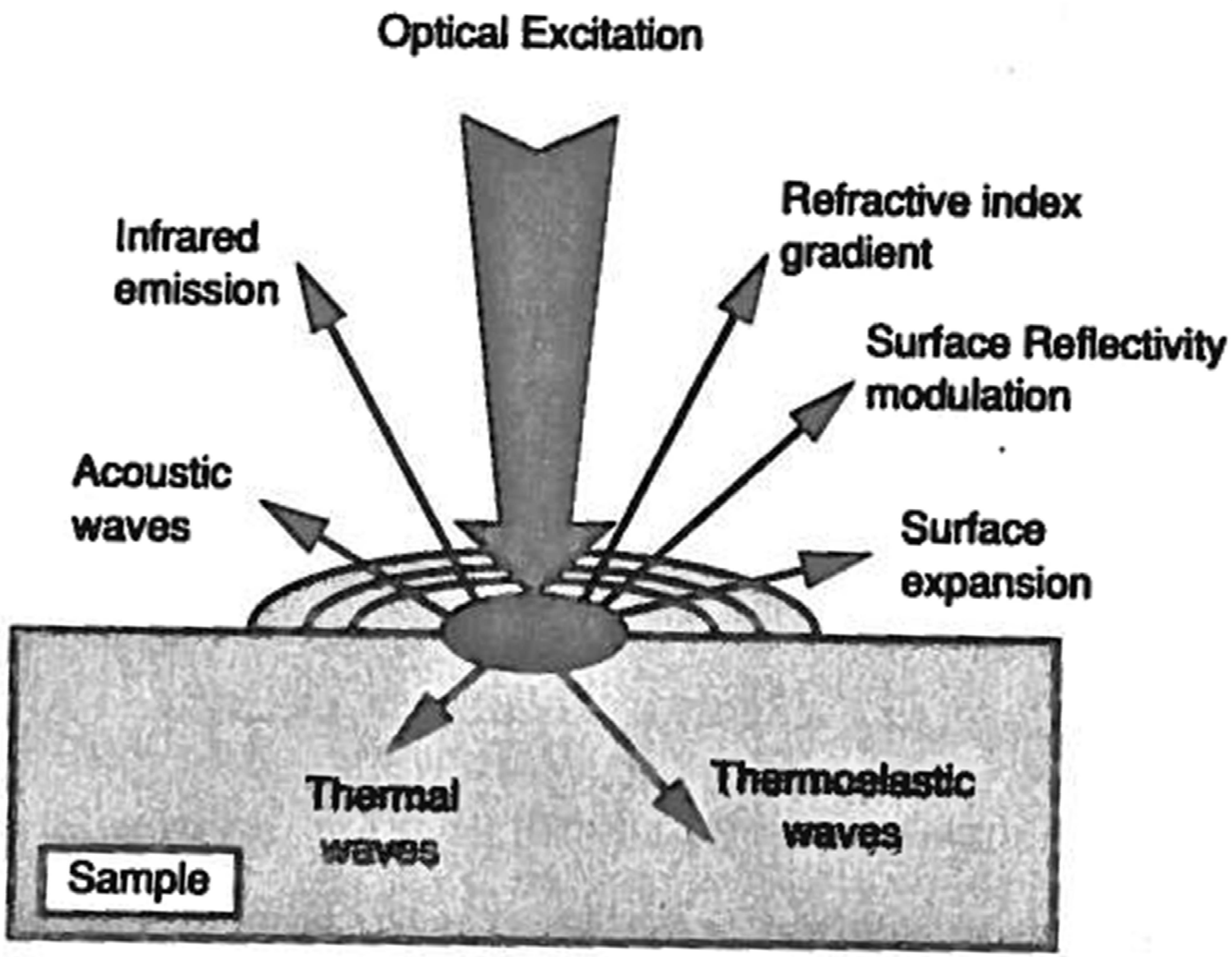

PHOTOTHERMAL TECHNIQUES

Photothermal reflection scheme

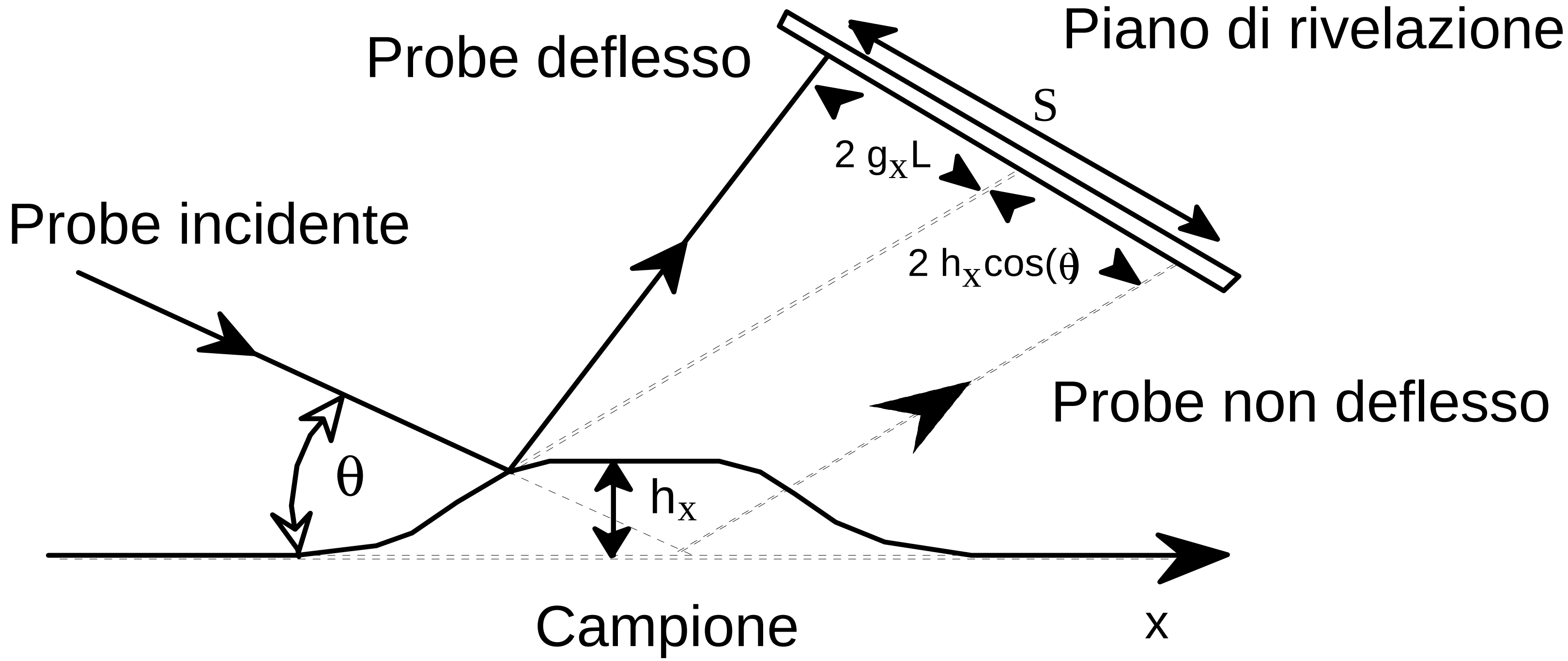

Photothermal reflection signal

$$S = 2h(x)\cos(\theta) + 2g(x)L$$

S displacement
L distance between sample and detector
h distortion height
g distortion gradient

PHOTOTHERMAL TECHNIQUES

Photoreflectance scheme

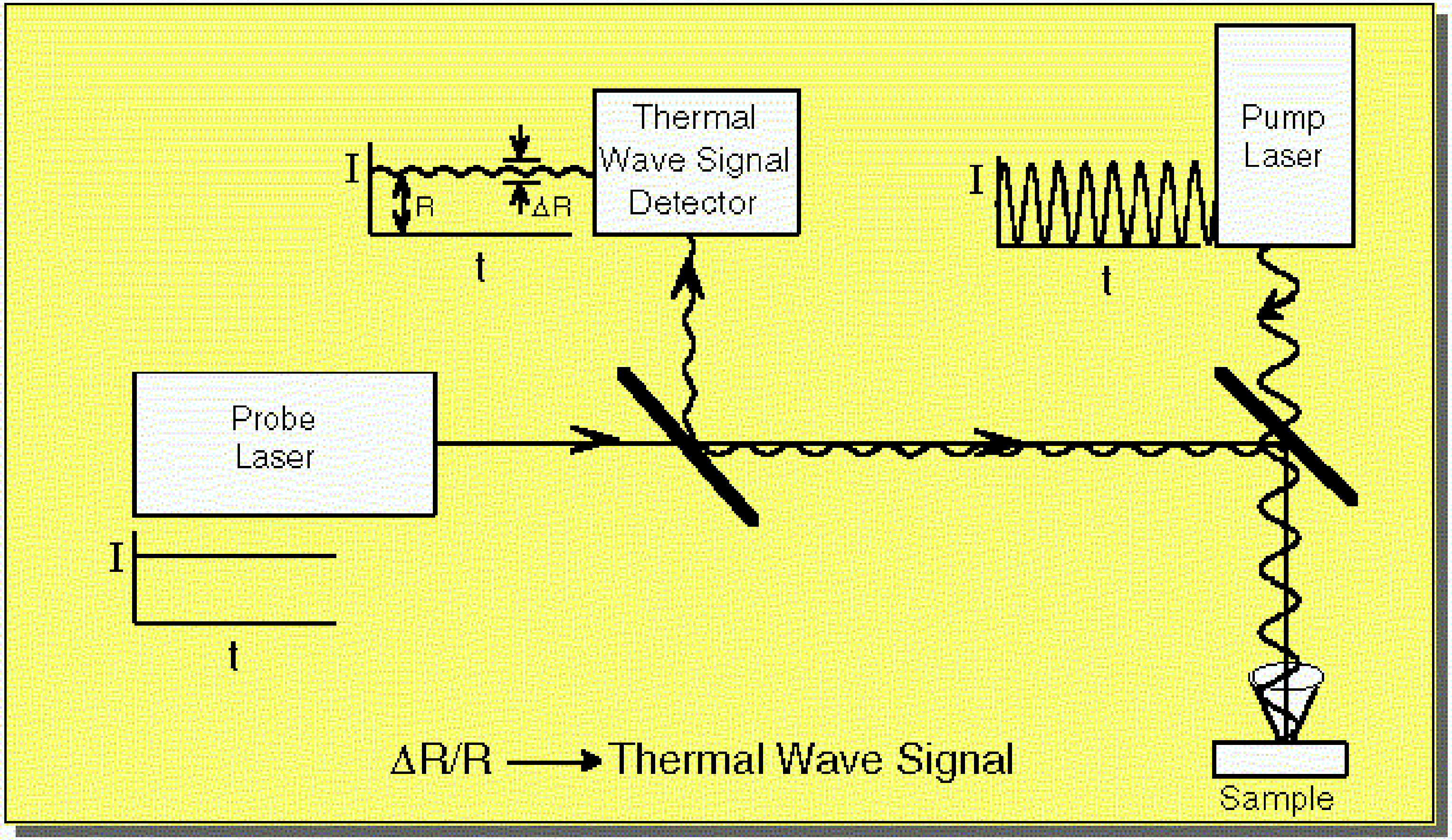

PHOTOTHERMAL TECHNIQUES
Photoreflectance microscope

Schematic set up

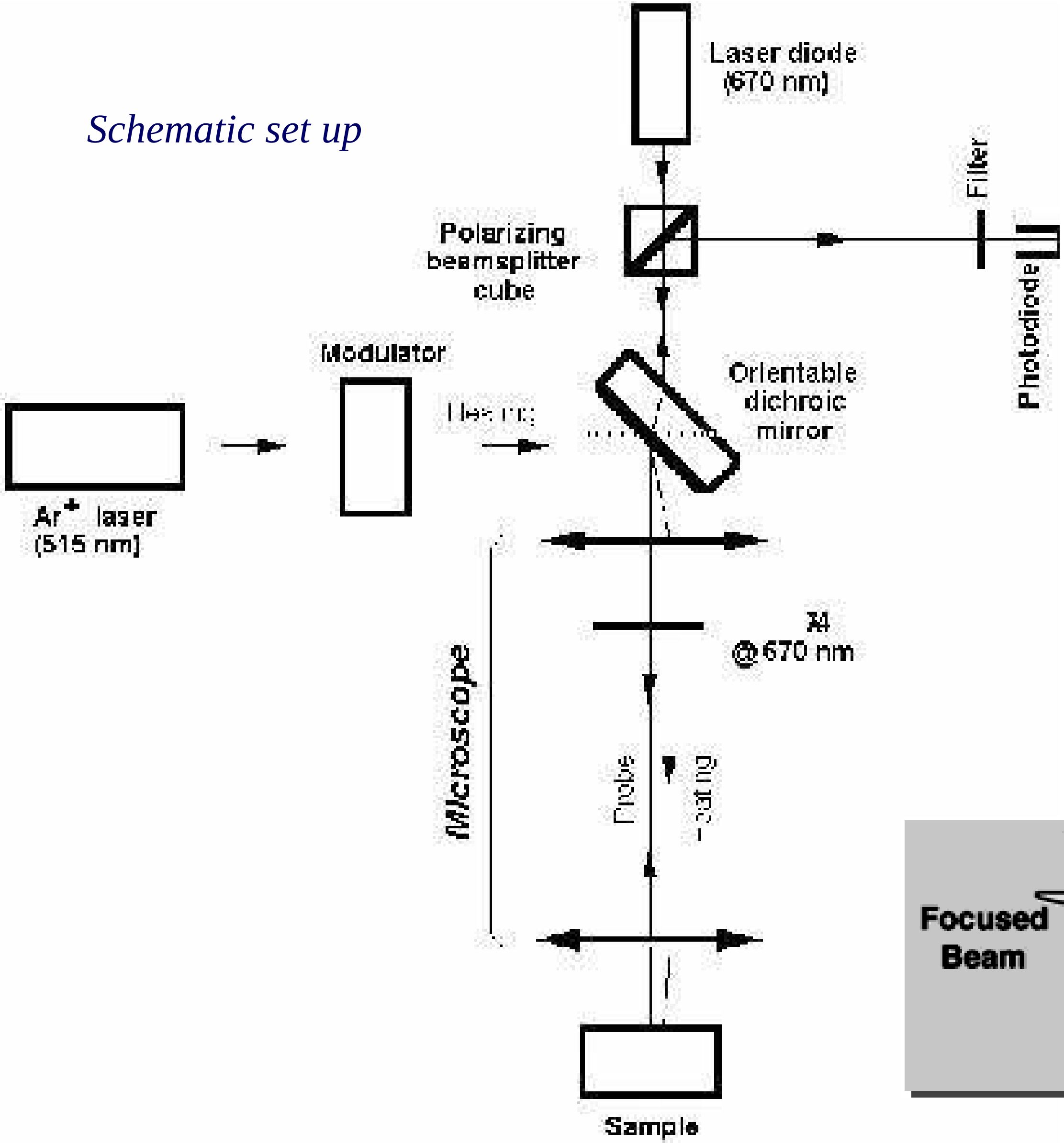

Magnification

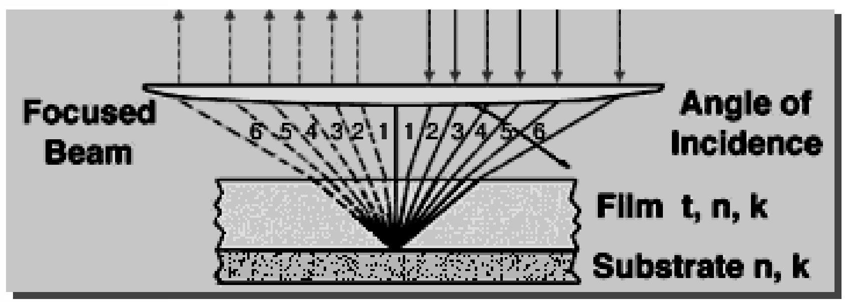

PHOTOTHERMAL TECHNIQUES
Radiometric technique

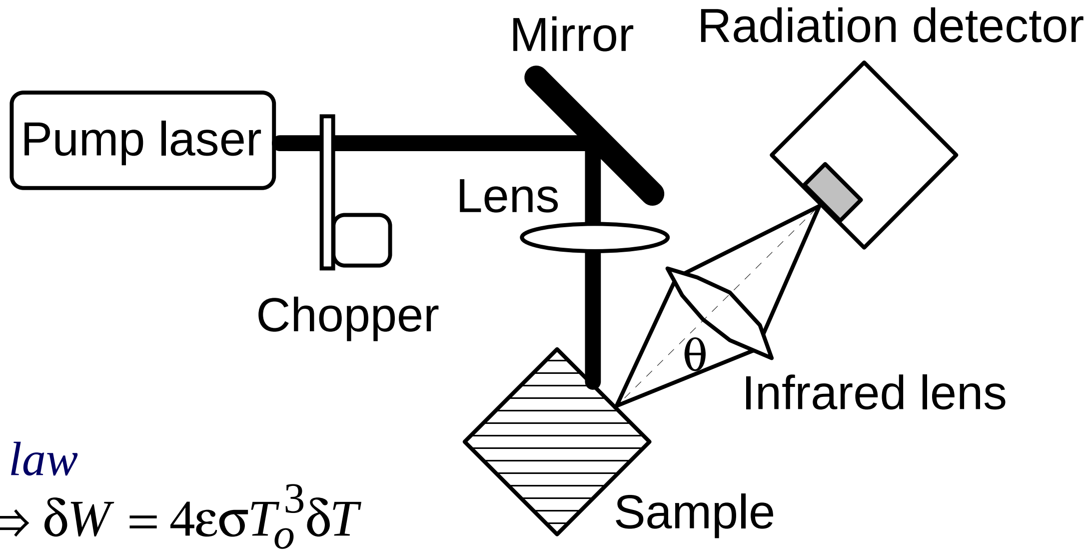

Stephan-Boltzman law

$$W = \varepsilon\,\sigma\,T^4 \Leftrightarrow \delta W = 4\varepsilon\sigma T_o^3 \delta T$$

$$\sigma = 5.67\text{x}10^{-12}\ \text{Wcm}^{-2}\text{K}^{-4}$$

Lambert law
Broadband filter

$$S = 4\varepsilon\sigma T_o^3 A\sin^2(\theta)\delta T$$

S, PTR signal

Lambert law
Selective filter at λ_d

$$S = \varepsilon A\sin^2(\theta) Tr(\lambda_d) R(\lambda_d) \frac{\partial W(\lambda_d)}{\partial T} \Delta\lambda \delta T$$

$$W(\lambda_d) = \frac{2\pi hc^2}{\lambda_d^5} \frac{1}{e^{hc/\lambda_d k_B T} - 1}$$

Tr transmission of the optics
R detector sensitivity

PHOTOTHERMAL TECHNIQUES
Photoacoustic technique

…you can hear the light (Bell,1880)

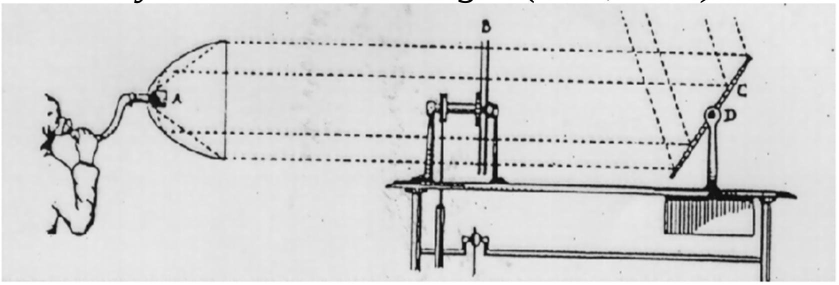

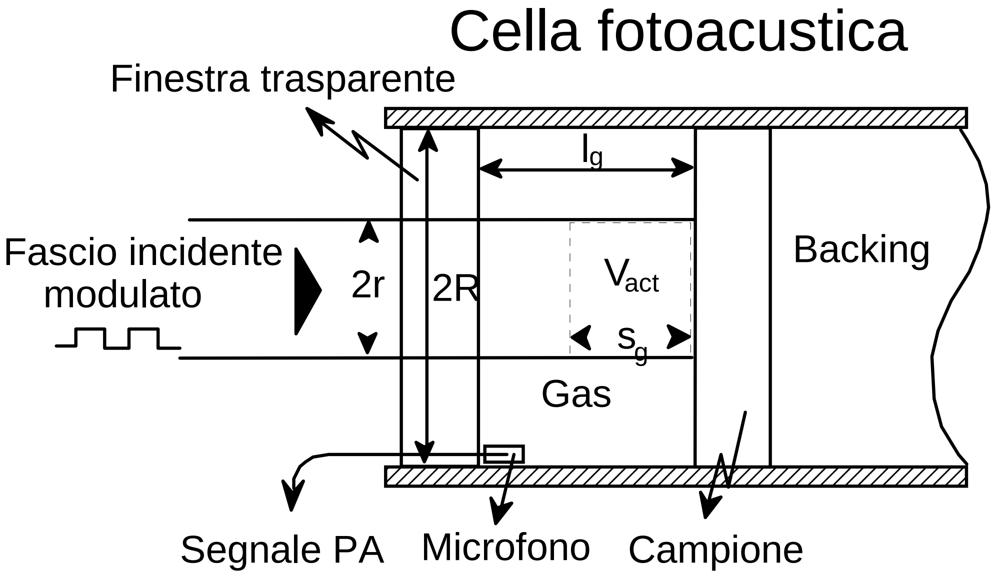

P acoustic pressure
T temperature
γ specific heat ratio
R radius of the cell
lg length of the cell
Vr residual volume
s_g effective length
D gas thermal diffusivity
f modulation frequency

Photoacoustic signal

$$dP = \frac{\gamma P r^2 s_g}{T\left(R^2 l_g + V_r/\pi\right)} dT$$

Effective cavity length

$$s_g = \min\left(l_g, \sqrt{D_g/\pi f}\right)$$

PHOTOTHERMAL TECHNIQUES
Photopyroelectric technique

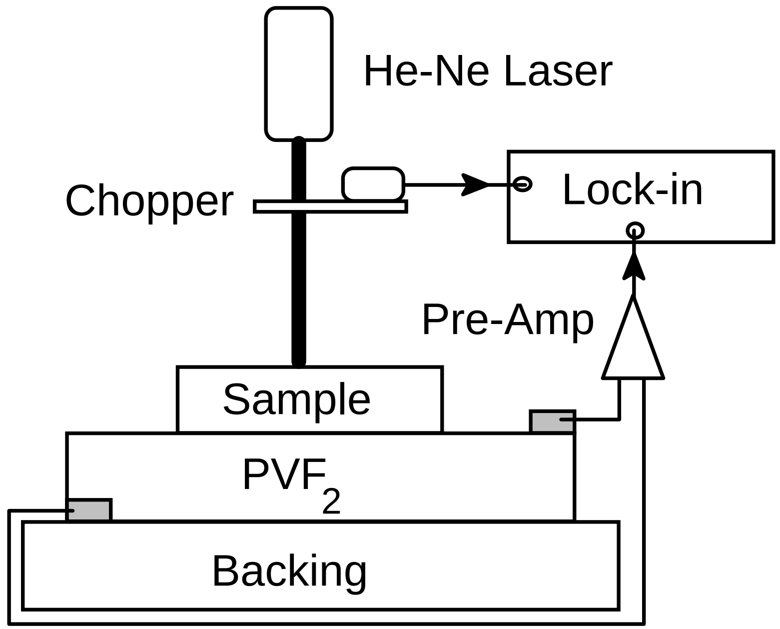

Photopyroelectric signal

$$i_p = \frac{-pA}{\ell_d}\frac{d}{dt}\int_0^{\ell_d} T(x,t)\,dx$$

p *pyroelectrica constant of the material*

A *area of the detector*

i_p *current*

T *temperature rise*

PHOTOTHERMAL TECHNIQUES

Other optical techniques

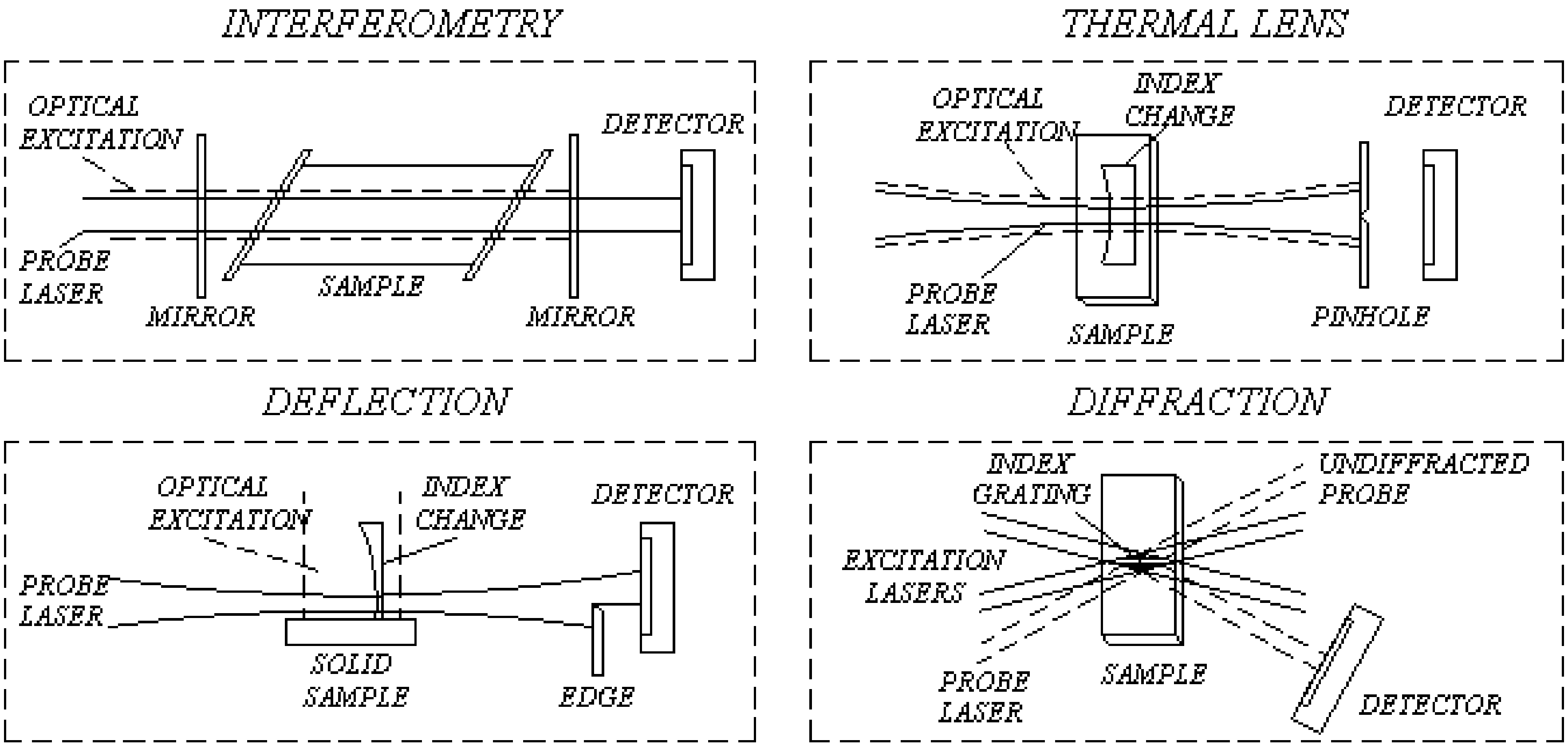

PHOTOTHERMAL TECHNIQUES

Photothermal deflection technique

Mirage effect

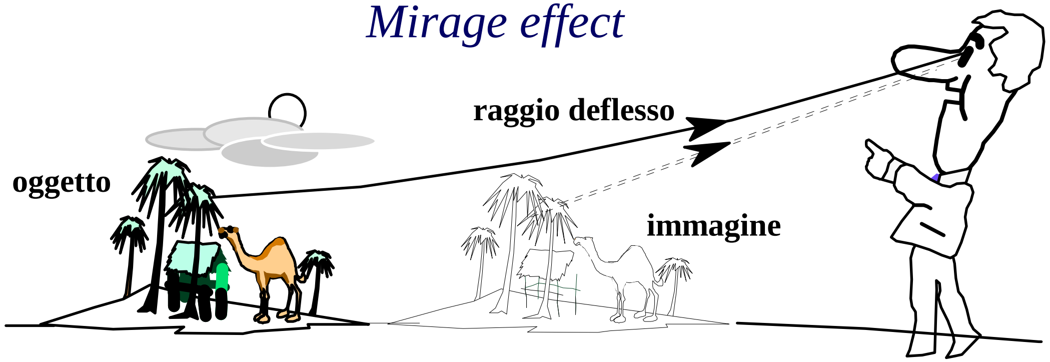

MIRAGGIO

Schematic set up

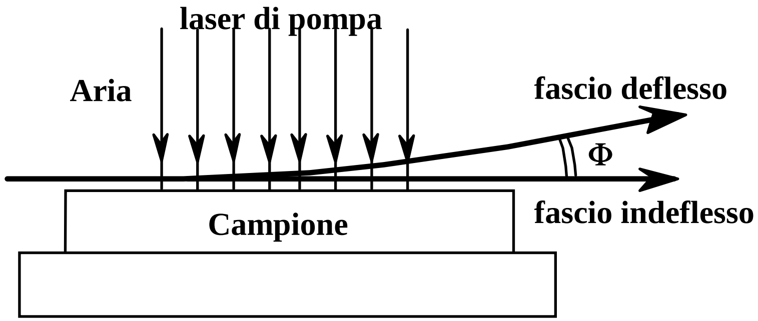

Deflection angle

$$\vec{\Phi} = \frac{1}{n}\frac{dn}{dT}\int_{path} \nabla_t T ds$$

Trace gas analysis device

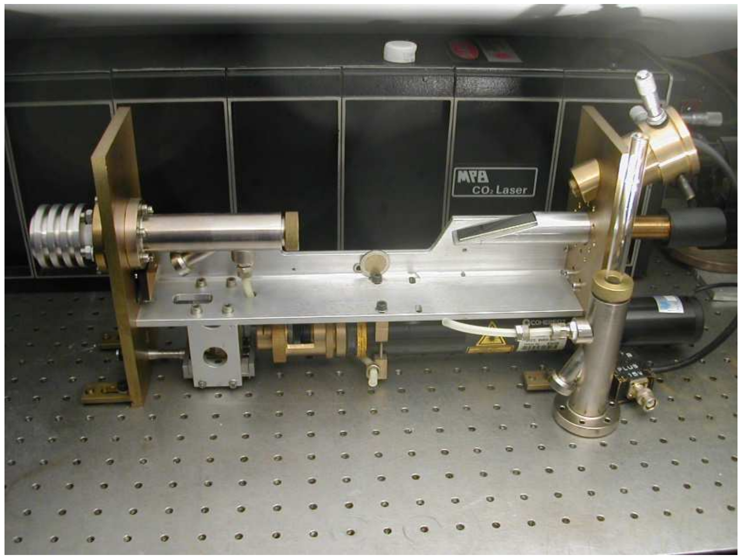

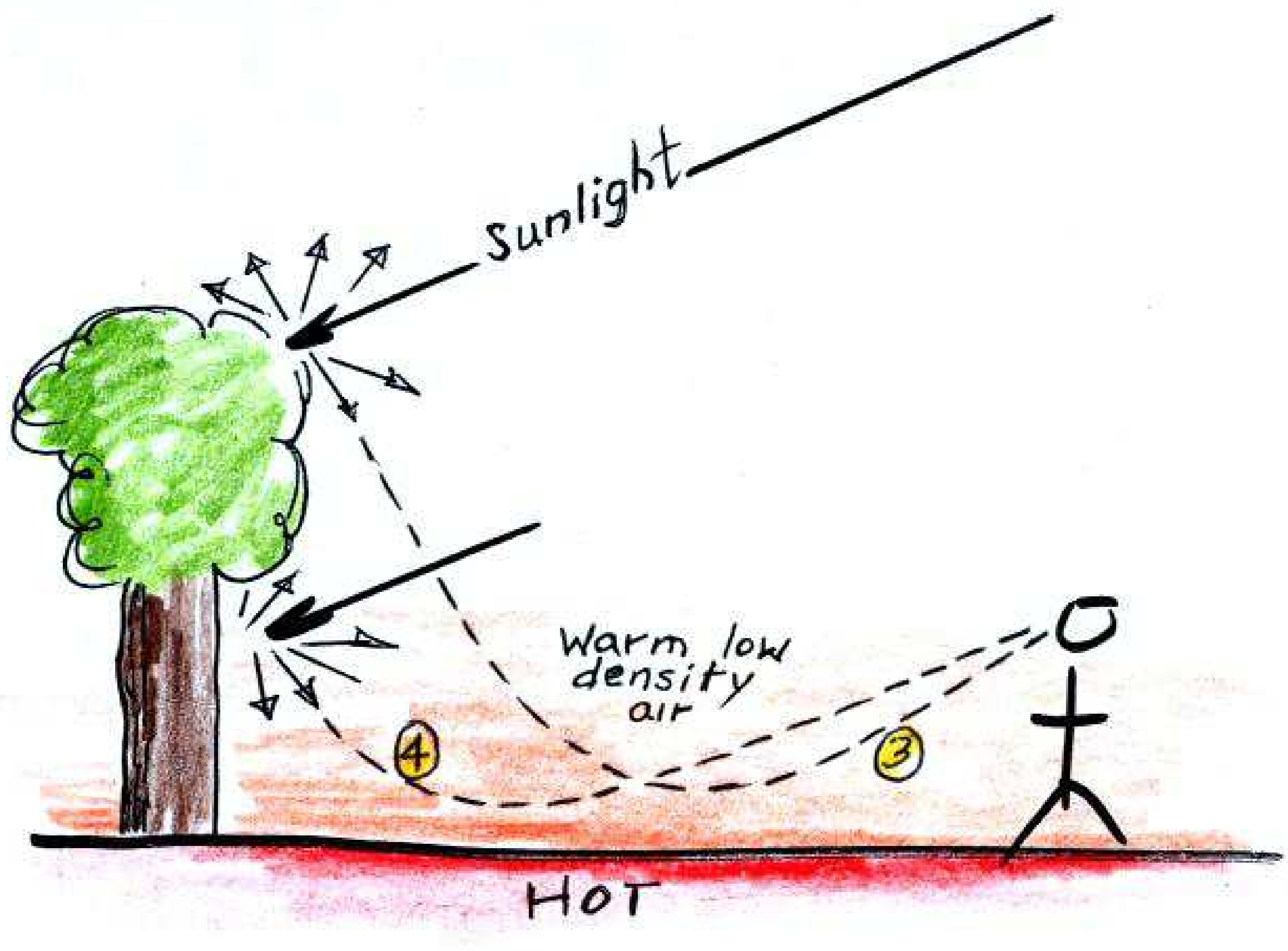
Sunlight
Warm low density air
4
3
HOT

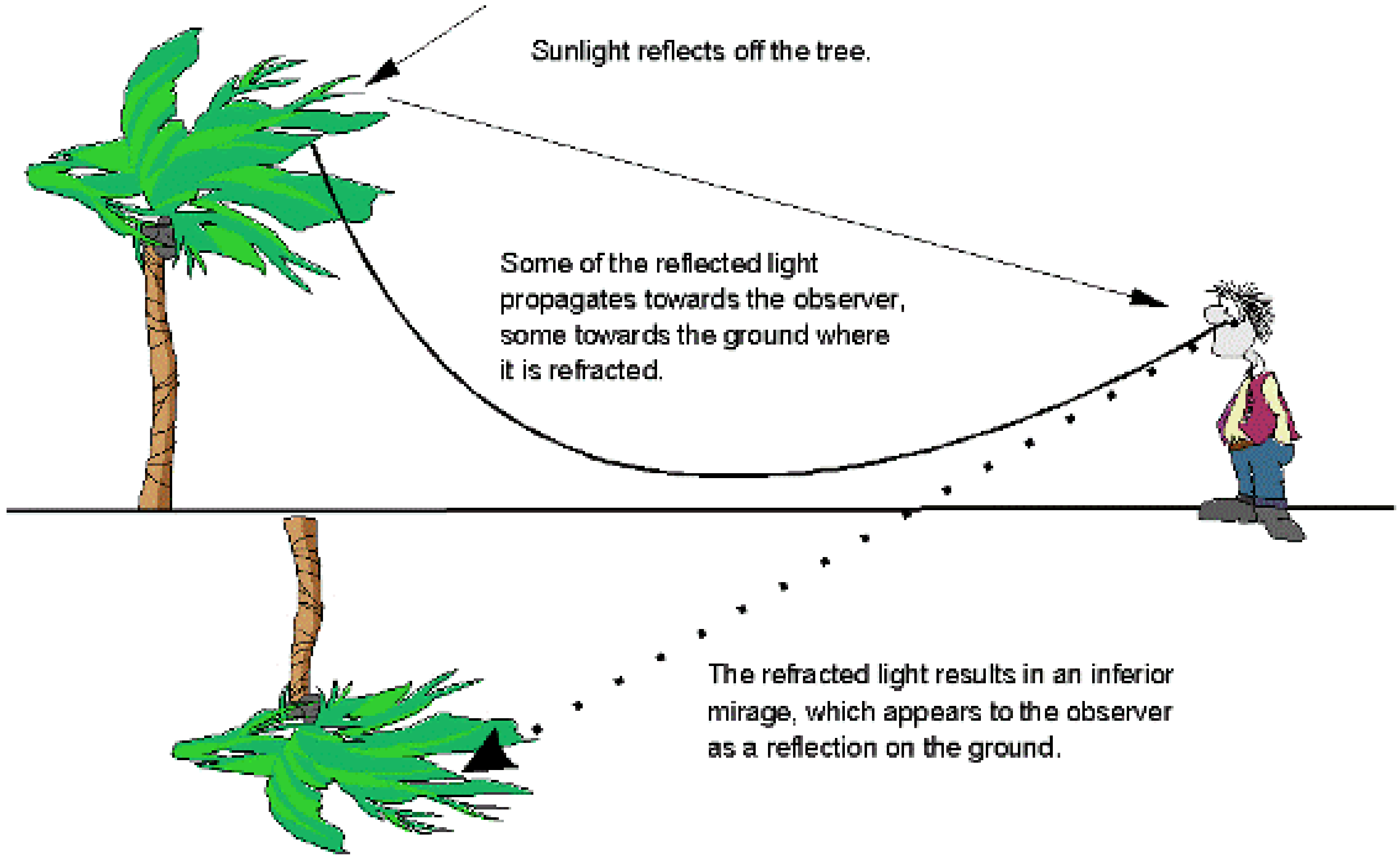
Sunlight reflects off the tree.
Some of the reflected light propagates towards the observer, some towards the ground where it is refracted.
The refracted light results in an inferior mirage, which appears to the observer as a reflection on the ground.


© Richard Fleet

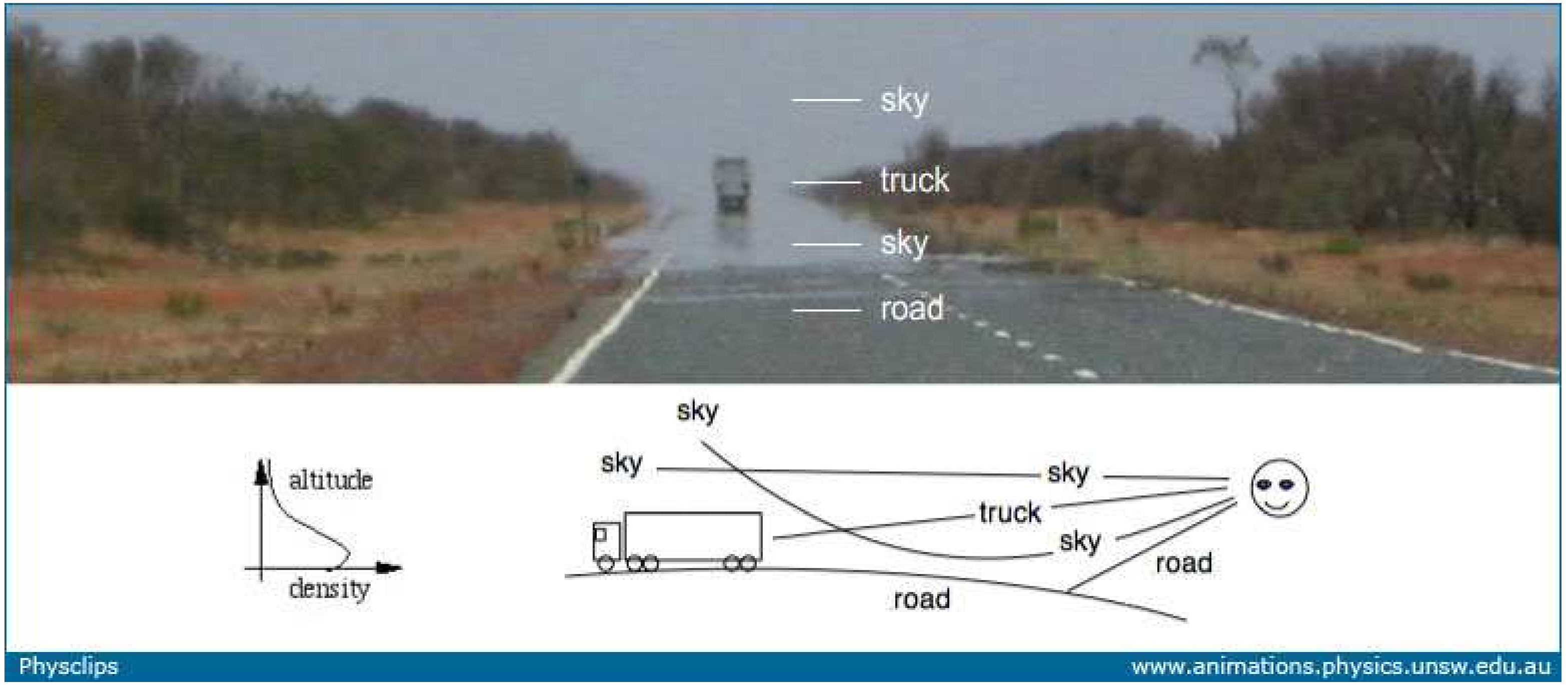
sky
truck
sky
road
altitude
density
sky
sky
sky
truck
sky
road
road
Physclips
www.animations.physics.unsw.edu.au

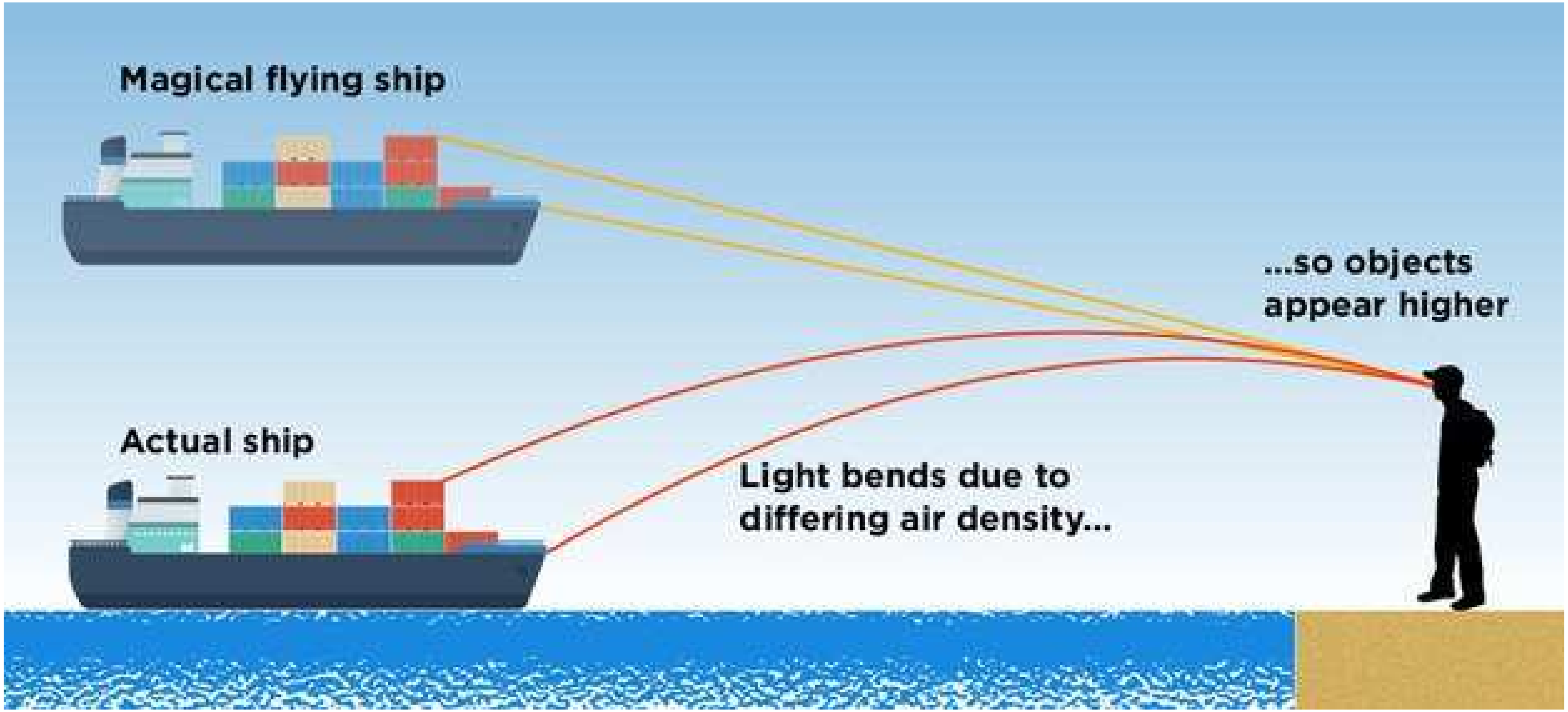
Magical flying ship
...so objects appear higher
Actual ship
Light bends due to differing air density...

Optical Beam Deflection

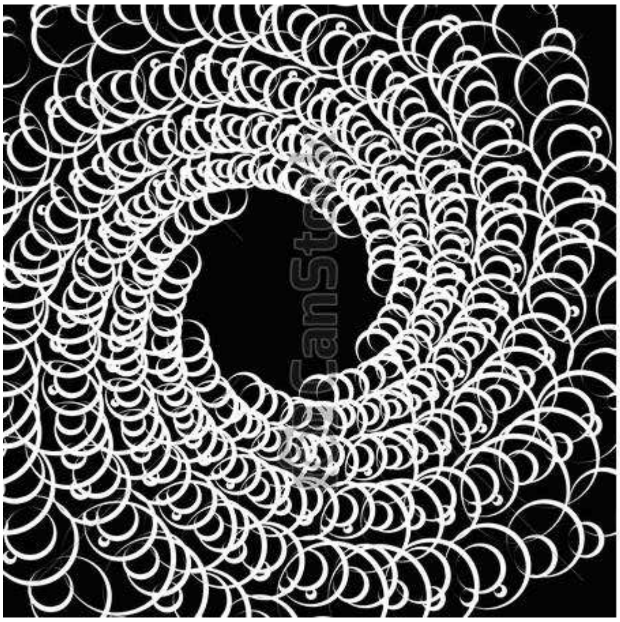

Mirage

Photothermal deflection

Thermo-optical spectroscopy: Detection by the "mirage effect"

A. C. Boccara, D. Fournier, and J. Badoz

Laboratoire d'Optique Physique, EPCI, ER N° 5 du CNRS, 10, rue Vauquelin, 75231 Paris Cedex 05, France

(Received 2 August 1979; accepted for publication 7 November 1979)

A new thermo-optical method based on the sensitive detection of thermal gradients adjacent to heated sample surfaces is described. Room- and low-temperature experiments were performed using this technique, and its advantages over different methods are discussed.

PACS numbers: 78.20.Nv, 07.65. − b, 44.30. + v, 67.40.Pm

When a conventional photoelectric measurement of the absorption coefficient is not feasible, i.e., for weakly absorbing samples and for opaque and diffusing samples, it is possible to use either calorimetric, interferometric, or photoacoustic techniques.[1,2]

The aim of this letter is to describe a new experimental

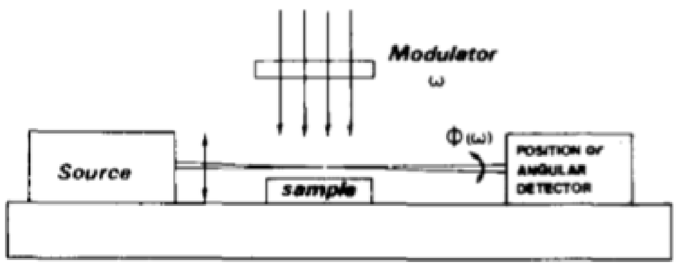

FIG. 1. Experimental setup. The sample is illuminated either by a 450-W Xe arc through a J.Y. $f/2$ monochromator (Figs. 2 and 3) or by a cw dye laser (Fig. 4).

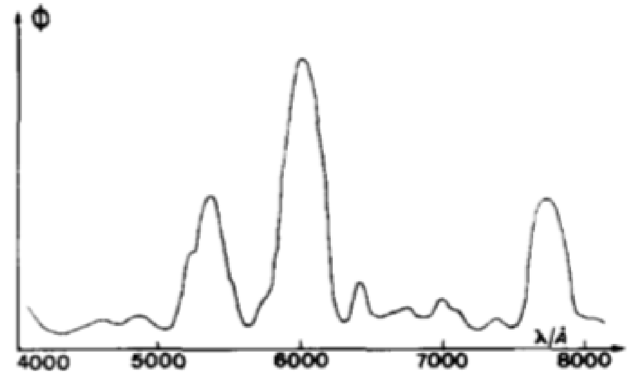

FIG. 3. Thermo-optical absorption spectrum of $Nd_2(MoO_4)_3$ crystal. Spectral bandwidth 100 Å, $\omega/2\pi = 80$ Hz.

The amplitude of the light beam deflection at modulation ω is given by $\phi = (l/n)(dn/dT)(dT/dx)$, where l is the interaction pathway between the probe beam and the tem-

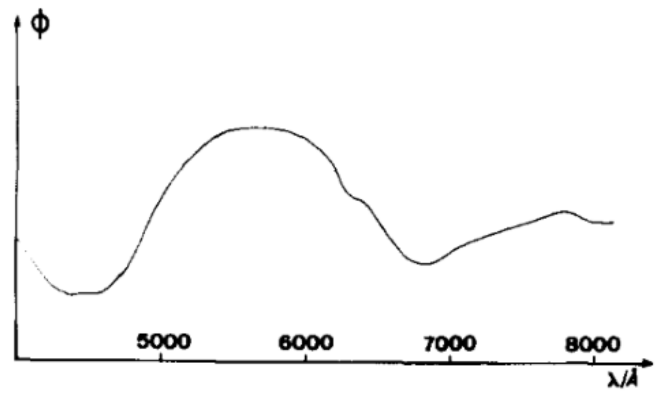

FIG. 2. Thermo-optical absorption spectrum of a $Cs_3Cr_3Cl_9$ powdered sample. Spectral bandwidth 100 Å, $\omega/2\pi = 300$ Hz.

spectra of a $Cs_3Cr_2Cl_9$ powdered sample and of a $Nd_2(MoO_4)_3$ monocrystal, respectively.

In order to perform thermo-optical measurements in liquid helium below the λ point, we have used the same technique instead of a conventional bolometer.[5] The time-dependent index of refraction gradient is generated by creating a heat standing wave (second sound) in the tail of the helium Dewar (~10 mm). Despite the weak dn/dT factor for liquid helium below 2 K, we were able to easily detect absorption

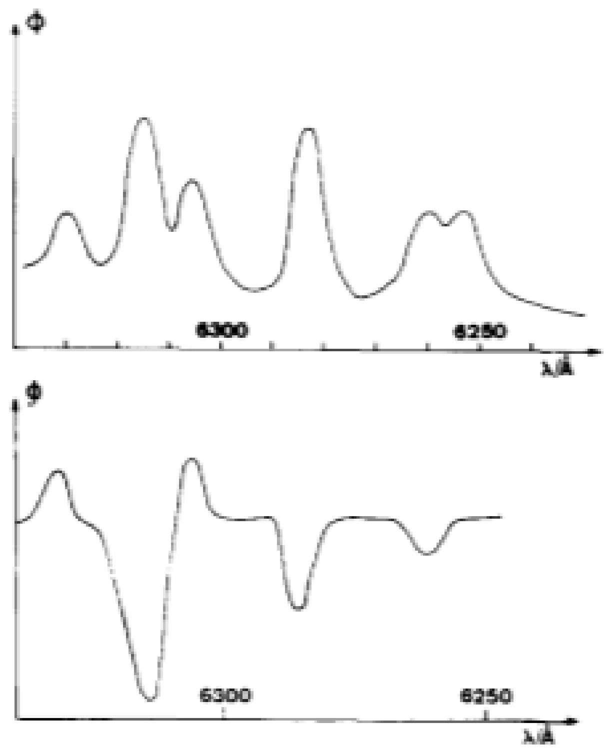

FIG. 4. $^4I_{9/2} \rightarrow {}^2H_{11/2}$ transition in $Nd_2(MoO_4)_3$ at 2 K, $\omega/2\pi = 3450$ Hz. Upper curve, thermo-optical absorption spectrum; lower curve, thermo-optical magnetic circular dichroism spectrum at 0.7 T.

Sensitive photothermal deflection technique for measuring absorption in optically thin media

A. C. Boccara and D. Fournier

Laboratoire d'Optique Physique, E.R. 5 du CNRS, Ecole Superieure de Physiqué et de Chimie Industrielles, 10, rue Vauquelin, 75231 Paris Cedex 05, France

Warren Jackson and Nabil M. Amer

Applied Physics and Laser Spectroscopy Group, Lawrence Berkeley Laboratory, University of California, Berkeley, California 94720

Received April 14, 1980

A highly sensitive and simple photothermal scheme for determining optical absorptions in condensed-matter samples is presented. αl values as low as 10^{-7} and 10^{-8} were measured for thin films and coatings and for liquids, respectively. A comparison with the thermal lens effect is given, and the experimental factors limiting our sensitivity are discussed.

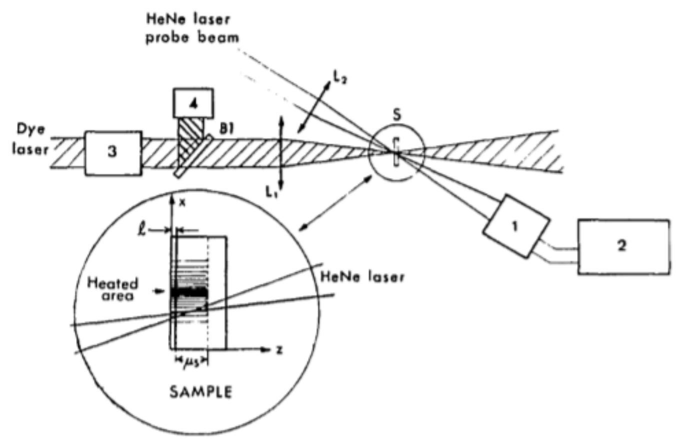

Fig. 1. Experimental setup. 1, Position sensor; 2, lock-in amplifier; 3, modulator; 4, power meter; L_1, 12-cm focal-length lens; L_2, 6-cm focal-length lens; B_1, beam splitter.

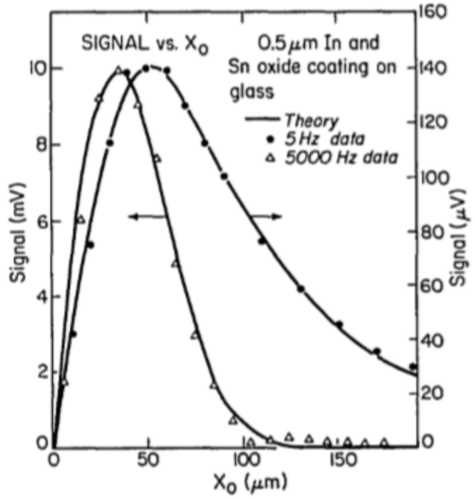

Fig. 2. Thermal-deflection signal versus the separation between the pump and probe beams. The solid lines are the results of the theory given in Ref. 4.

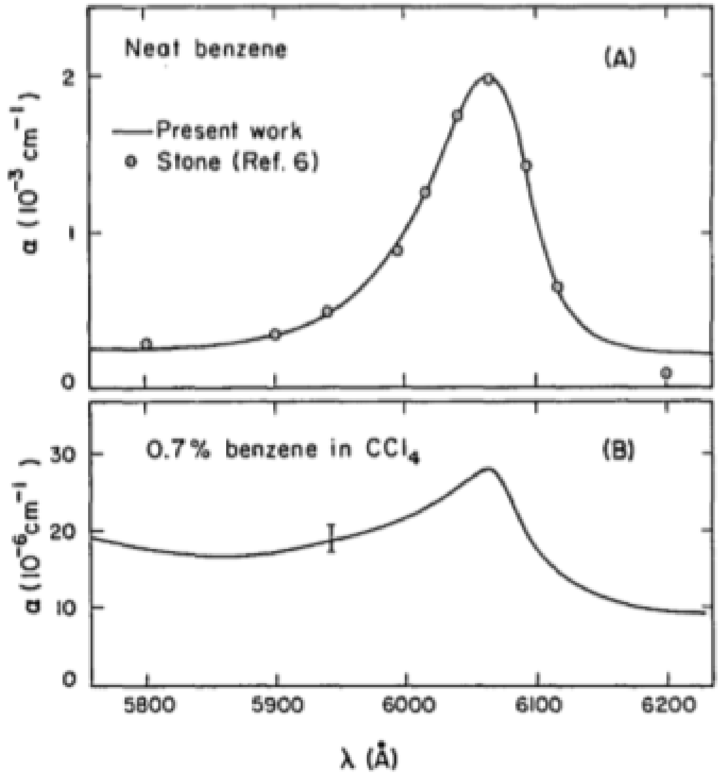

Fig. 3. (A) absorption spectrum of the sixth harmonic of the C—H stretching excitation of neat benzene. l = 0.5 mm; beam power, 60 mW. (B) the absorption of 0.7% benzene in CCl_4. l = 0.5 mm; beam power, 60 mW; lock-in-amplifier time constant, 0.3 sec. Bar represents typical errors of $\pm 2 \times 10^{-6}$ cm^{-1}.

References

1. A. Hordvik, Appl. Opt. **16,** 2827 (1977).
2. See, for example, D. C. Smith, IEEE J. Quantum Electron. **QE-5,** 600 (1969).
3. D. Fournier, A. C. Boccara, N. M. Amer, and R. Gerlach, Appl. Phys. Lett. (to be published, September 15, 1980).
4. W. Jackson, N. M. Amer, A. C. Boccara, and D. Fournier, in preparation.
5. Silicon Detector Corporation, Newbury Park, California.
6. J. Stone, Appl. Opt. **17,** 2876 (1978).
7. A. C. Tam, C. K. N. Patel, and R. J. Kerl, Opt. Lett. **4,** 81 (1979).
8. M. S. Burberry, J. A. Morrell, and A. C. Albrecht, J. Chem. Phys. **70,** 5522 (1979).
9. R. Swofford, M. Long, and A. Albrecht, J. Chem. Phys. **65,** 179 (1976).
10. R. Swofford and J. Morrell, J. Appl. Phys. **49,** 3667 (1978):
11. C. Hu and J. R. Whinnery, Appl. Opt. **12,** 72 (1973).

Photothermal deflection spectroscopy and detection

W. B. Jackson, N. M. Amer, A. C. Boccara, and D. Fournier

The theory for a sensitive spectroscopy based on the photothermal deflection of a laser beam is developed. We consider cw and pulsed cases of both transverse and collinear photothermal deflection spectroscopy for solids, liquids, gases, and thin films. The predictions of the theory are experimentally verified, its implications for imaging and microscopy are given, and the sources of noise are analyzed. The sensitivity and versatility of photothermal deflection spectroscopy are compared with thermal lensing and photoacoustic spec-

1334 APPLIED OPTICS / Vol. 20, No. 8 / 15 April 1981

References

1. See, for example, J. Stone, J. Opt. Soc. Am. 62, 327 (1972); Appl. Opt. 12, 1828 (1973).
2. J. R. Whinnery, Acc. Chem. Res. 7, 225 (1974) and references therein.
3. R. L. Swofford and J. A. Morrell, J. Appl. Phys. 49, 3667 (1978) and references therein.
4. For an overview of photoacoustic spectroscopy, see Y.-H. Pao, Ed., *Optoacoustic Spectroscopy and Detection* (Academic, New York, 1977).
5. D. Fournier, A. C. Boccara, and J. Badoz, in *Digest of Topical Meeting on Photoacoustic Spectroscopy* (Optical Society of America, Washington, D.C., 1979), paper ThA1.
6. A. C. Boccara, D. Fournier, W. Jackson, and N. M. Amer, Opt. Lett. 5, 377 (1980).
7. D. Fournier, A. C. Boccara, N. M. Amer, and R. Gerlach, Appl. Phys. Lett. 37, 519 (1980).
8. A. C. Boccara, D. Fournier, and J. Badoz, Appl. Phys. Lett. 36, 130 (1980).
9. J. C. Murphy and L. C. Aamodt, J. Appl. Phys. 51, 4580 (1980).

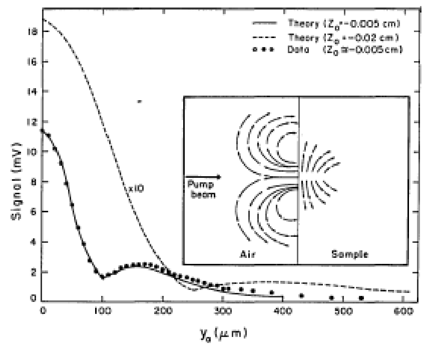

Fig. 10. Transverse PDS. Signal amplitude vs off-axis displacement y_0 for various z_0 offsets. Material is 600-nm edge filter glass, frequency is 48 Hz, tilt angle is 0°, and beam radius is 70 μm. Inset shows direction of heat flow and origin of the second maximum.

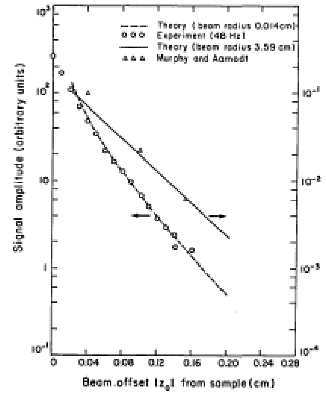

Fig. 12. Transverse PDS. Signal amplitude vs beam offset y_0 at 48 Hz. Tilt angle is 0°.

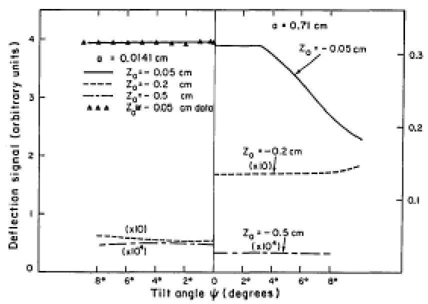

Fig. 11. Transverse PDS. Signal amplitude vs tilt angle ψ. Frequency is 48 Hz, and the sample is 600-nm edge filter glass.

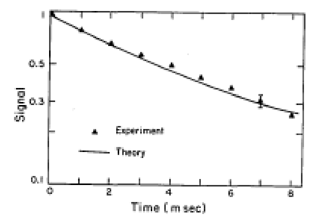

Fig. 13. Signal vs time for benzene at 607 nm. Collinear PDS with the probe beam at $x_0 = a/2$.

Photothermal spectroscopy using optical beam probing: Mirage effect [a)]

J. C. Murphy and L. C. Aamodt
Applied Physics Laboratory, The Johns Hopkins University, Laurel, Maryland 20810

(Received 17 January 1980; accepted for publication 2 June 1980)

Optical beam deflection near a heated surface was recently introduced as a method of photothermal spectroscopy. Photothermal spectroscopy (PTS) is closely related to photoacoustic spectroscopy (PAS) in its ability to measure optical properties of opaque solids and liquids. This paper develops a theory of this effect and compares this theory with extensive experimental observations. Both are in excellent agreement. The relationship between this form of PTS and PAS is explicitly developed. Applications to the measurement of thermal diffusivity of gases is described.

PACS numbers: 07.65. — b, 43.35.Sx, 78.20.Hp

in the sample and the justification for the name photo*acoustic* spectroscopy. The low detection threshold of photoacoustic systems is attributable to the excellent sensitivity of available microphones. Recently Fournier, Boccara, and Bodoz[9] have introduced an optical means for carrying out PAS experiments ("mirage" detection). In this method, temperature-induced changes in the index of refraction of the gas in contact with the sample surface are used to detect light absorption. They report successful measurement of PAS spectra as a function of temperature into the liquid helium range. A significant advantage of this method is that the spatial gradient of the total gas temperature rise associated

[1] Allan Rosencwaig, Anal. Chem. **47**, 592 (1975).
[2] J.C. Murphy and L.C. Aamodt, J. Appl. Phys. **48**, 3502 (1977).
[3] Robert G. Peterson and Richard C. Powell, Chem. Phys. Lett. **53**, 366 (1978).
[4] P. Nordal and S.O. Kanstad, Opt. Commun. **24**, 95 (1978).
[5] L.C. Aamodt, J.C. Murphy, and J.G. Parker, J. Appl. Phys. **48**, 927 (1977).
[6] L.C. Aamodt and J.C. Murphy, J. Appl. Phys. **49**, 3036 (1978).
[7] A. Rosencwaig and A. Gersho, J. Appl. Phys. **47**, 64 (1976).
[8] F.A. McDonald and G.C. Wetsel, Jr., J. Appl. Phys. **49**, 2313 (1978).
[9] D. Fournier, A.C. Boccara, and J. Badoz, Topical Meeting on Photoacoustic Spectroscopy, 1–3 August 1979, Iowa State University, paper ThA1 (unpublished); A. C. Boccara, D. Fournier, and J. Badoz, Appl. Phys. Lett. **36**, 130 (1980).
[10] J.C. Murphy and L.C. Aamodt, J. Appl. Phys. **31**, 728 (1977).
[11] H.S. Carslaw and J.C. Jaeger, *Conduction of Heat in Solids* (Clarendon, Oxford, 1959).
[12] *International Critical Tables*, National Research Council (McGraw Hill, New York, 1930), Vol VII, p. 4.
[13] Y.S. Touloukian, R.W. Powell, I.Y. Ho, and M.C. Nicolaou, *Thermal Diffusivity*, (IFI/Plenum, New York, 1973), Vol. 10, p. 128.

PRINCIPLE OF PHOTOTHERMAL DEFLECTION

HELMOLTZ Equation

$$\nabla^2 V(r) + k^2 n^2(r) V(r) = 0$$

$$V(r) = A(r)\cdot e^{i\,k\,S(r)}$$

RAY OPTICS Equation

$$\begin{cases} \cancel{\nabla^2 A} + k^2 A\cdot\left(n^2 - |\nabla S|^2\right) = 0 \\ A\nabla^2 S + 2\nabla A\cdot\nabla S = 0 \end{cases}$$

RAY OPTICS Solution

$$|\nabla S|^2 = n^2 \quad \Rightarrow \quad \nabla S = n\cdot\vec{\sigma}$$

- n → **Refractive index**
- $\vec{\sigma}$ → **Ray unit vector**

BENDING EFFECT $\dfrac{dS}{ds} = n$

$$\nabla n = \nabla\left(\frac{dS}{ds}\right)$$

$$\nabla_t n = n\frac{d\vec{\sigma}}{ds} = \frac{n}{\rho}\vec{v}$$

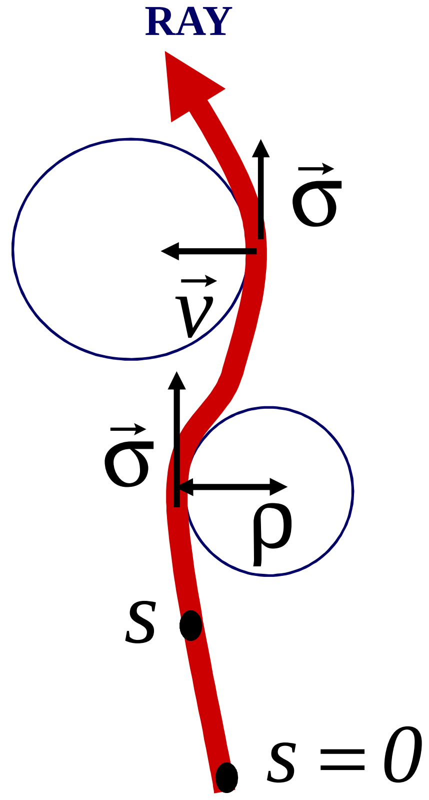

Light bends only due to the transverse gradient

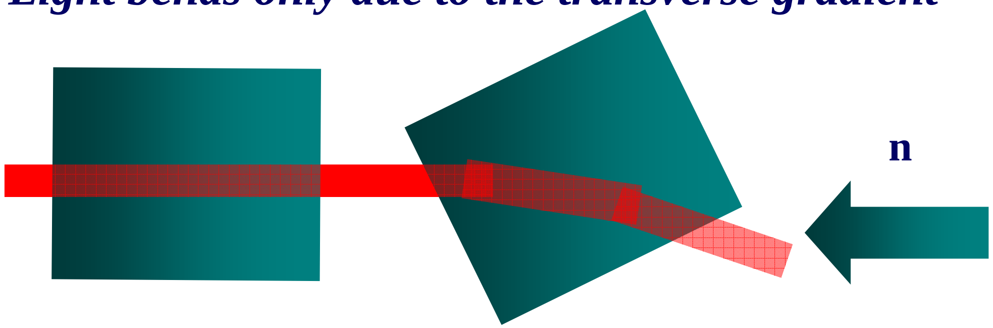

WEAK DEFLECTION

$$\nabla_t n = n\frac{d\vec{\sigma}}{ds} \quad \xrightarrow{\textit{Integration over } s} \quad \vec{\sigma}(s)-\vec{\sigma}(0)=\int_0^s \frac{\nabla_t n}{n}ds$$

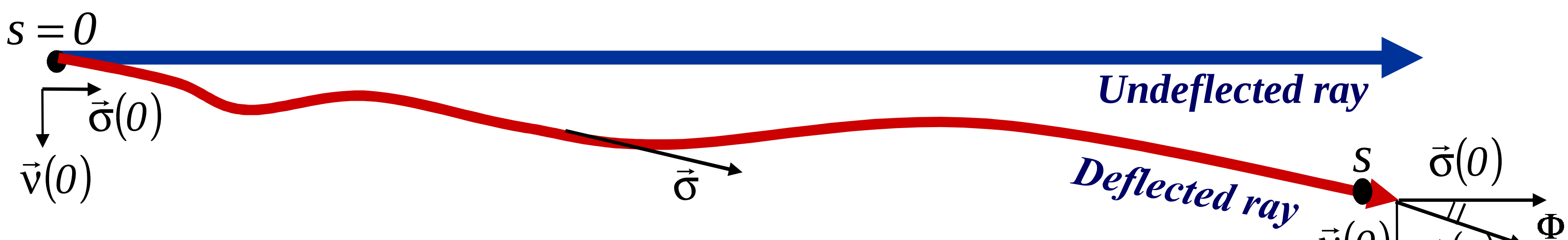

Final ray $\vec{\sigma}(s)=\mathrm{sen}\,\Phi\cdot\vec{v}(0)+\cos\Phi\cdot\vec{\sigma}(0)\cong\Phi\cdot\vec{v}(0)+\vec{\sigma}(0)$

Deflection formula $\Phi=\int_{path}\frac{\nabla_t n\cdot\vec{v}}{n}ds$

2-D WEAK DEFLECTION

$$\Phi_{h_1}=\int_{path}\frac{\nabla_t n\cdot\vec{h}_1}{n}ds=\int_{path}\frac{1}{n}\frac{\partial n}{\partial h_1}ds$$

$$\Phi_{h_2}=\int_{path}\frac{\nabla_t n\cdot\vec{h}_2}{n}ds=\int_{path}\frac{1}{n}\frac{\partial n}{\partial h_2}ds$$

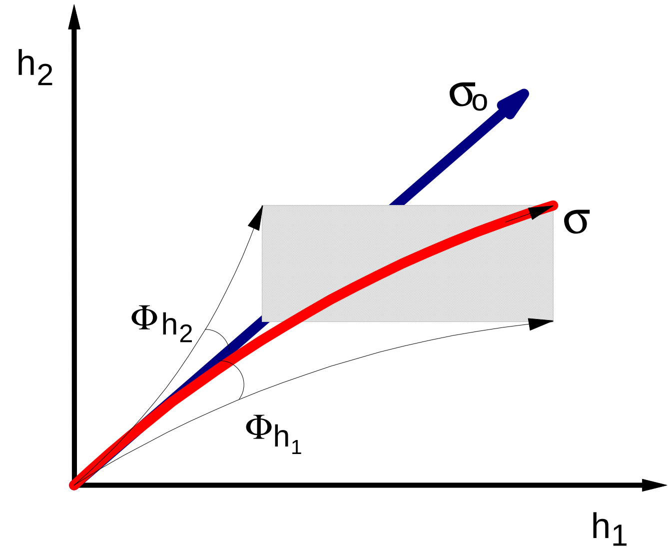

NATURE OF THE DEFLECTION

Taylor expansion of the refractive index

$$dn = \frac{\partial n}{\partial T}\cdot(T - T_0) + \frac{\partial n}{\partial f_1}\cdot(f_1 - f_{10}) + \ldots + \frac{\partial n}{\partial f_n}\cdot(f_n - f_{n0})$$

Photothermal deflection

$$\begin{cases} \vec{\Phi} = \vec{\Phi}_{\mathbf{T}} + \vec{\Phi}_{\mathbf{f_1}} + \ldots + \vec{\Phi}_{\mathbf{f_n}} \\ \vec{\Phi} = \int_{path} \frac{\partial n}{\partial T}\cdot\frac{\nabla_t \mathrm{T}}{\mathrm{n}}\,\mathrm{ds} + \sum_i \int_{path} \frac{\partial n}{\partial f_i}\cdot\frac{\nabla_t \mathrm{f_i}}{\mathrm{n}}\,\mathrm{ds} \end{cases}$$

$$\vec{\Phi} = \frac{1}{n}\frac{dn}{dT}\int_{path} \nabla_t \mathrm{T}\;\;\mathrm{ds}$$

In gases

$$n(p,T) = 1 + \frac{3Ap}{2RT}$$

Tipo di composto	A [m³ mol⁻¹] *10⁻⁶
Aria	4.6
Ossigeno	4.05
HCl	6.68
Vapore acqueo	3.72
CS_2	22
C_3H_6O	16.2

$$\begin{cases} \left.\dfrac{dn}{dT}\right|_{To} = \dfrac{-3Ap}{2RT_o^2} \\ \left.\dfrac{d^2n}{dT^2}\right|_{To} = \dfrac{3Ap}{RT_o^3} \end{cases}$$

AIR OPTOTHERMAL COEFFICIENT

Best approximation

$$\frac{dn}{dT} = -7.856 \cdot 10^{-5} \frac{p\left(1 + 3.34 \cdot 10^{-6} p\right)}{T_o^2}$$

AIR OPTOTHERMAL COEFFICIENT

$$\frac{dn}{dT} = -7.856 \cdot 10^{-5} \frac{p\left(1 + 3.34 \cdot 10^{-6}\, p\right)}{T_o^2}$$

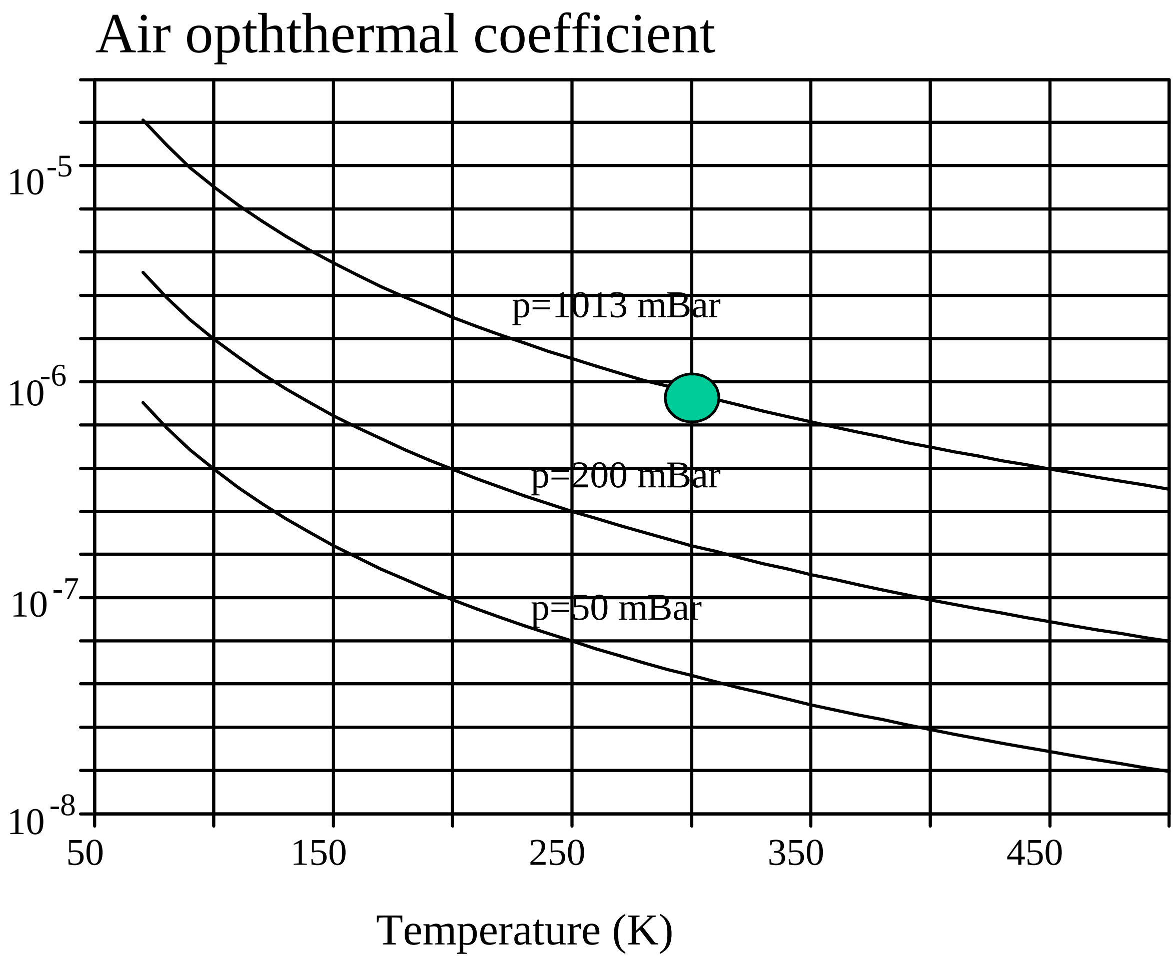

EXPERIMENTAL RESULTS ON THE AIR OPTOTHERMAL COEFFICIENT

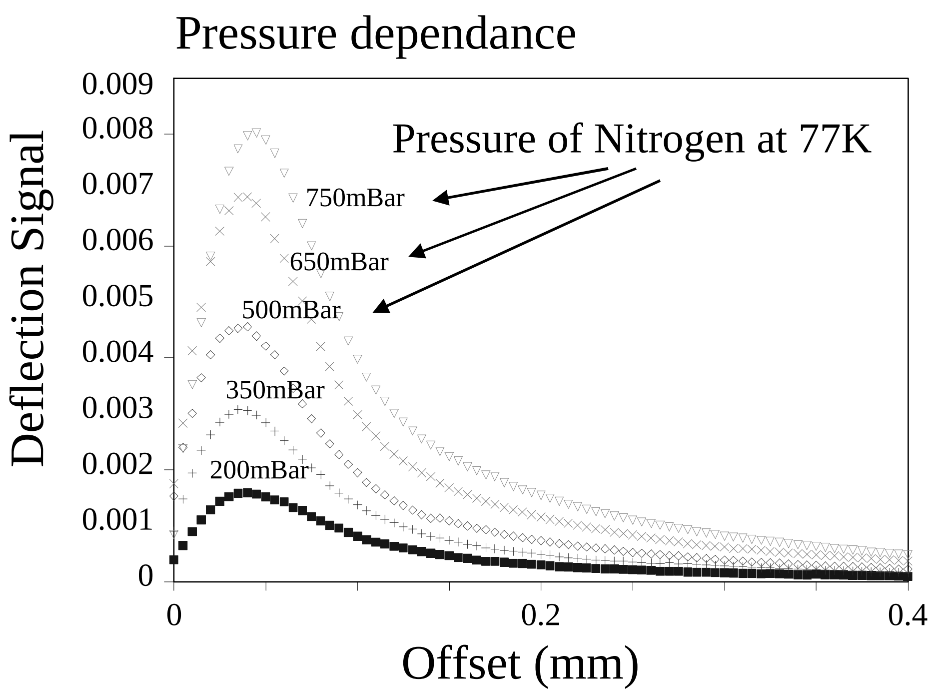

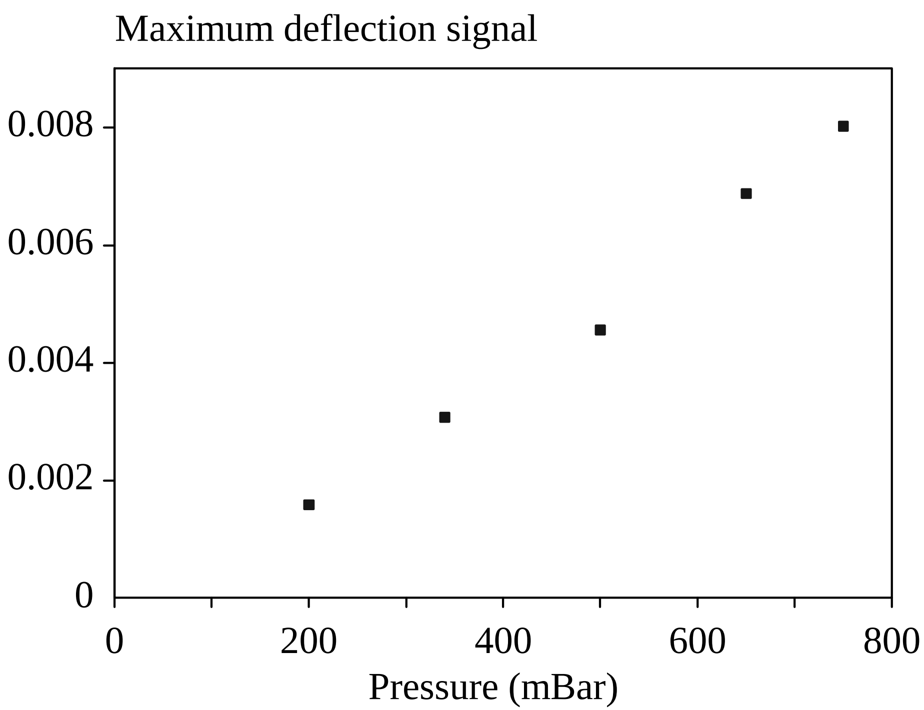

SIGNAL DETECTION

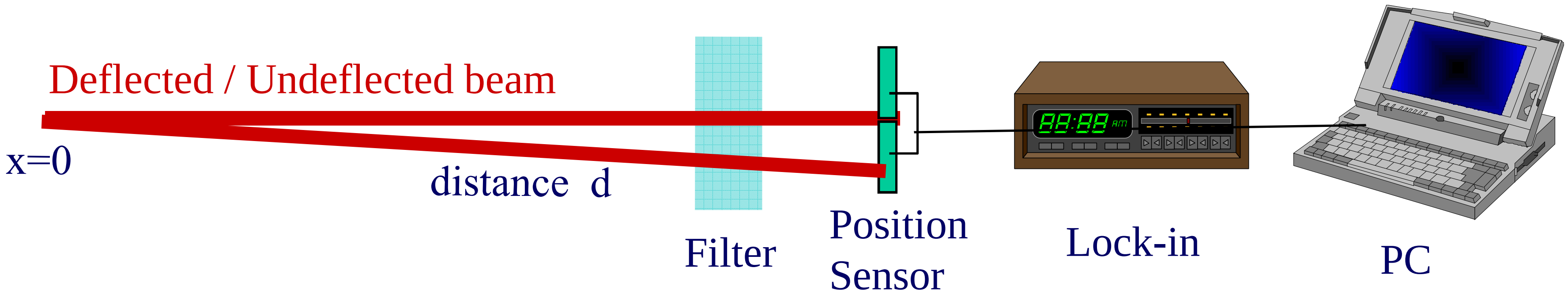

POSITION SENSOR EQUATIONS

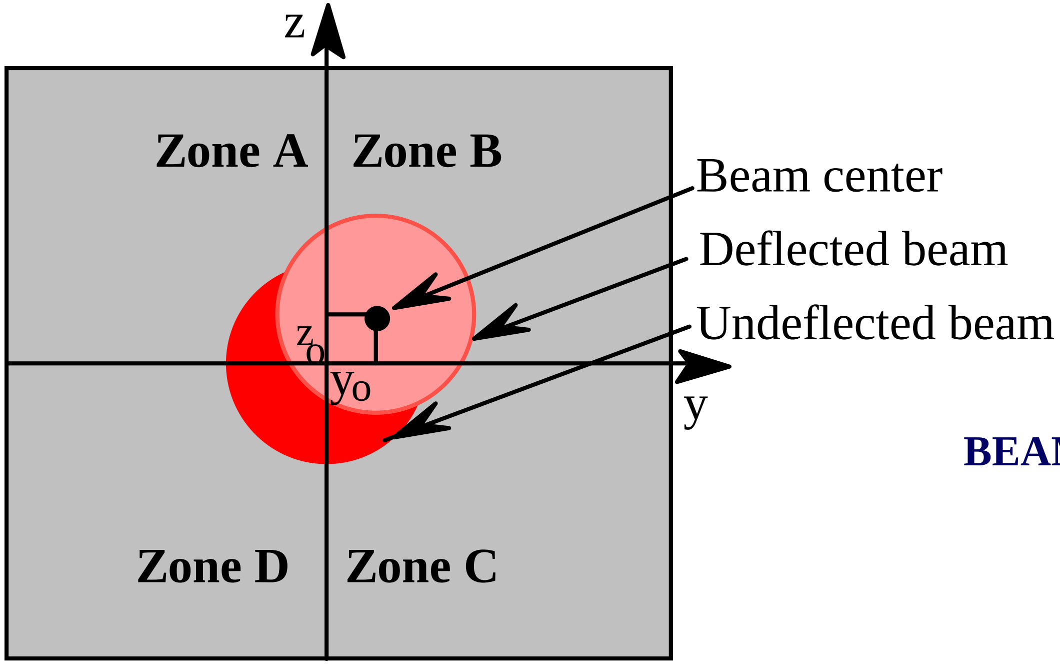

BEAM CENTER

$$\begin{cases} y_0 = \Phi_y d \\ z_0 = \Phi_z d \end{cases}$$

SPOT-SIZE BROADENING

$$w(d) = w_0 \cdot \sqrt{1 + \left(\frac{\lambda d}{\pi n w_0^2}\right)^2} \cong \frac{\lambda d}{\pi w_0^2}$$

BEAM INTENSITY ON THE DETECTOR

$$I(y,z) = \frac{2P}{\pi w^2(d)} \cdot e^{-2\frac{(y-y_0)^2+(z-z_0)^2}{w^2(d)}}$$

POWER ON THE DETECTOR

Weak deflection approximation $erf(z) \cong \frac{2}{\sqrt{\pi}} z$

$$P_A = \frac{P}{4} \cdot \frac{\sqrt{8}}{\sqrt{\pi}} \cdot \left(\frac{z_0 - y_0}{w(d)} \right) = \frac{P w_0 \sqrt{\pi}}{\lambda \sqrt{2}} \cdot \left(\Phi_z - \Phi_y \right)$$

$$P_B = \frac{P}{4} \cdot \frac{\sqrt{8}}{\sqrt{\pi}} \cdot \left(\frac{z_0 + y_0}{w(d)} \right) = \frac{P w_0 \sqrt{\pi}}{\lambda \sqrt{2}} \cdot \left(\Phi_z + \Phi_y \right)$$

$$P_C = \frac{P}{4} \cdot \frac{\sqrt{8}}{\sqrt{\pi}} \cdot \left(\frac{y_0 - z_0}{w(d)} \right) = \frac{P w_0 \sqrt{\pi}}{\lambda \sqrt{2}} \cdot \left(\Phi_y - \Phi_z \right) = -P_A$$

$$P_D = -\frac{P}{4} \cdot \frac{\sqrt{8}}{\sqrt{\pi}} \cdot \left(\frac{z_0 + y_0}{w(d)} \right) = -\frac{P w_0 \sqrt{\pi}}{\lambda \sqrt{2}} \cdot \left(\Phi_z + \Phi_y \right) = -P_B$$

DEFLECTION SIGNAL

Vertical signal

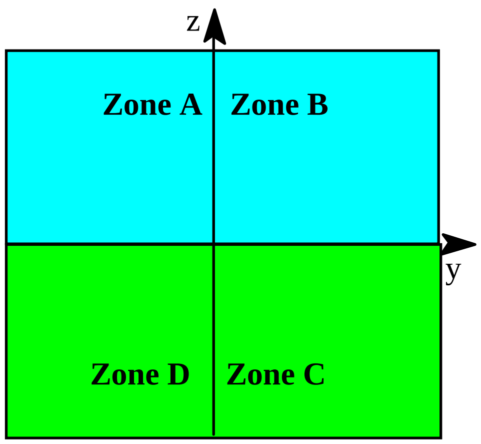

$$\begin{cases} \dfrac{\Delta V_v}{V_o} = \dfrac{P_A + P_B - P_C - P_D}{P_A + P_B + P_C + P_D} \\ \dfrac{\Delta V_l}{V_o} = \dfrac{-P_A + P_B + P_C - P_D}{P_A + P_B + P_C + P_D} \end{cases}$$

$$\begin{cases} \Delta V_v = \sqrt{8\pi} \dfrac{w_0}{\lambda} \Phi_z \\ \Delta V_l = \sqrt{8\pi} \dfrac{w_0}{\lambda} \Phi_y \end{cases}$$

Lateral signal

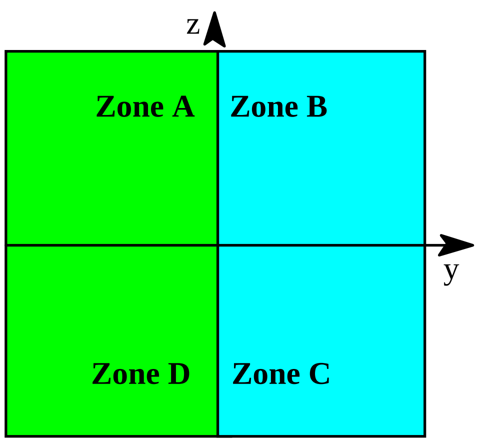

Main applications

- *Thermal diffusivity and effusivity measurements*
- *Absorption spectroscopy*
- *Effusivity and optical absorption depth profiling*
- *Measurement of the attenuation in optical waveguides*
- *Evaluation of the thickness of thin layers*
- *Trace gas analysis*
- *Characterization of metallic surfaces*

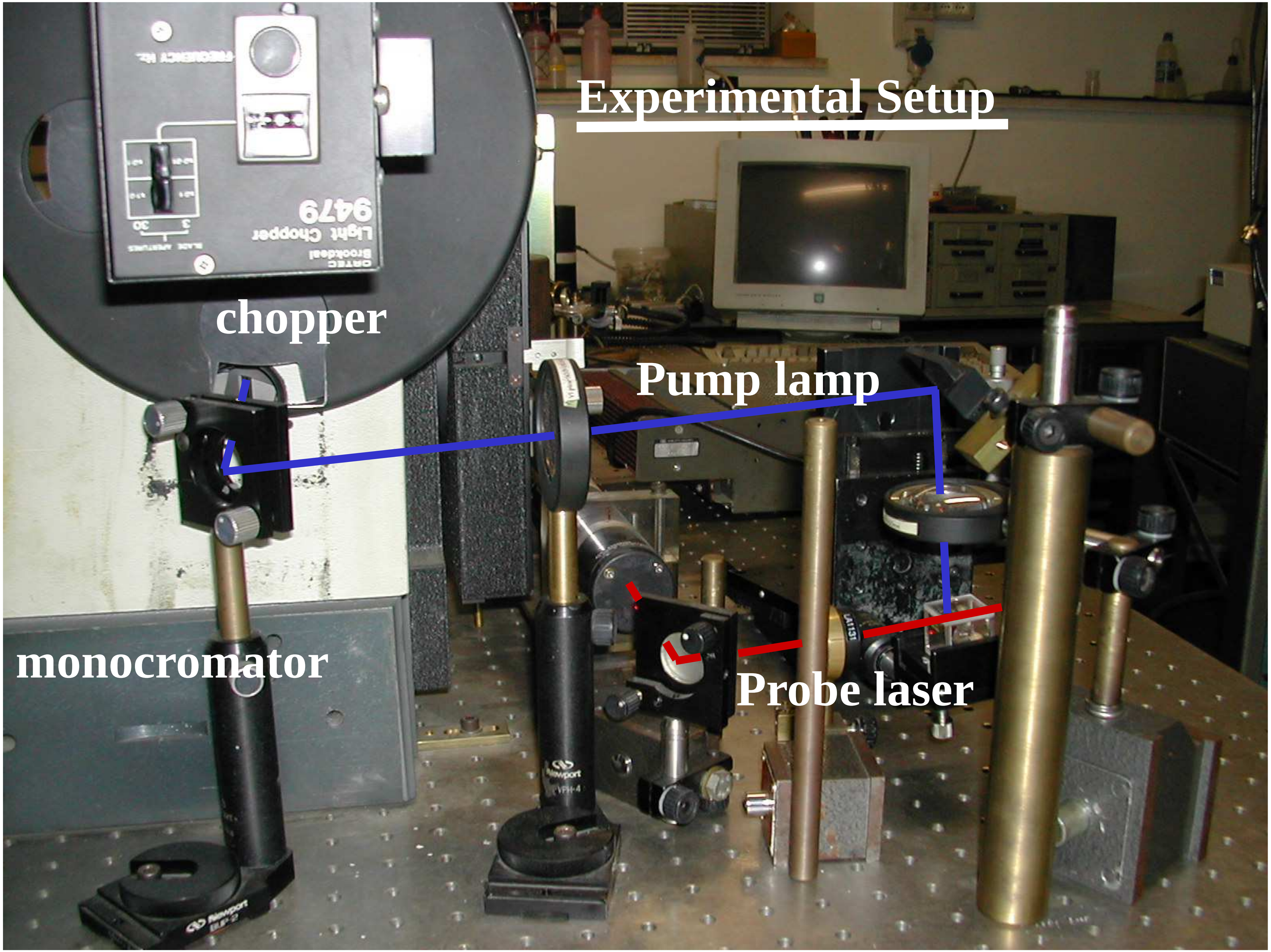
Experimental Setup
chopper
Pump lamp
monocromator
Probe laser

Photothermal Deflection Spectroscopy Set-up

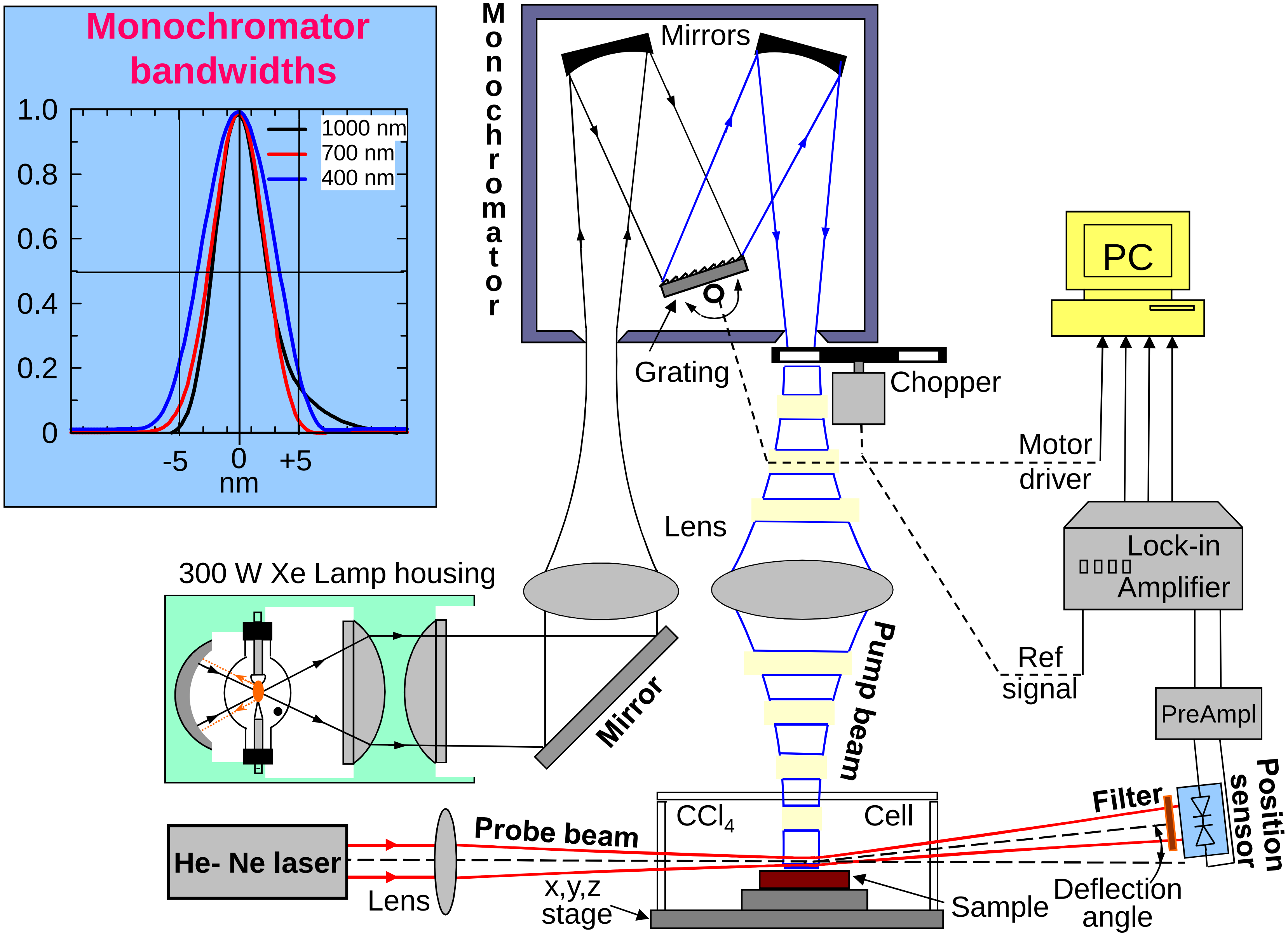

Optical Reflectance Spectroscopy

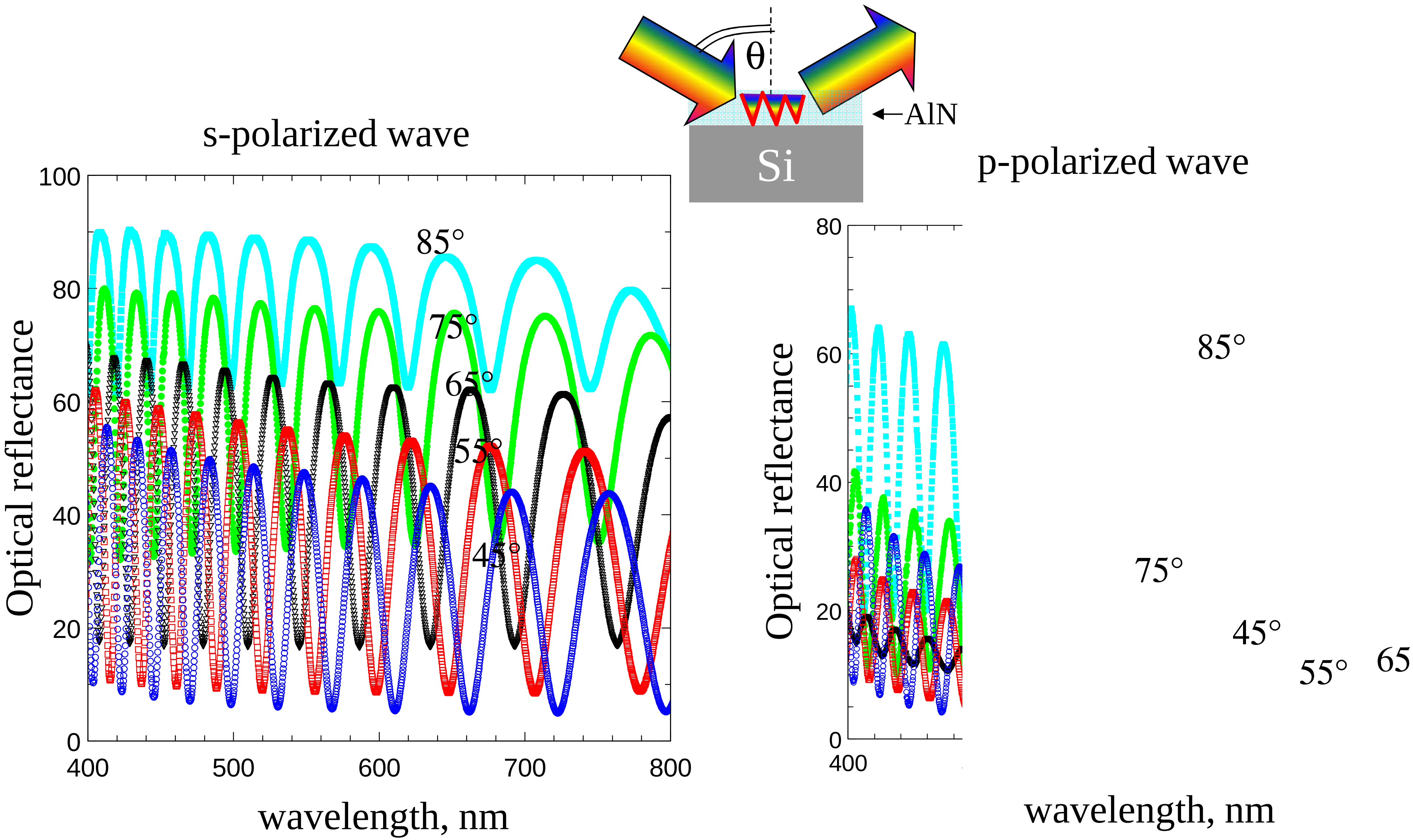

Courtesy of A.Passaseo

Photothermal Deflection Spectroscopy on AlN

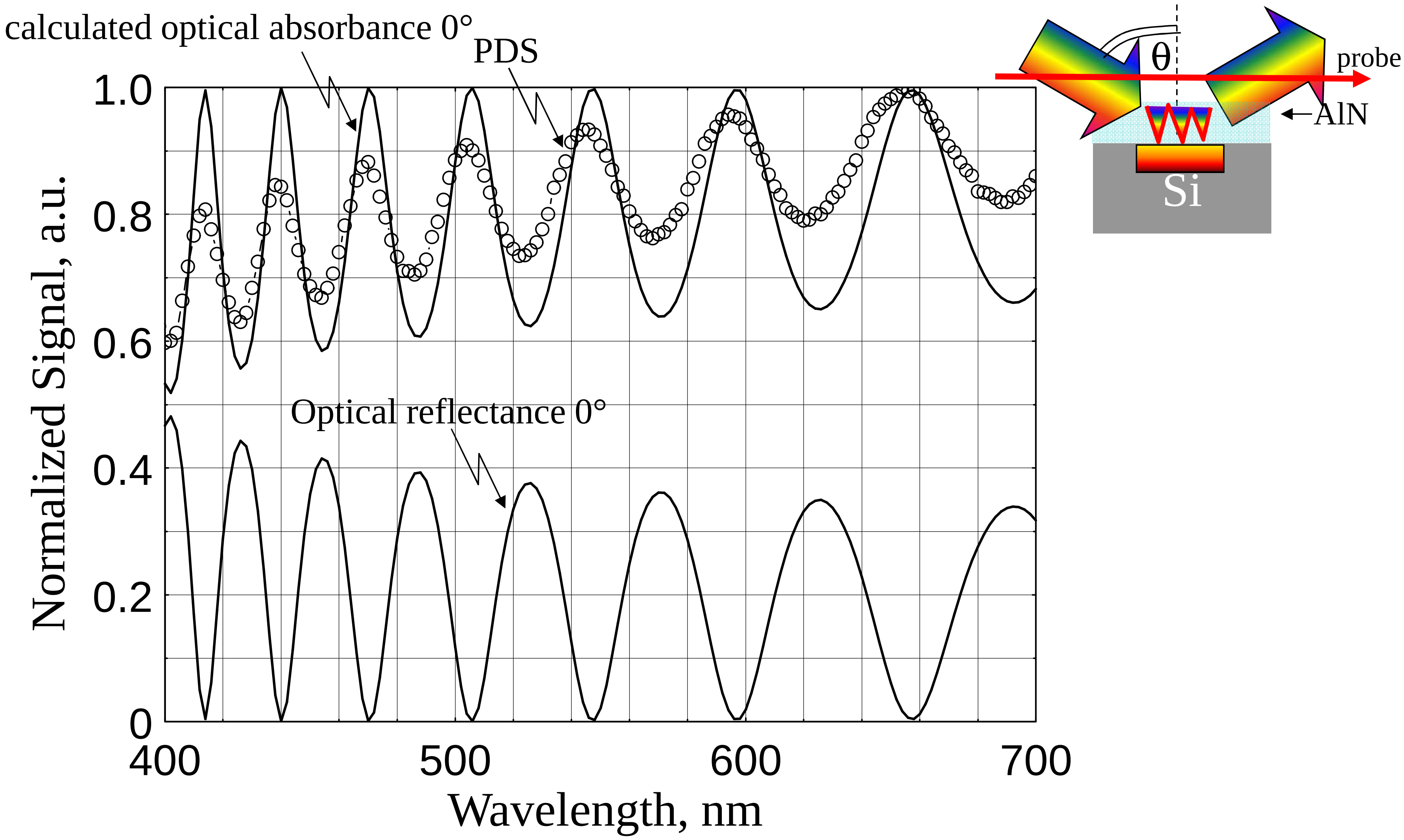

Device under test

section

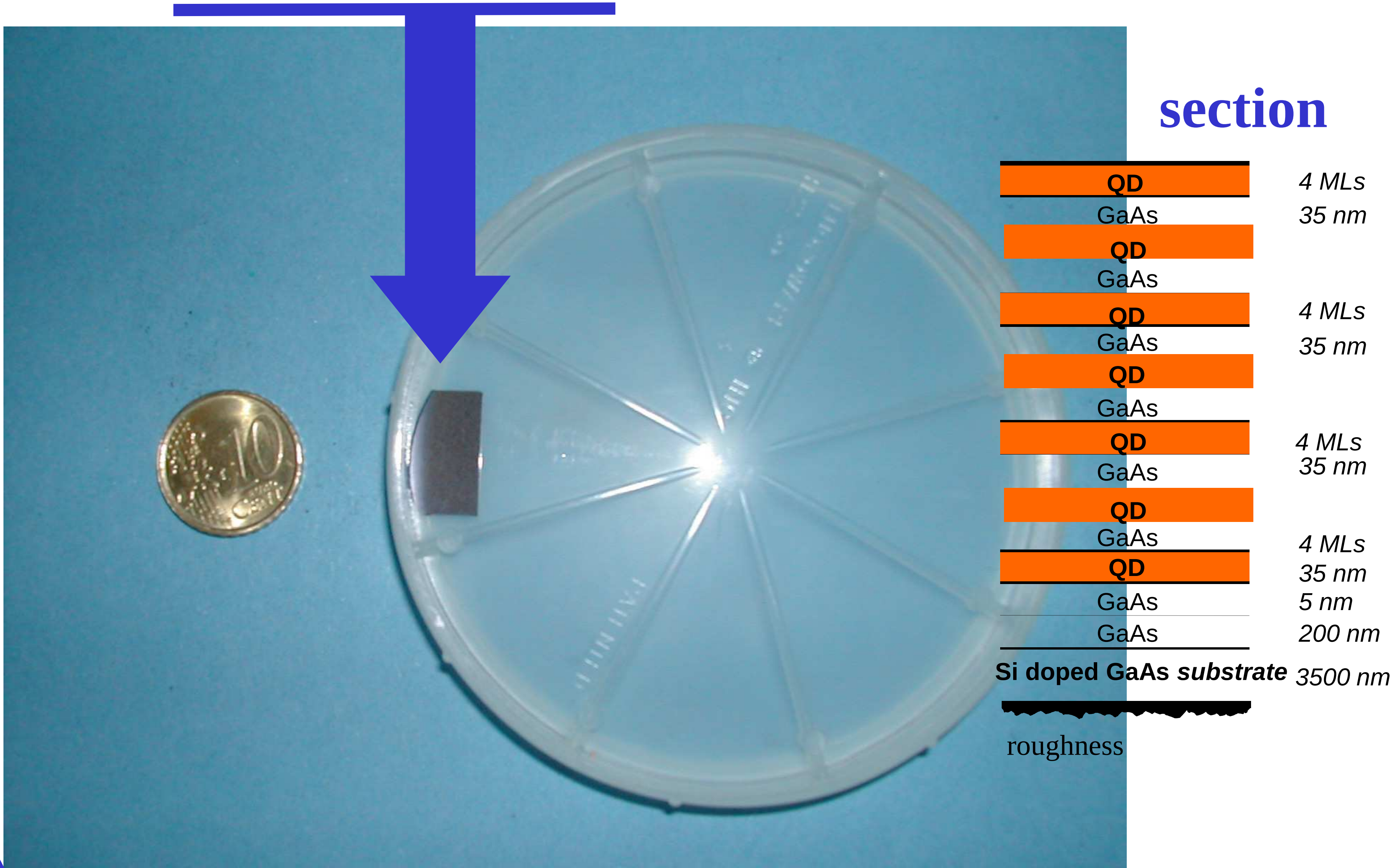

Courtesy of A.Passaseo

Photothermal Deflection Spectroscopy

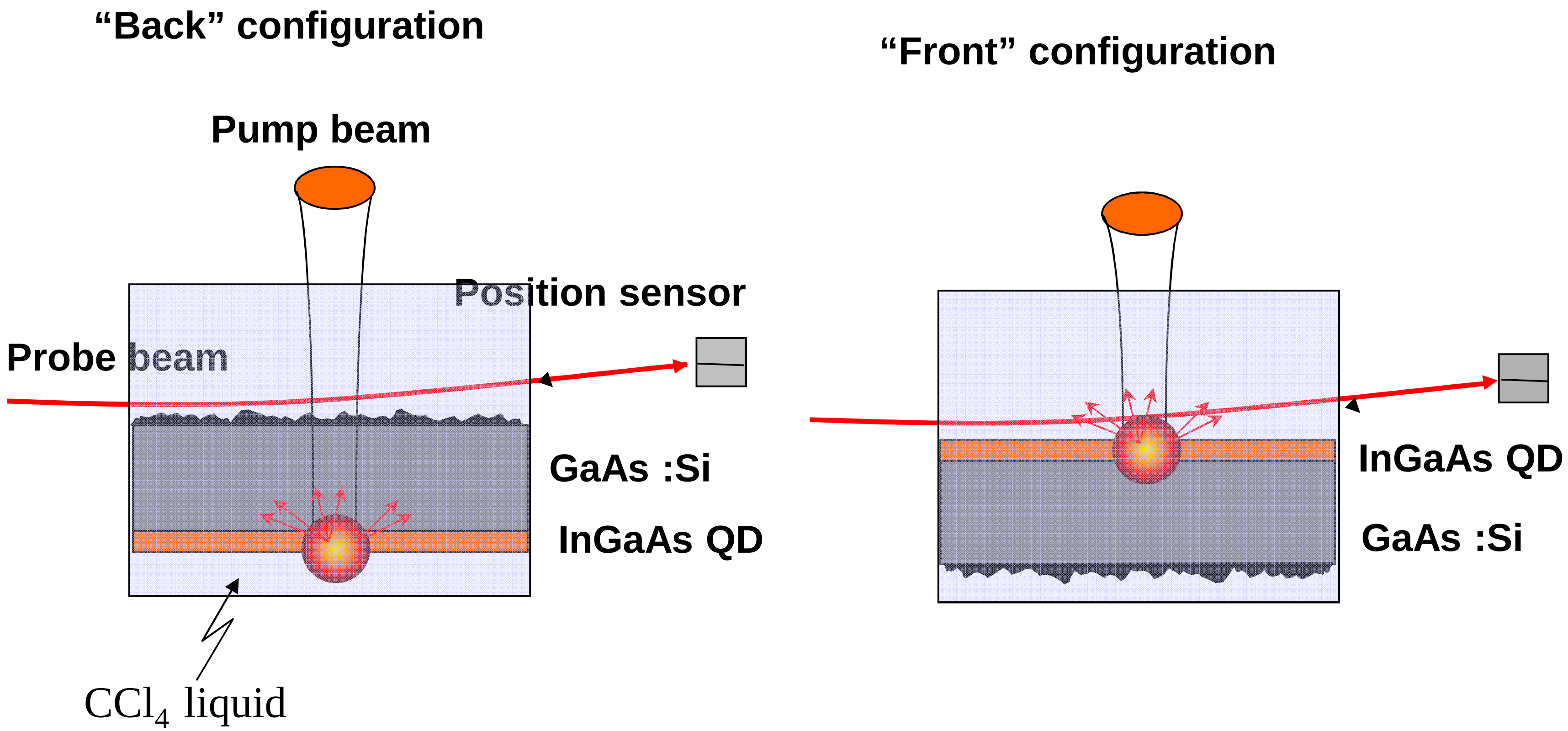

Experimental Results on Quantum Dots

PTD, QD-InGaAs/GaA-SI

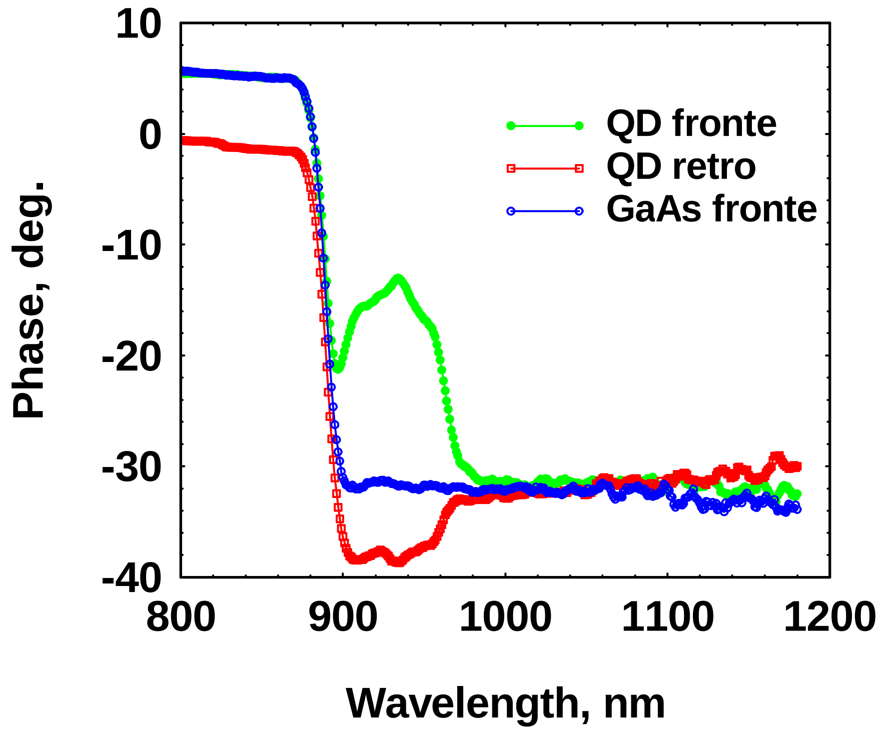

PDS, QD-InGaAs/GaA-SI

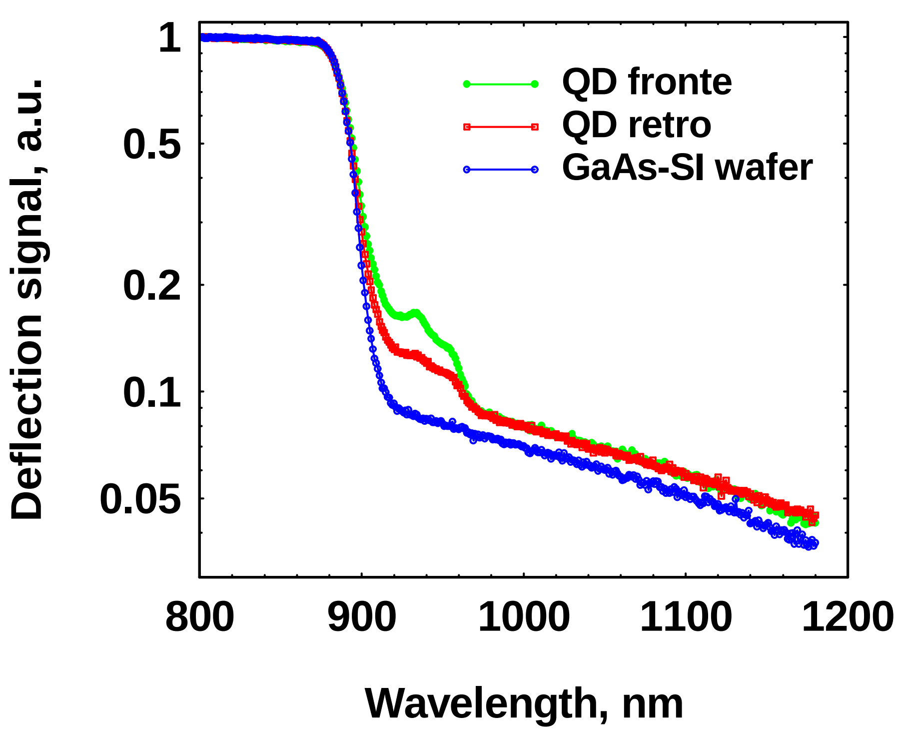

3D Photonic crystal: SiO_2 synthetic opal

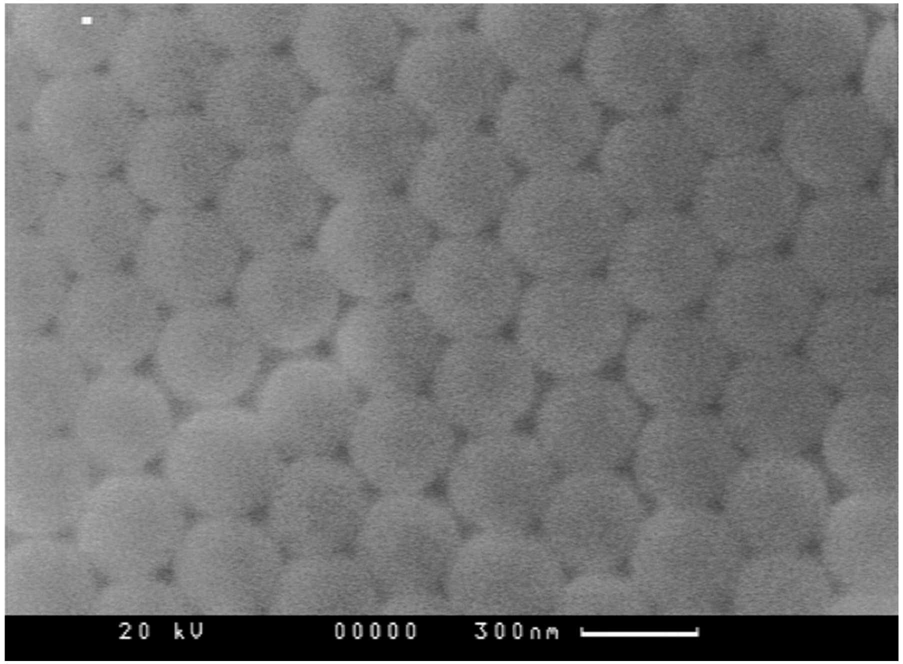

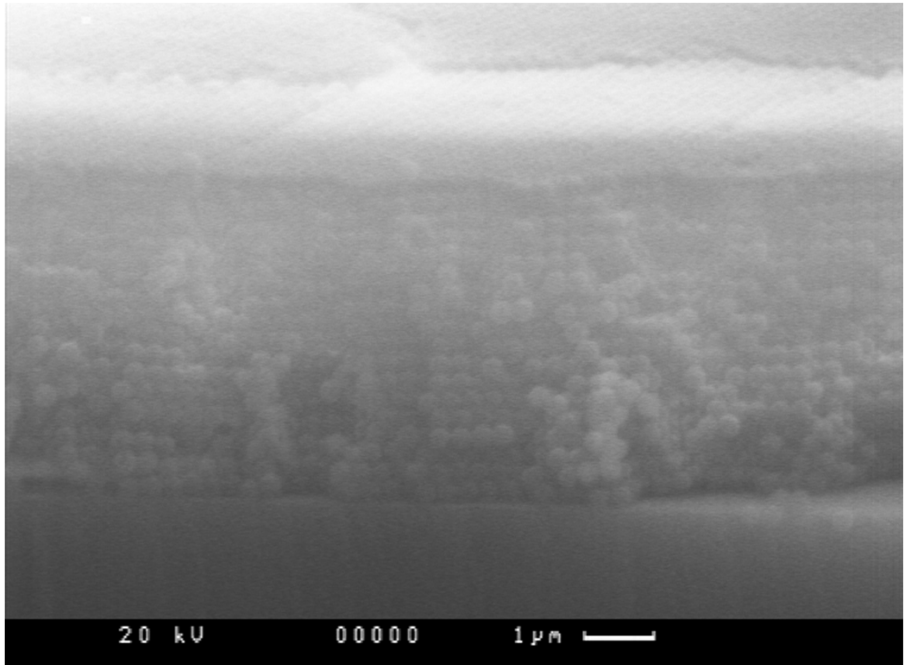

Characterization of VO_2/SiO_2 invese opals

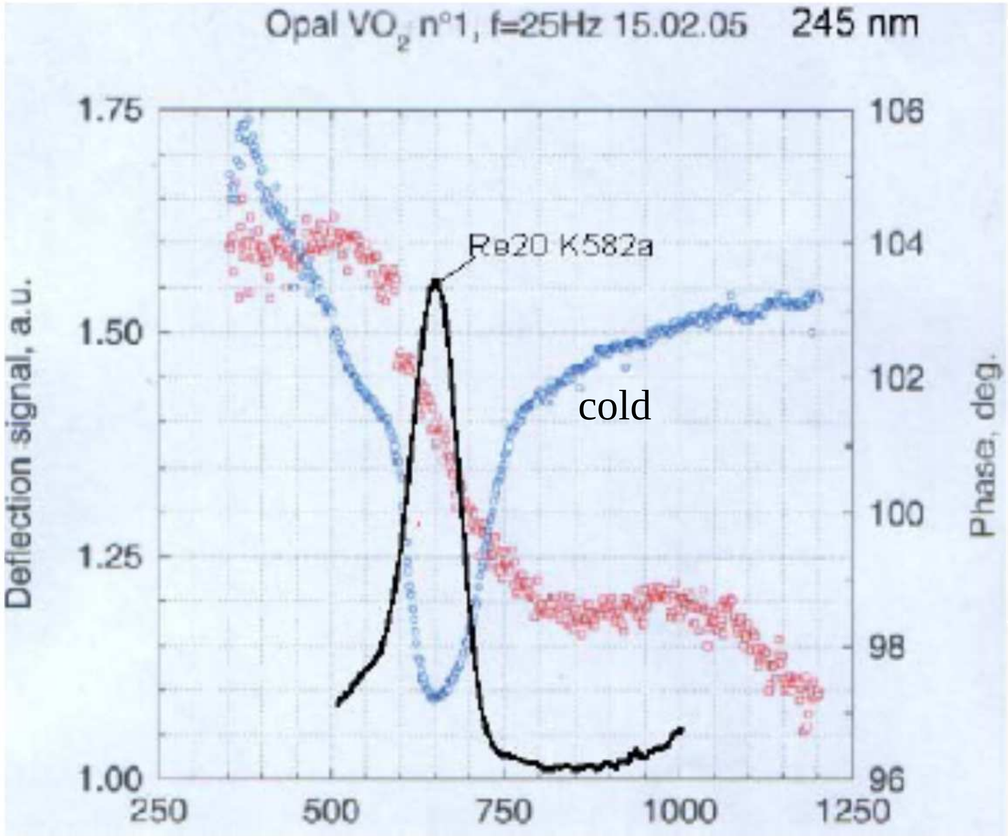

wavelength, nm

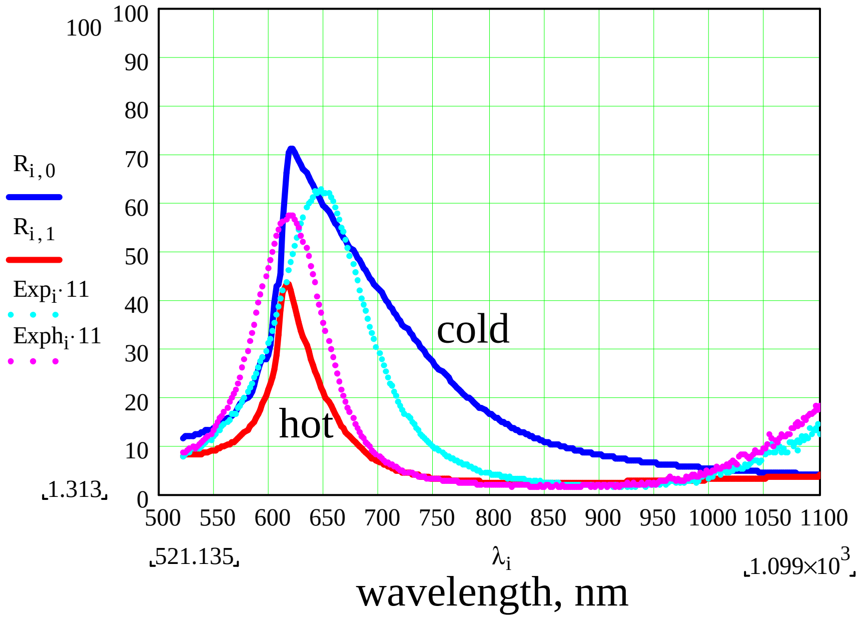

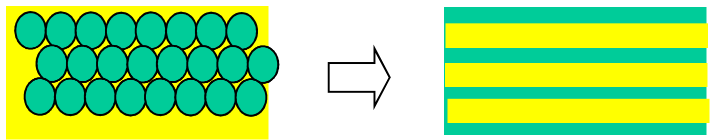

Main applications

- *Thermal diffusivity measurements*
- *Absorption spectroscopy*
- *Effusivity and optical absorption depth profiling*
- *Measurement of the attenuation in optical waveguides*
- *Evaluation of the thickness of thin layers*
- *Trace gas analysis*
- *Characterization of metallic surfaces*

THE HEAT DIFFUSION

$$\begin{cases} \vec{F} = - k \nabla T \\ \nabla \cdot \vec{F} + \rho c \dfrac{\partial T}{\partial t} = w \end{cases}$$

Heat flux

Energy conservation law

$$\nabla^2 T - \frac{1}{D}\frac{\partial T}{\partial t} = -\frac{w}{k}$$

Fourier diffusion equation

F	*heat flux*
T	*temperature rise*
w	*power density*
k	*thermal conductivity*
D	*thermal diffusivity*
ρ	*density*
c	*specific heat*

PULSED REGIME

Green function in pulsed regime

Temperature solution for unitary pulse placed in the origin at t=0

$$G_1(x,y,z,t) = \frac{1}{8\rho c[\pi D t]^{3/2}} e^{-(x^2+y^2+z^2)/4Dt}$$

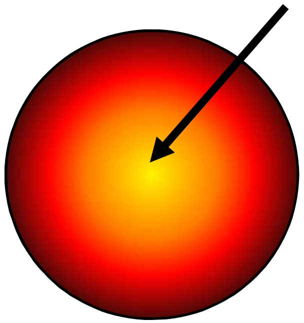

Thermal waves

$$\frac{\partial^2 T}{\partial x^2} - \frac{1}{D}\frac{\partial T}{\partial t} = -\frac{w e^{j\omega t}}{k}$$

$$\frac{d^2 \tilde{T}}{dx^2} - \beta^2 \tilde{T} = -\frac{\tilde{w}}{k}$$

"thermal wave"

$$\tilde{T}(x,\omega) = A e^{-\beta x} = A e^{-(1+j)x/\ell}$$

$$T(x,t) = A e^{-x/\ell} \cos(\omega t - x/\ell - \pi/4)$$

Thermal diffusion length

$$\ell = \sqrt{D/\pi f}$$

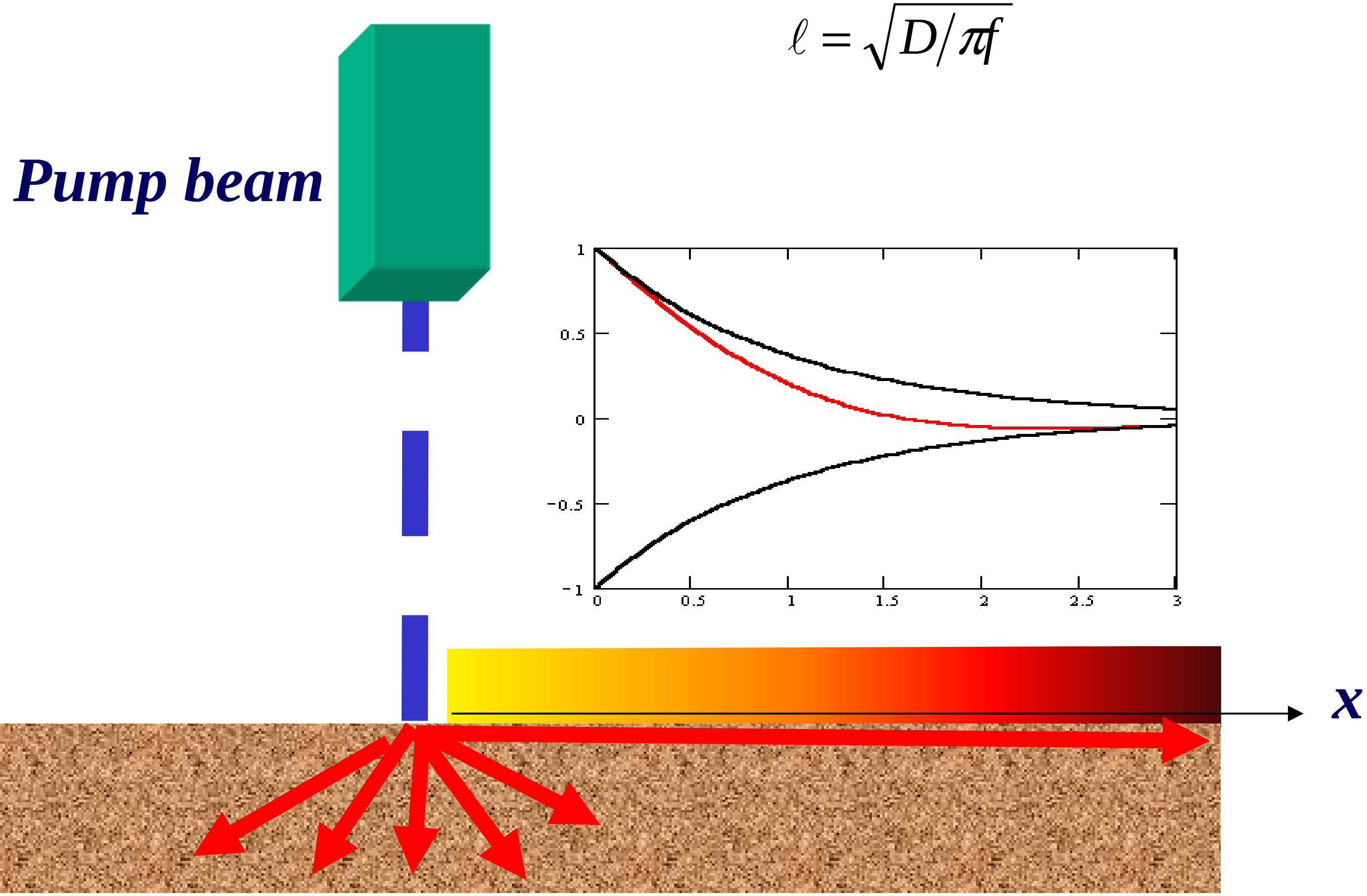

THEORY OF THERMAL WAVES

Plane "thermal wave"

$$\tilde{T}(z,\omega) = Ae^{-\vec{\beta}\cdot\vec{r}} = Ae^{-\beta z} = Ae^{-(1+j)z/\ell}$$

$$T(z,t) = \mathrm{Re}\left[\tilde{T}(z,\omega)e^{j\omega t}\right] = Ae^{-z/\ell}\cos(\omega t - z/\ell + \varphi)$$

Thermal diffusion length

$$\ell = \sqrt{D/\pi f}$$

Heating period Cooling period

Plane source

Complex quantity method

Amplitude of temperature $Ae^{-z/\ell}$

Phase of the temperature $-z/\ell$

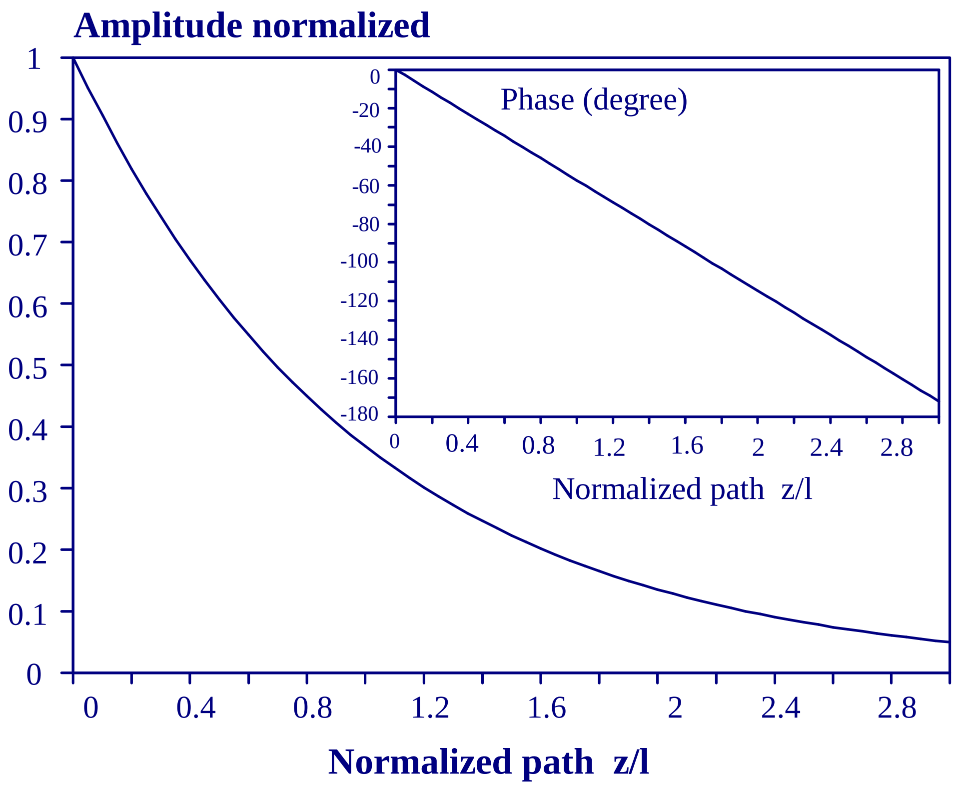

PLANE THERMAL WAVE

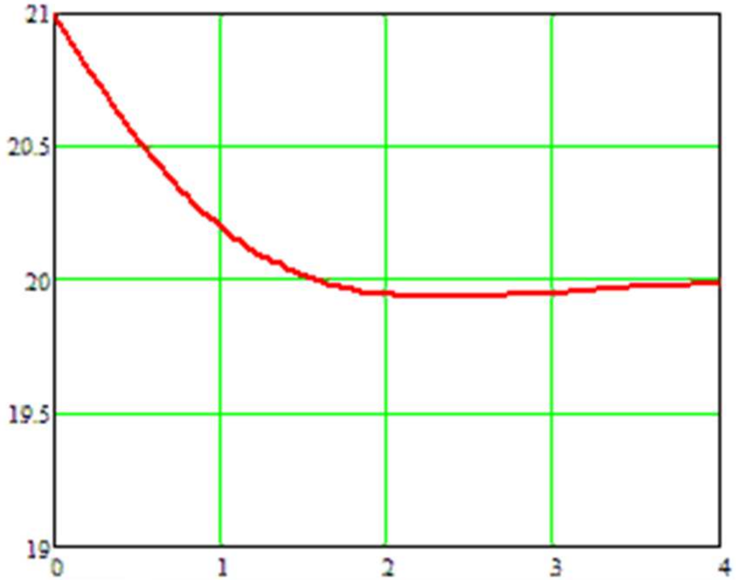

THE HEAT DIFFUSION

PLANE THERMAL WAVE

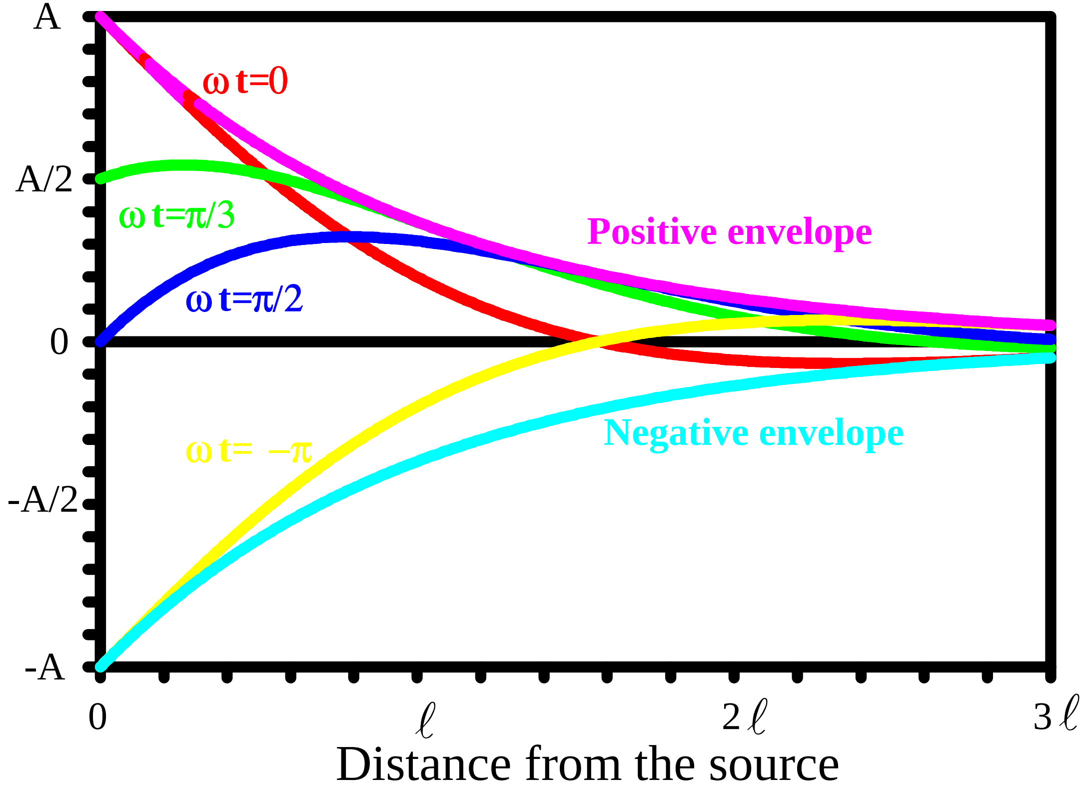

THE HEAT DIFFUSION

THERMAL WAVE GENERATION

1D - PLANE THERMAL WAVE

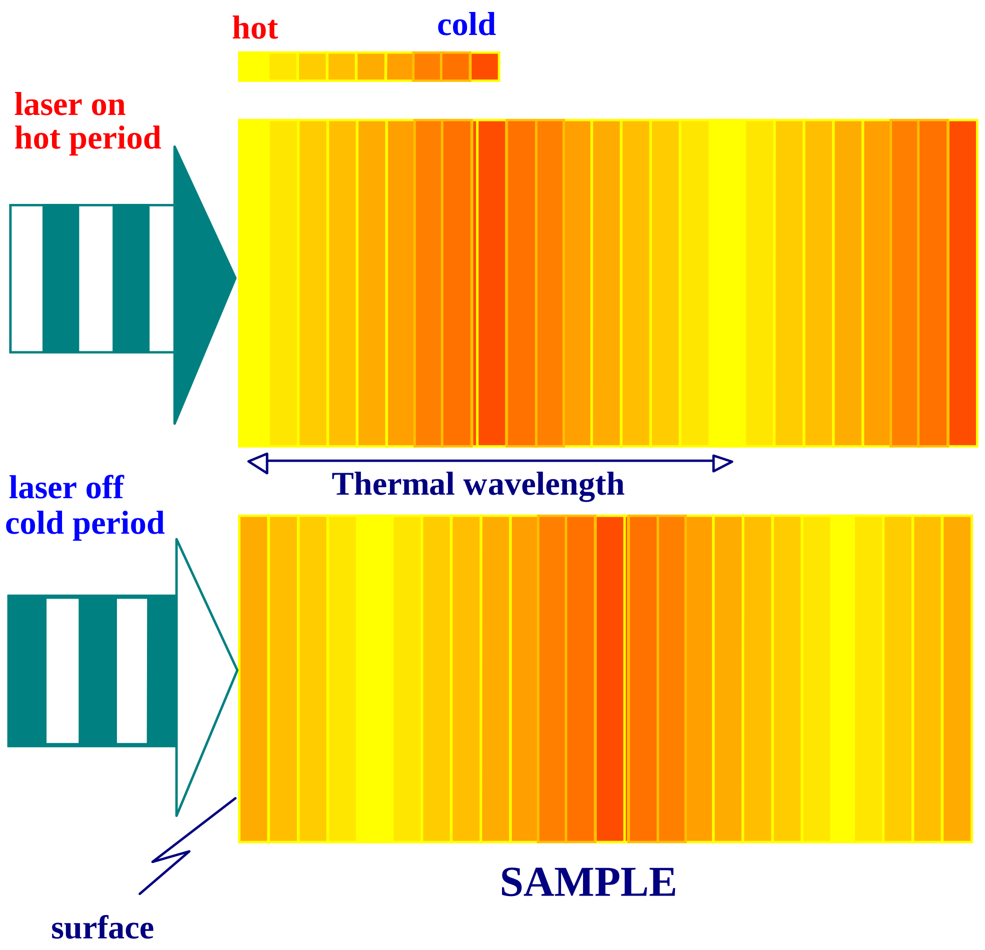

SPHERICAL THERMAL WAVE

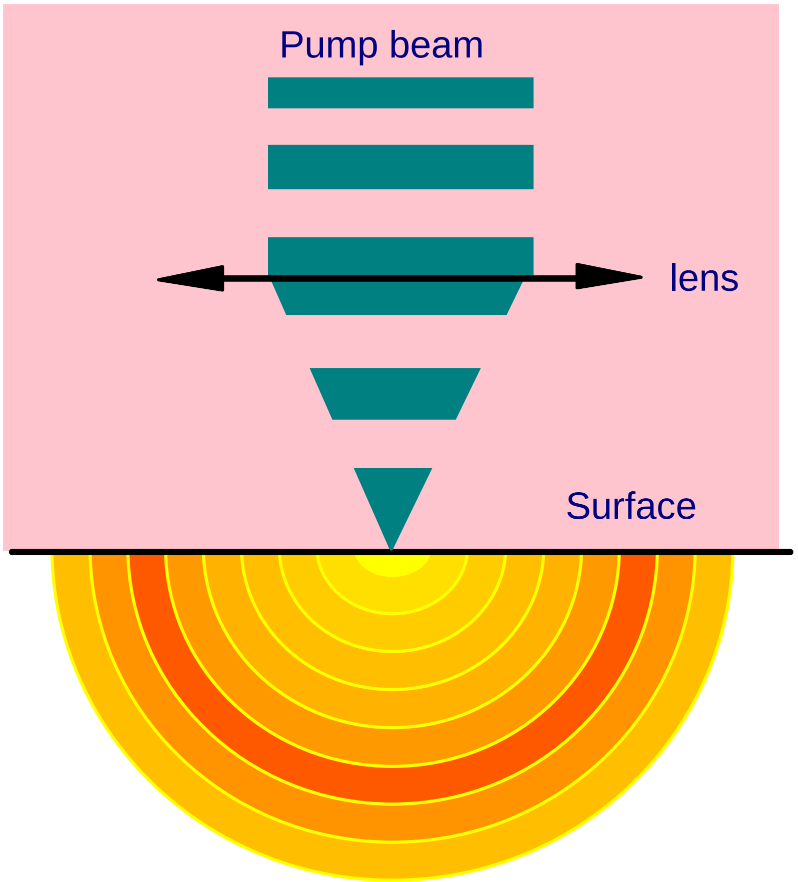

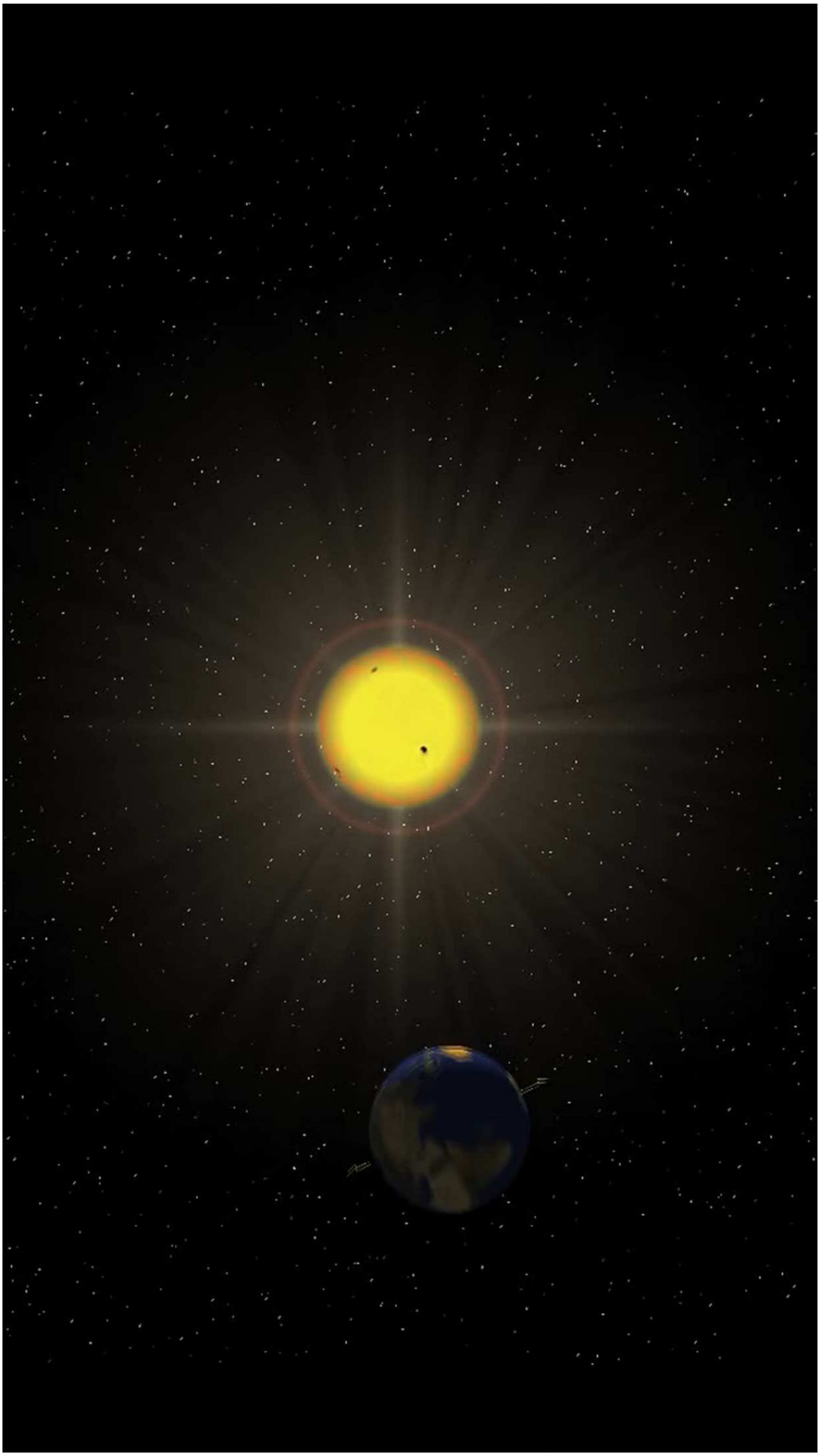

PLANE THERMAL WAVE GENERATION

on the soil due to the seasonal light oscillations

z=depth

Heat diffusion equation in harmonic regime

$$\frac{d^2\tilde{T}}{dz^2} - \underbrace{\left(\frac{j\omega}{D}\right)}_{\beta^2}\tilde{T} = 0$$

Plane "thermal wave"

$$\tilde{T}(z,\omega) = A\cdot e^{-\beta z} = A\cdot e^{-\sqrt{\frac{j\omega}{D}}\cdot z} = A\cdot e^{-(1+j)\frac{z}{\ell}}$$

Thermal diffusion length

$$\ell = \sqrt{D/\pi f}$$

Boundary condition on heat flux at the surface

$$-k\frac{d\tilde{T}}{dz}\bigg|_{z=0} + h\tilde{T} = I \longrightarrow (k\cdot\beta + h)\cdot A = I \longrightarrow A = \frac{I}{k\beta + h}$$

$$\tilde{T}(z,\omega) = \frac{I}{k\beta + h}\cdot e^{-\beta z} = \frac{I}{k\sqrt{\frac{j\omega}{D}} + \cancel{h}}\cdot e^{-\sqrt{\frac{j\omega}{D}}\cdot z}$$

$$T(z,t) = \mathrm{Re}\left[\tilde{T}(z,\omega)e^{j\omega t}\right] = \frac{I}{e_g\sqrt{\omega}}e^{-z/\ell}\cos\left(\omega t - \frac{z}{\ell} - \frac{\pi}{4}\right)$$

ROMA CIAMPINO (1961-1990)	Mesi												Stagioni				Anno
	Gen	Feb	Mar	Apr	Mag	Giu	Lug	Ago	Set	Ott	Nov	Dic	Inv	Pri	Est	Aut	
T. max. media (°C)	11,8	13,0	15,2	18,1	22,9	27,0	30,4	30,3	26,8	21,8	16,3	12,6	**12,5**	**18,7**	**29,2**	**21,6**	**20,5**
T. min. media (°C)	2,7	3,5	5,0	7,5	11,1	14,7	17,4	17,5	14,8	10,8	6,8	3,9	**3,4**	**7,9**	**16,5**	**10,8**	**9,6**
T. max. assoluta (°C)	20,8 (1965)	21,2 (1978)	26,6 (1981)	27,2 (1977)	33,0 (1977)	37,8 (1982)	39,4 (1983)	40,6 (1981)	38,4 (1982)	30,4 (1966)	25,0 (1971)	20,3 (1963)	**21,2**	**33,0**	**40,6**	**38,4**	**40,6**
T. min. assoluta (°C)	-11,0 (1985)	-6,0 (1965)	-6,5 (1963)	-0,2 (1966)	1,8 (1962)	5,6 (1962)	9,1 (1966)	9,3 (1963)	4,3 (1964)	0,8 (1981)	-5,2 (1973)	-5,6 (1964)	**-11,0**	**-6,5**	**5,6**	**-5,2**	**-11,0**
Giorni di calura ($T_{max} \geq$ 30 °C)	0	0	0	0	0,6	5,9	18,1	17,0	3,9	0,1	0,0	0,0	**0,0**	**0,6**	**41,0**	**4,0**	**45,6**
Giorni di pioggia	9	9	9	9	6	4	2	3	6	8	11	10	**28**	**24**	**9**	**25**	**86**
Umidità relativa media (%)	77	75	72	73	71	68	67	66	69	74	78	78	**76,7**	**72**	**67**	**73,7**	**72,3**
Eliofania assoluta (ore al giorno)	3,9	4,7	5,4	6,7	8,5	9,5	10,7	9,6	7,9	6,3	4,3	3,6	**4,1**	**6,9**	**9,9**	**6,2**	**6,8**
Radiazione solare globale media (centesimi di MJ/m²)	652	941	1 396	1 916	2 401	2 623	2 653	2 298	1 769	1 201	722	557	**2 150**	**5 713**	**7 574**	**3 692**	**19 129**
Pressione a 0 metri s.l.m. (hPa)	1 017	1 016	1 013	1 015	1 015	1 016	1 015	1 015	1 017	1 017	1 015	1 014	**1 015,7**	**1 014,3**	**1 015,3**	**1 016,3**	**1 015,4**
Vento (direzione-m/s)	NE 4,2	S 4,4	S 4,4	S 4,3	S 4,0	SW 4,0	SW 4,1	SW 4,0	S 3,9	S 3,9	S 4,3	NE 4,3	**4,3**	**4,2**	**4,0**	**4,0**	**4,1**

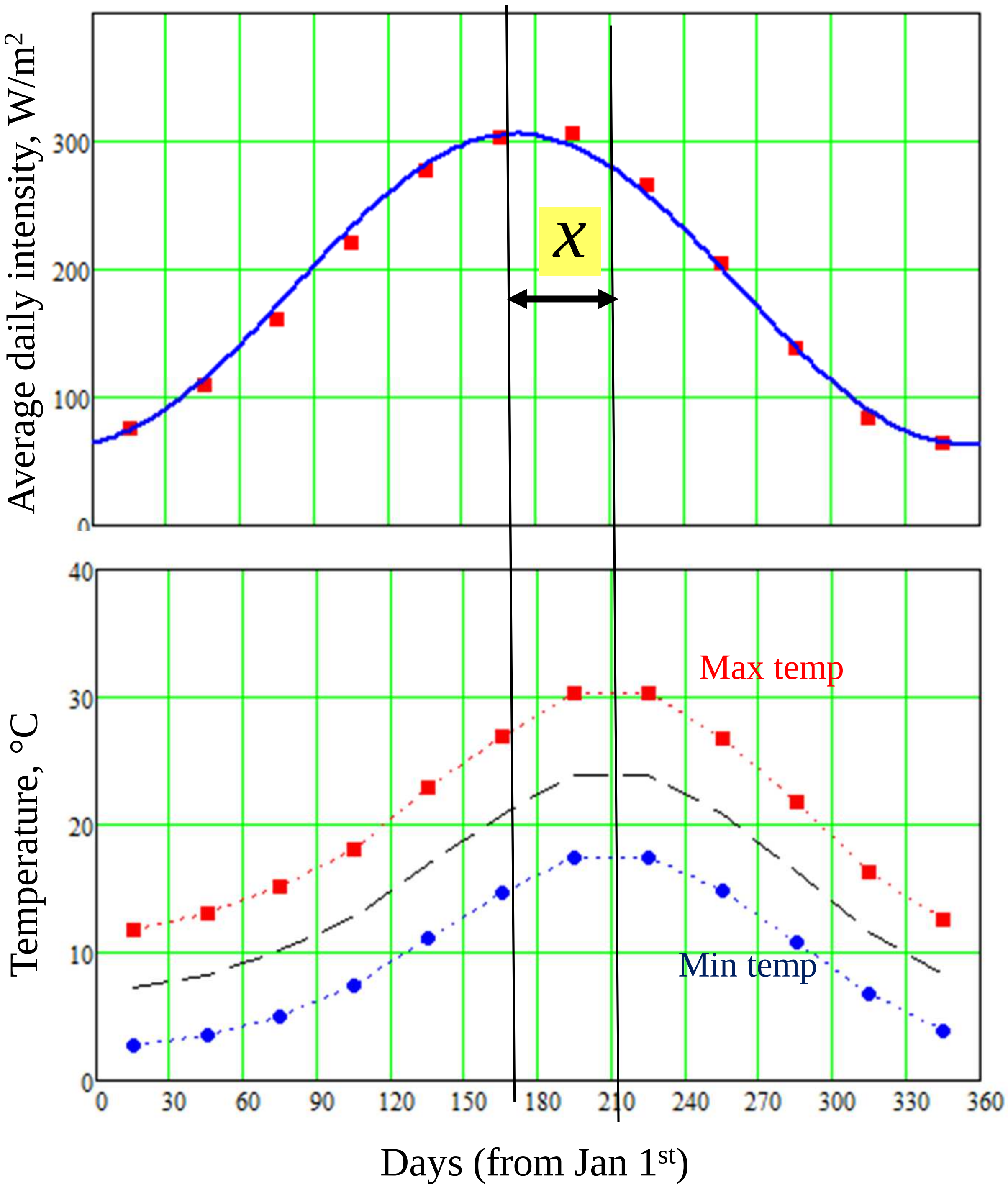

$$\frac{\pi}{4} : 2\pi = x : 365d$$

$$x = 45 \quad day$$

Measured temperature oscillations during the year in depth

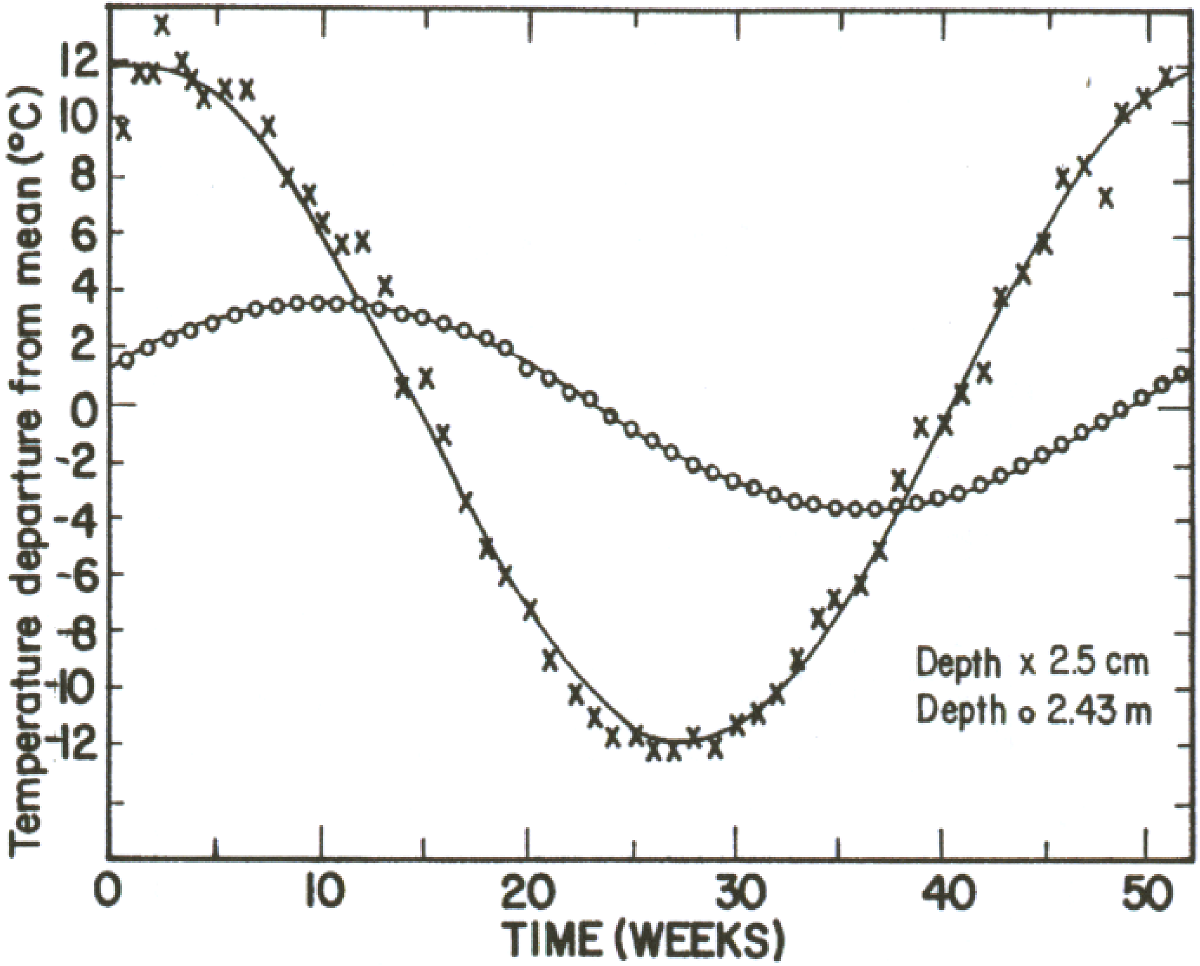

$$T(z,t)=\frac{A\cdot I}{e\sqrt{\omega}}e^{-z/\ell}\cos\left(\omega t-\frac{z}{\ell}-\frac{\pi}{4}\right)\qquad \omega=\frac{2\pi}{T_{year}}=\frac{2\pi}{365*86400}\frac{rad}{s}$$

Collinear configuration

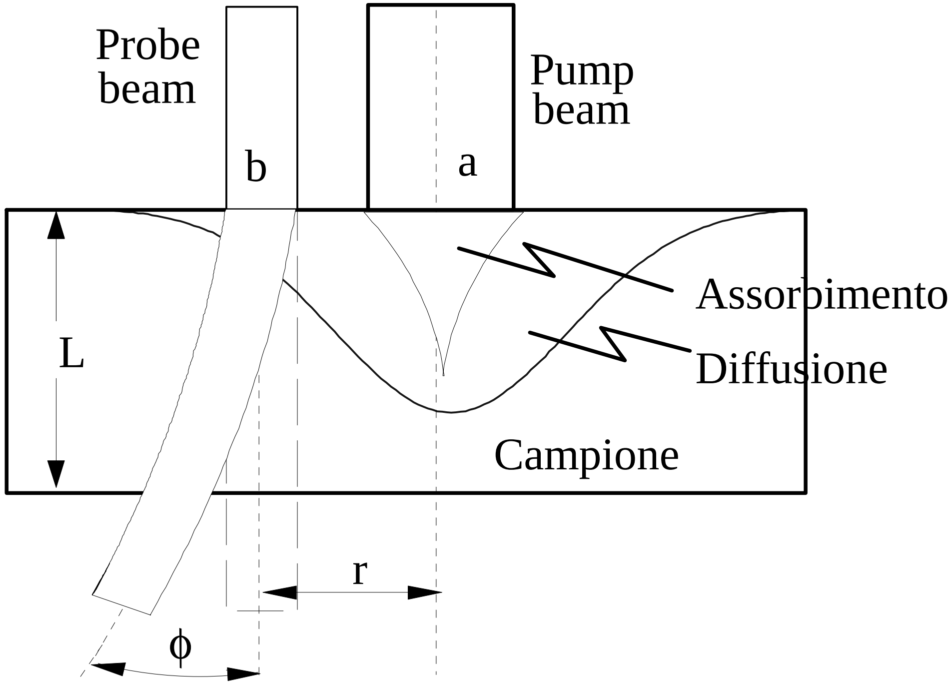

$$\Phi = -\left(\frac{dn}{dT}\right)\frac{P\left(1-e^{-\alpha L}\right)}{2\pi k\ell}\int_0^\infty \frac{\delta^2 J_1\left(\delta\frac{r}{\ell}\right)e^{-\frac{1}{8}\left(\delta\sqrt{a^2+b^2}/\ell\right)^2}}{\delta^2+2j}d\delta = -\left(\frac{dn}{dT}\right)\frac{P\left(1-e^{-\alpha L}\right)(1+j)}{2\pi k\ell}K_1\left[(1+j)r/\ell\right]$$

Phase method

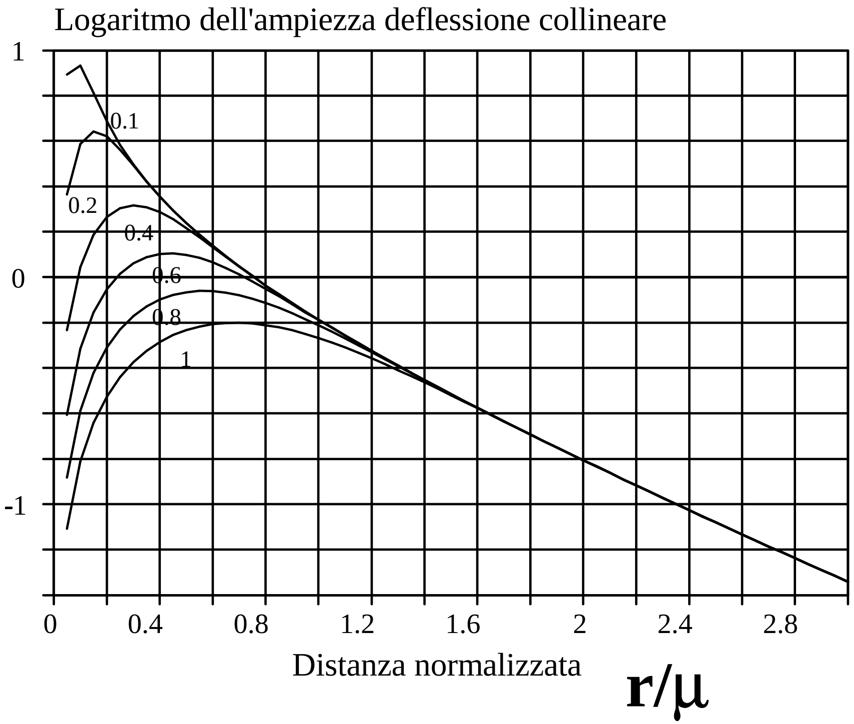

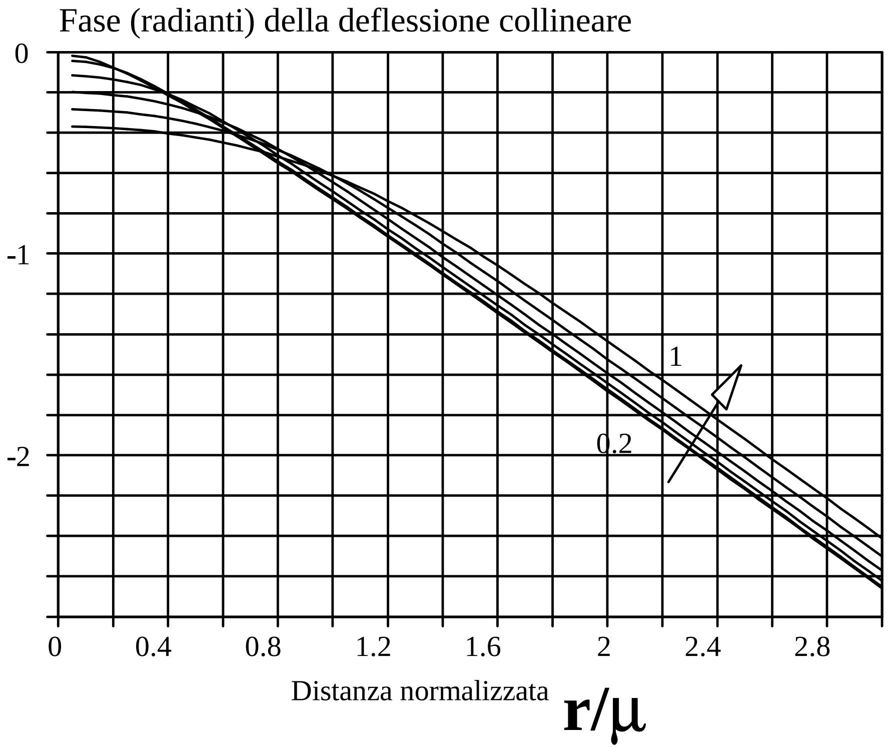

$$\varphi(y) = \varphi_o - r/\mu \qquad \mu = \left|\frac{\Delta r}{\Delta \phi}\right|$$

Transverse configuration

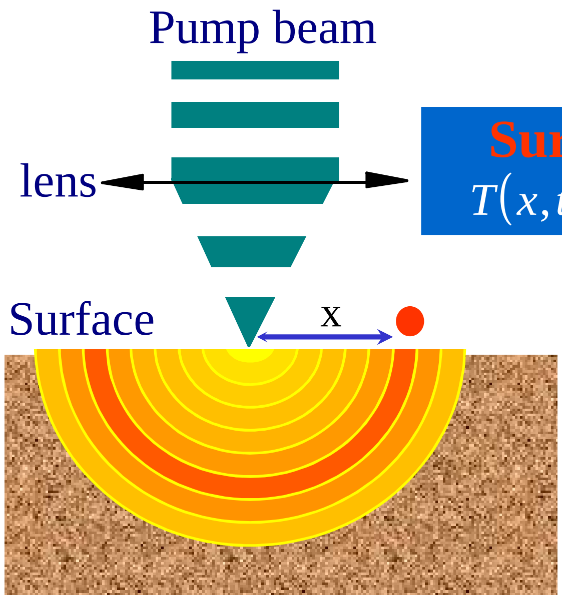

Surface thermal wave

$$T(x,t) = Ae^{-x/\ell}\cos(\omega t - x/\ell)$$

Thermal diffusion length

$$\ell = \sqrt{D/\pi f}$$

Amplitude

Phase ϕ

Thermal Diffusivity

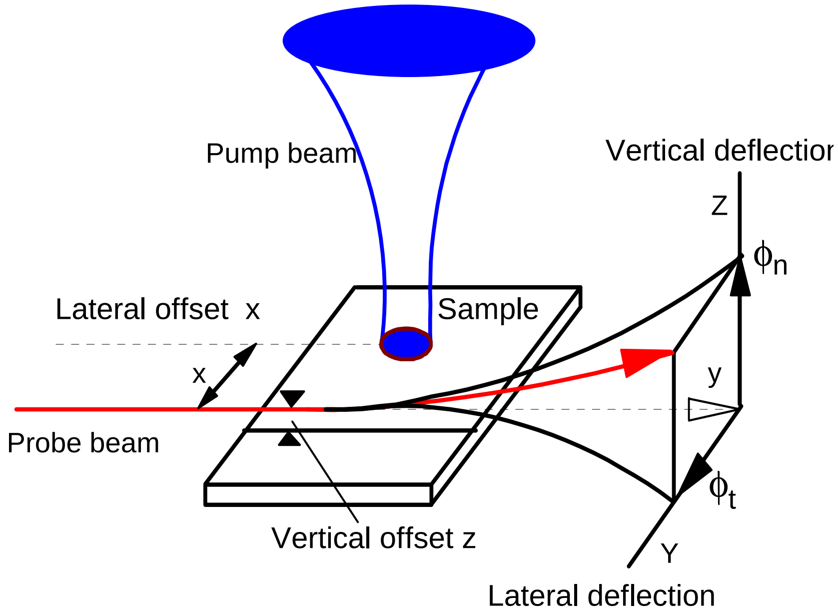

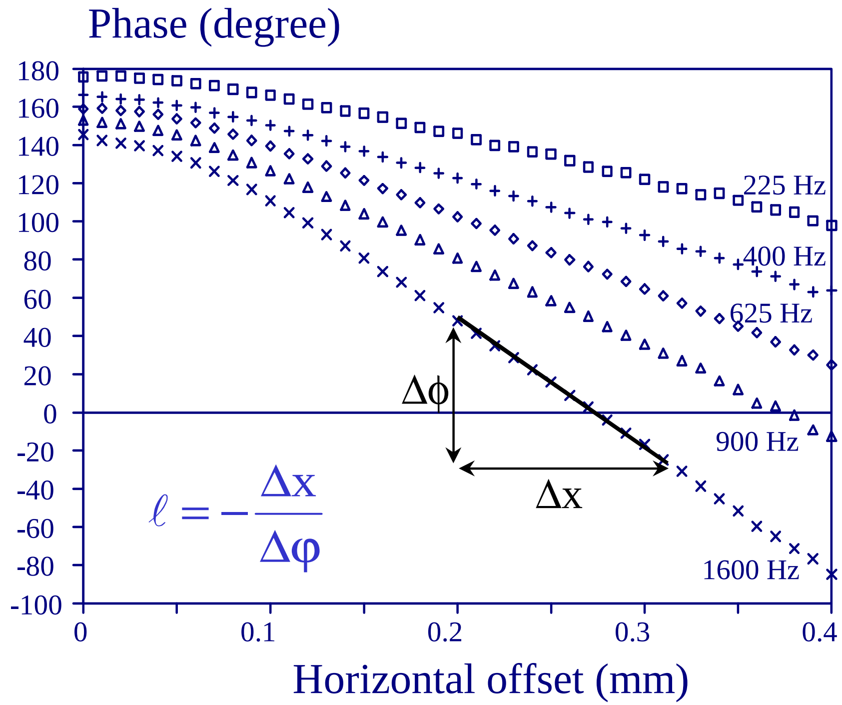

Transverse configuration

Schema Skimming

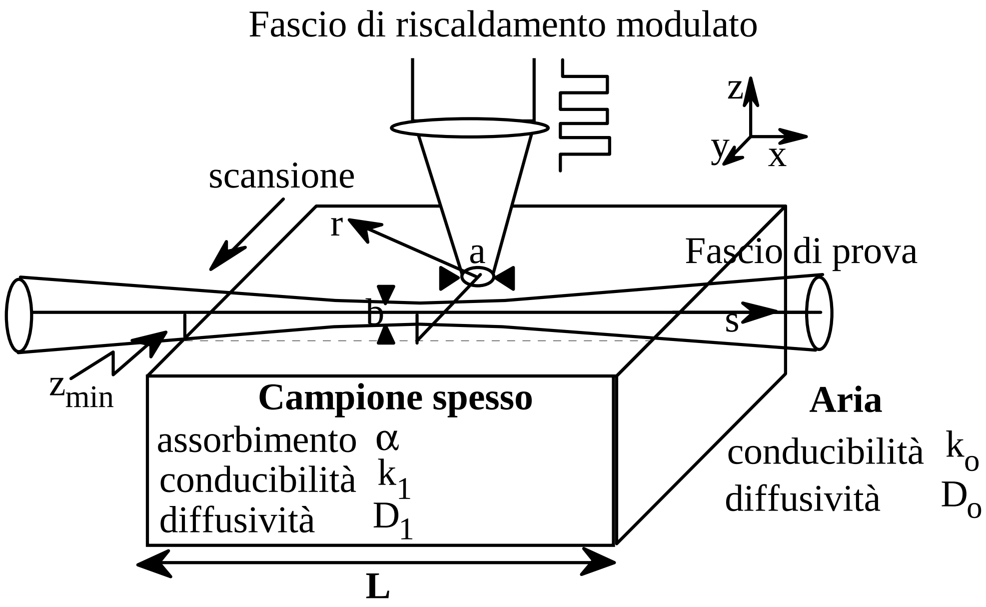

$$\Phi_z = \frac{1}{\pi}\left(\frac{dn}{dT}\right)_o \frac{\alpha P}{k_1} e^{\frac{j\omega b^2}{8D_o}} \int_0^{\infty} \frac{\sqrt{\delta^2 + 2j\, D_1/D_o}\; e^{-\left(\delta \frac{a}{\ell}\right)^2 \Big/ 8 - \frac{z}{\ell}\sqrt{\delta^2 + 2j\, D_1/D_o}} \cos\left(\delta \frac{y}{\ell}\right)}{\left(\sqrt{\delta^2 + 2j} + \alpha\ell\right)\left(\sqrt{\delta^2 + 2j} + k_o/k_1 \sqrt{\delta^2 + 2j\, D_1/D_o}\right)} d\delta$$

$$\Phi_y = \frac{-1}{\pi}\left(\frac{dn}{dT}\right)_o \frac{\alpha P}{k_1} e^{\frac{j\omega b^2}{8D_o}} \int_0^{\infty} \frac{\delta\, e^{-\left(\delta \frac{a}{\ell}\right)^2 \Big/ 8 - \frac{z}{\ell}\sqrt{\delta^2 + 2j\, D_1/D_o}} \sin\left(\delta \frac{y}{\ell}\right)}{\left(\sqrt{\delta^2 + 2j} + \alpha\ell\right)\left(\sqrt{\delta^2 + 2j} + k_o/k_1 \sqrt{\delta^2 + 2j\, D_1/D_o}\right)} d\delta$$

$$\Phi_y = \frac{-1}{\pi}\left(\frac{dn}{dT}\right)_o \frac{\alpha P}{k_1}\int_0^{\infty}\frac{\delta \sin\left(\delta \frac{y}{\ell}\right) d\delta}{\left(\sqrt{\delta^2+2j}+\alpha\ell\right)\left(\sqrt{\delta^2+2j}\right)}\begin{cases}\alpha\ell \to 0 & \left(\frac{dn}{dT}\right)_o \frac{-\alpha P}{k_1}\frac{e^{-(1+j)y/\ell}}{2} \\ \alpha\ell \to \infty & \left(\frac{dn}{dT}\right)_o \frac{-(1+j)P}{\pi k_1 \ell} K_1\left[(1+j)\frac{y}{\ell}\right]\end{cases}$$

$$\varphi(y) = \varphi_o - y/\mu \qquad \mu = \left|\frac{\Delta y}{\Delta \phi}\right|$$

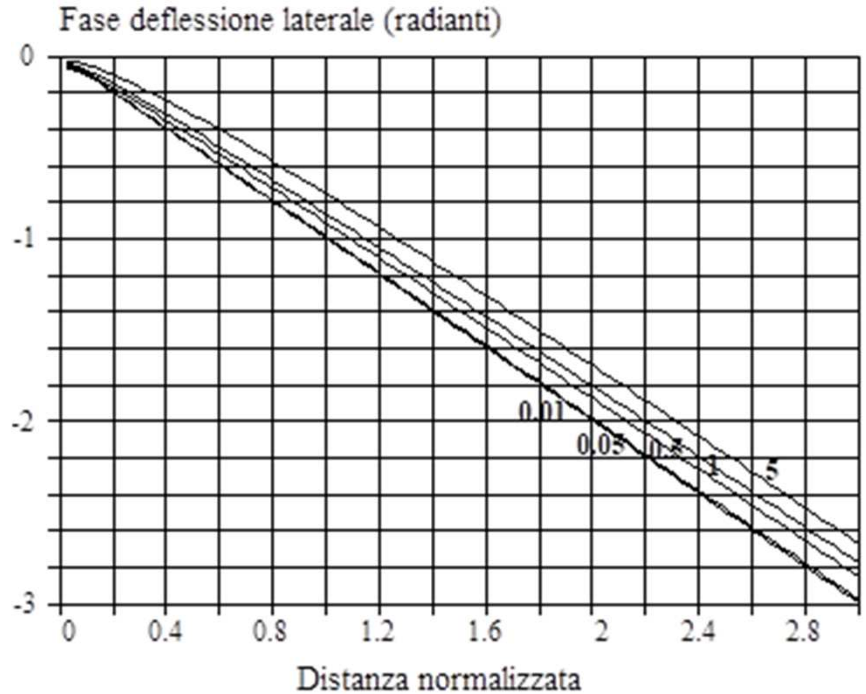

On the photodeflection method applied to low thermal diffusivity measurements

M. Bertolotti and R. Li Voti
Dipartimento di Energetica, Universita' di Roma "La Sapienza," Via Scarpa 16-00161, Roma and GNEQP of CNR, Italy

G. Liakhou
Polytechnique Institute of Kishinev, Kishinev, Moldavia

C. Sibilia
Dipartimento di Energetica, Universita' di Roma "La Sapienza," Via Scarpa 16-00161, Roma and GNEQP of CNR, Italy

(Received 18 August 1992; accepted for publication 24 February 1993)

The photodeflection method when applied to measure the low thermal diffusivity of some materials gives inconsistent results. In this article a way to extend the thermal diffusivity range of measurements using the phase of the photodeflection signal is presented. A comparison with computer simulations and experimental results shows good agreement.

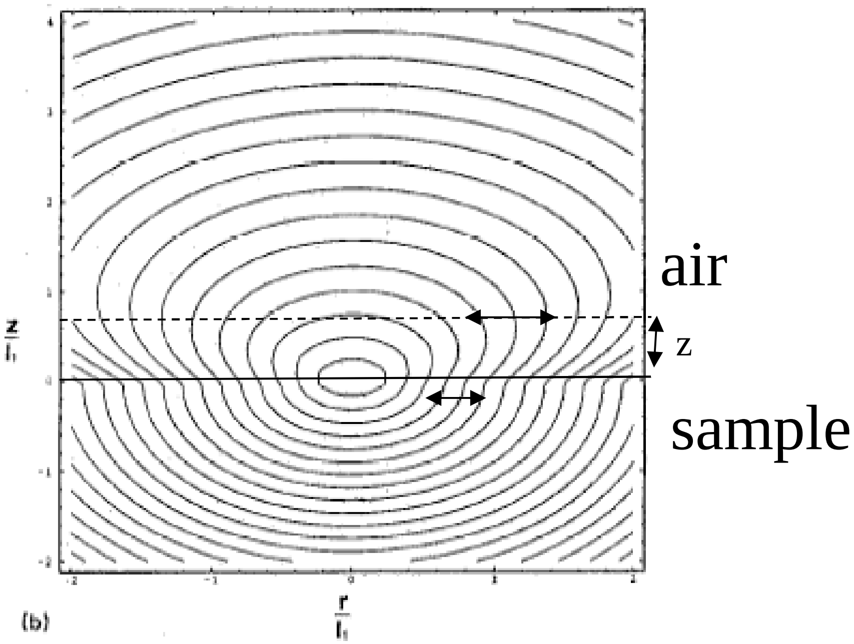

FIG. 4. Equimodulus (a) and equiphase (b) thermal surfaces for a diffusivity ratio $D_1/D_0=0.25$ and $a/l_1=0.2$, as a function of the r/l_1 (abscissa) and z/l_1 (ordinate), respectively. The phase shift between two contiguous surfaces is $\pi/10$.

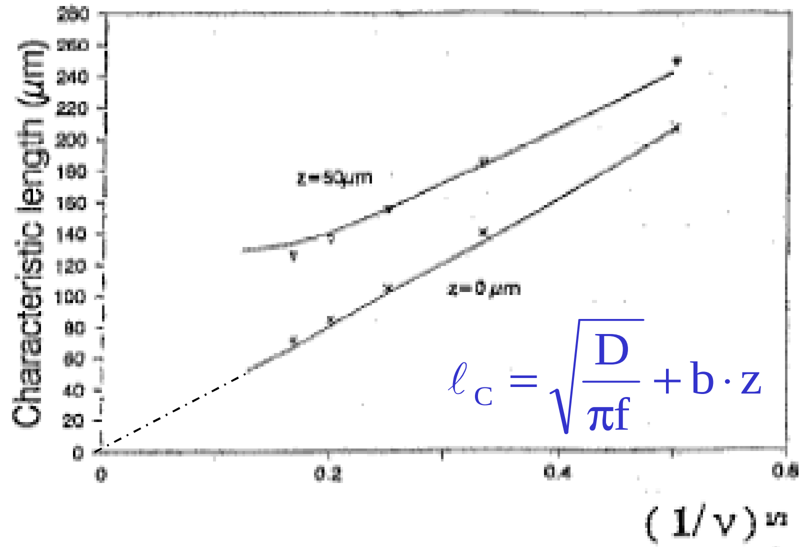

FIG. 16. Characteristic length as a function of $1/\sqrt{\nu}$. Comparison between experimental data and numerical analysis: (×) exp. $z=0$ μm, (Δ) exp. $z=50$ μm, (—) theory. Pump power = 15 mW, chopper frequency = 9 Hz, $D_1=0.005$ cm^2/s.

Analysis of the photothermal deflection technique in the surface reflection scheme: Theory and experiment

M. Bertolotti,[a] G. L. Liakhou,[b] R. Li Voti, S. Paoloni, and C. Sibilia
Dipartimento di Energetica, Università degli Studi di Roma ''La Sapienza'' Via A. Scarpa 16, 00161 Roma, Italy and GNEQP of CNR and INFM, Italy

(Received 18 June 1997; accepted for publication 3 October 1997)

The photothermal deflection technique has been usually applied, for the thermal diffusivity measurements, in the transverse skimming scheme. To overcome some limitations of the skimming, a surface reflection scheme (i.e., bouncing scheme) has been introduced in which the probe beam is reflected from the sample surface. In this configuration the probe beam deflection is obtained as a result of two different mechanisms: the thermal gradient in the gas near to the heated sample (mirage) and the sample surface deformation due to the thermal expansion (displacement). The superposition of these two effects must be taken into account when deriving the thermal diffusivity. In this article the mirage and the displacement have been studied from a theoretical and experimental point of view, and a new method for the measurement of thermal diffusivity in the bouncing scheme is presented. A special setup is described to obtain separately the mirage and the displacement signals from which the thermal diffusivity and the thermal expansion coefficient can be derived. The experimental values for different samples obtained by applying our method are in agreement with the literature values.
[S0021-8979(98)00102-9]

966 J. Appl. Phys. 83 (2), 15 January 1998

TABLE I. Thermal diffusivity end expansion for several materials.

Sample Type of material (1)	Thermal diffusivity (cm^2/s) Measured in skimming scheme (2)	Measured in bouncing scheme (3)	Expansion (K^{-1})[a] (4)
InP	0.44	0.44 ± 0.02	$4.6 \cdot 10^{-6}$
silicon	0.89	0.95 ± 0.07	$4.6 \cdot 10^{-6}$
As_2S_3	0.003	0.003 ± 0.0001	$2.5 \cdot 10^{-6}$
glass	0.0077 ± 10%	0.008 ± 10%	$5 \cdot 10^{-7}$

[a]See Ref. 27.

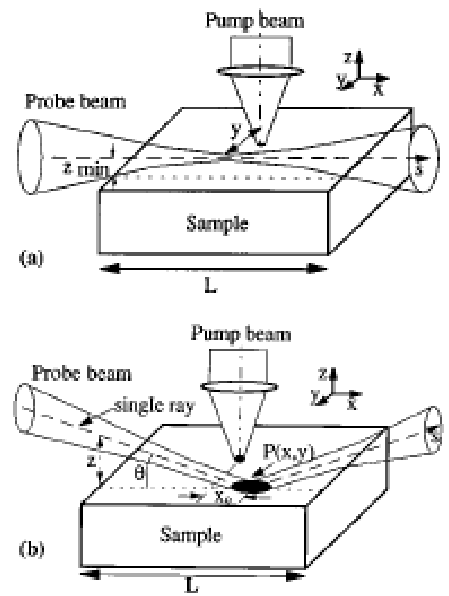

FIG. 1. Schematic representation of the photodeflection transverse configuration: (a) the skimming scheme, (b) the bouncing scheme.

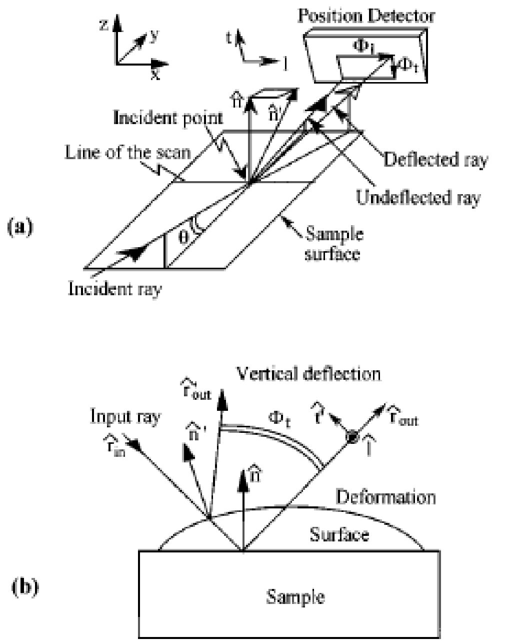

FIG. 8. Schematic representation of the probe beam deflection pro
the surface deformation: (a) 3D view, (b) lateral view.

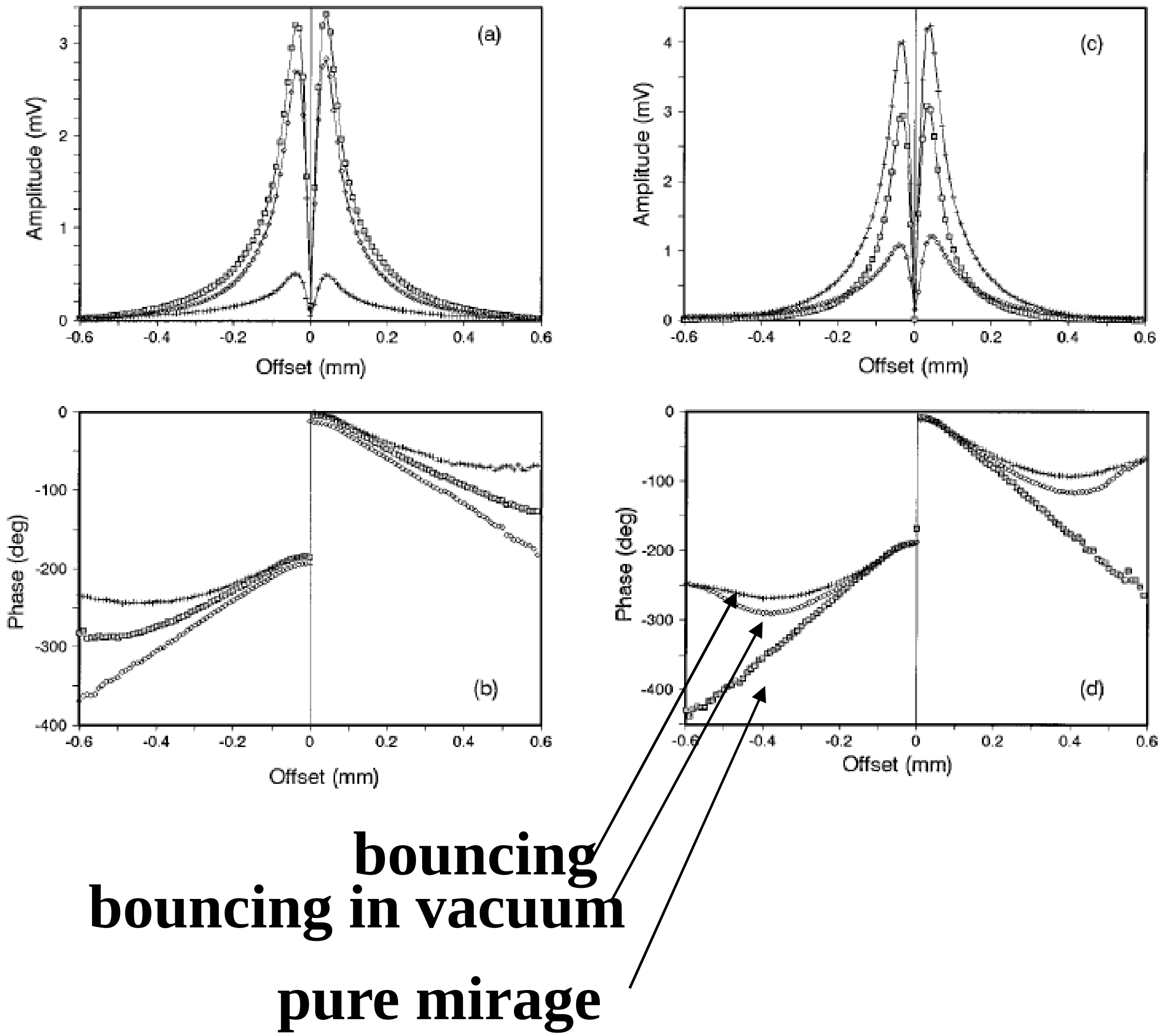

New photothermal deflection method for thermal diffusivity measurement of semiconductor wafers

M. Bertolotti,[a] V. Dorogan,[b] G. Liakhou,[b] R. Li Voti, S. Paoloni, and C. Sibilia
Dipartimento di Energetica, Università di Roma ''La Sapienza,'' GNEQP of CNR, INFM,
Via Scarpa 16, 00161 Roma, Italy

(Received 10 September 1996; accepted for publication 3 December 1996)

The photothermal deflection technique is applied in transverse configuration to measure the thermal diffusivity of semiconductor wafers. The large size of these samples inhibits the possibility to make the probe beam skim the sample at a small height which is required for a direct thermal diffusivity measurement. To overcome this problem, three new experimental schemes are proposed, each one based on a different geometry of the heat diffusion (one-, two-, or three-dimensional scheme). In particular for the 3D experimental scheme, a new mirage setup is described which uses two crystalline prisms 6 mm apart from each other to let the probe beam skim 50±3 μm high over the sample surface, with a spot size of 22 μm. The main advantages of this setup, here discussed, are the obtained low probe beam height which is, moreover, independent of the sample dimensions, and the cheap technology to produce the necessary high-quality prisms. The performances of the new schemes have been tested by comparing, for well-known semiconductor wafers (InSb, InAs, InP, GaAs, GaP, Ge, and Si), the experimentally measured thermal diffusivity with the values reported in the literature. [S0034-6748(97)03703-9]

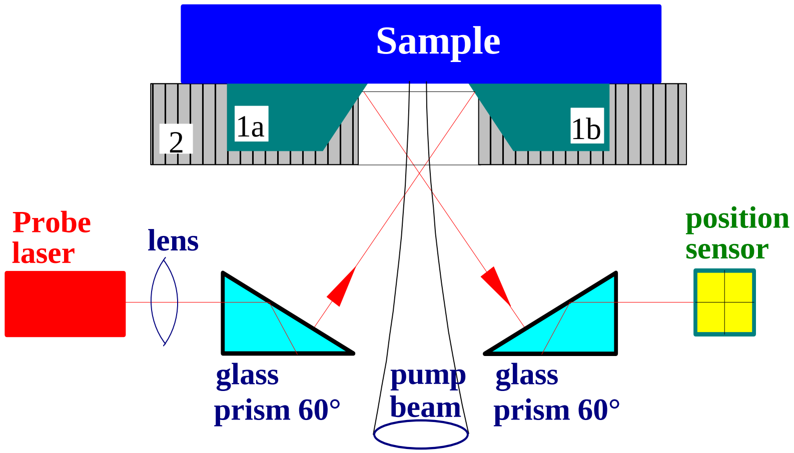

Sample	Type	L (μm)	D_{th} (cm^2/s) (Fig. 1)	D_{th} (cm^2/s) (Fig. 2)	D_{th} (cm^2/s) (Fig. 3)	Nominal value (cm^2/s)	Ref.
InSb	*n*	550	0.20	0.19	0.21	0.19	12
	n	350	0.20	0.19	0.19		
InAs	*n*	1300	0.21	0.20	0.21	0.19	2
	n	350	0.20	0.21	0.19	0.22	3
InP	*i*	330	0.40	0.45	0.44	0.46	2
	p	400	0.39	0.43	0.42	0.45	3
GaAs	*i*	360	0.25	0.26	0.25	0.25	3
	n	350	0.28	0.27	0.28	0.26	2
	p	350	0.23	0.24	0.24		
GaP	*i*	360	0.43	0.46	0.45	0.45	12
Ge	*n*	400	0.36	0.38	0.38	0.37	12
Si	*n*	470	0.76	0.85	0.80	0.88	12
	p	250	0.67	0.66	0.64		

A cryostatic setup for the low-temperature measurement of thermal diffusivity with the photothermal method

M. Bertolotti
Dipartimento di Energetica, Università di Roma "La Sapienza," Via Scarpa 16, 00161 Roma, Italy, GNEQP of CNR, Italy, and INFM, Italy

G. Liakhou
Technical University of Moldova, Stephan Cel Mare, 277012 Kishinev, Moldova

R. Li Voti, S. Paoloni, and C. Sibilia
Dipartimento di Energetica, Università di Roma "La Sapienza," Via Scarpa 16, 00161 Roma, Italy, GNEQP of CNR, Italy, and INFM, Italy

N. Sparvieri
ALENIA, Via Tiburtina Km 12.4, 00131 Roma, Italy

(Received 5 June 1995; accepted for publication 5 July 1995)

A cryostatic setup is described to perform photothermal deflection measurements from room temperature to 77 K. The setup uses gaseous nitrogen as a medium where the photodeflection is produced. The ability of the system to work is demonstrated presenting some measurements of thermal diffusivity of high-temperature superconductor samples and of yttrium-iron garnets with variable aluminum content. © *1995 American Institute of Physics.*

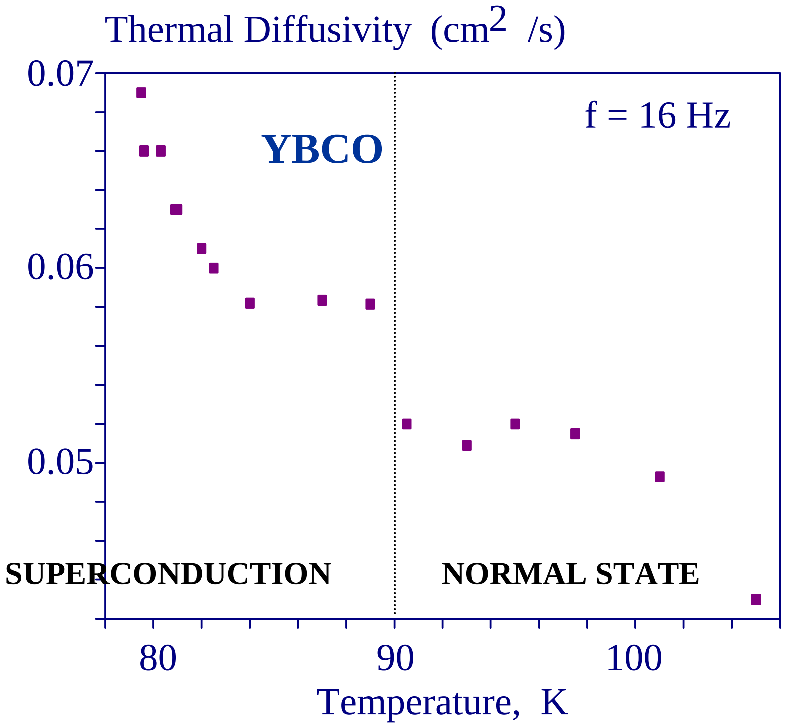

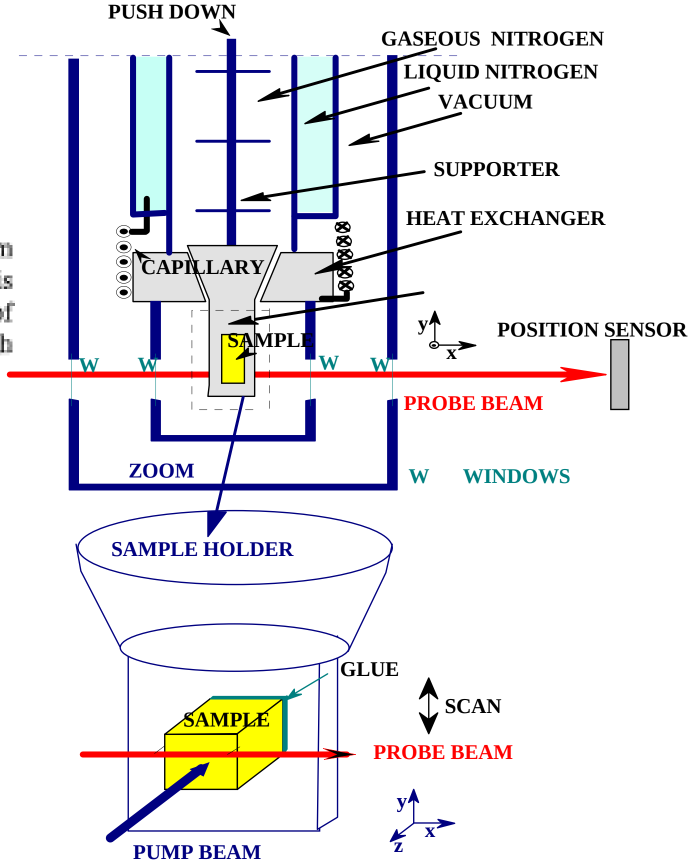

Collaboration

CSM, Alenia, IRTEC CNR, Univ. Trieste

New method for the study of mirror heating of a semiconductor laser diode and for the determination of thermal diffusivity of the entire structure

M. Bertolotti, G. L. Liakhou,[a] R. Li Voti, C. Sibilia, A. Syrbu,[a] and R. P. Wang[b]
Dipartimento di Energetica, Università Roma I, Via Scarpa 16-00161, Roma, Italy

(Received 20 July 1994; accepted for publication 24 July 1994)

A new method based on the photothermal deflection technique is described to determine the mirror temperature of a semiconductor laser diode as a function of intensity of drive current. The device's effective thermal diffusivity can also be measured. A short theoretical discussion is presented together with experimental measurements performed on three different kinds of laser diodes.

Es. LASER DIODE DOUBLE HETEROSTRUCTURE AlGaAs/GaAs, λ=800 nm

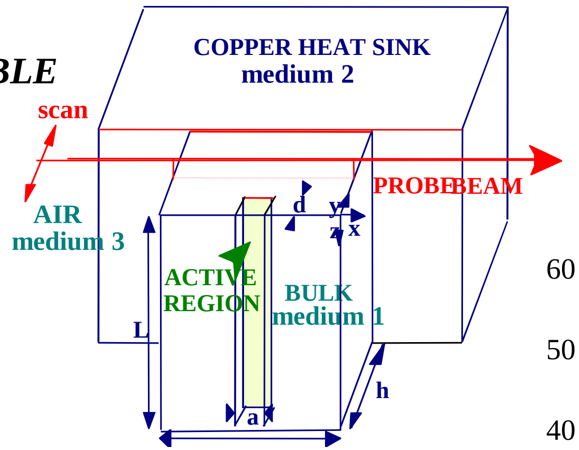

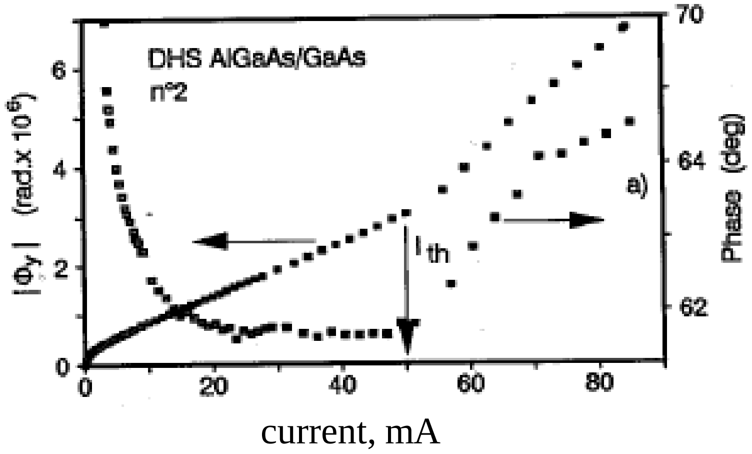

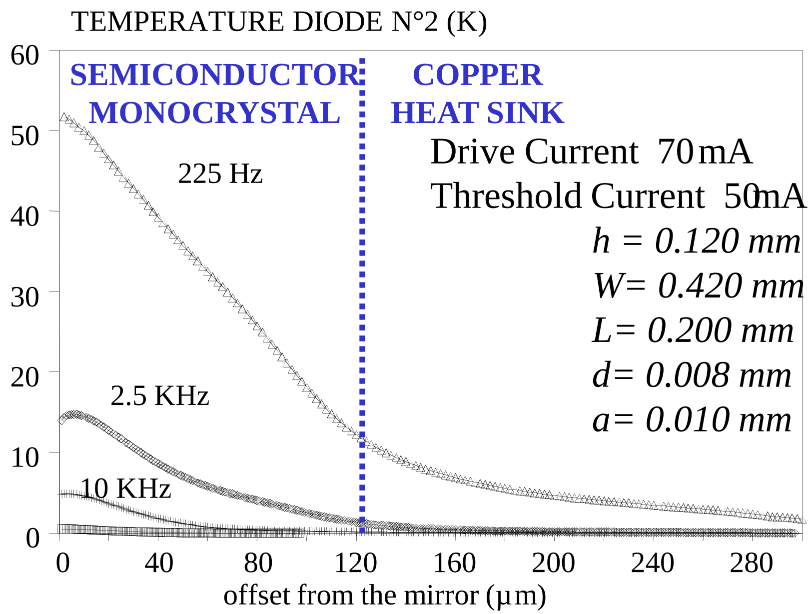

Characterization of SiO_2 /GaN opal sample

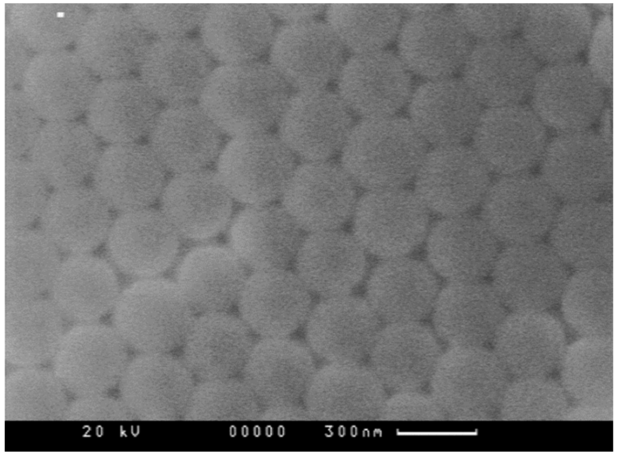

Sample	n.1	n.2	n.3	n.4
Composition	SiO_2 unfilled	SiO_2/GaN 25%	SiO_2/GaN 70%	SiO_2/GaN 70% inverted
Thermal diffusivity, cm^2/s	$1.4\ 10^{-3}$	$1.6\ 10^{-3}$	$3.2\ 10^{-3}$	$0.62\ 10^{-3}$

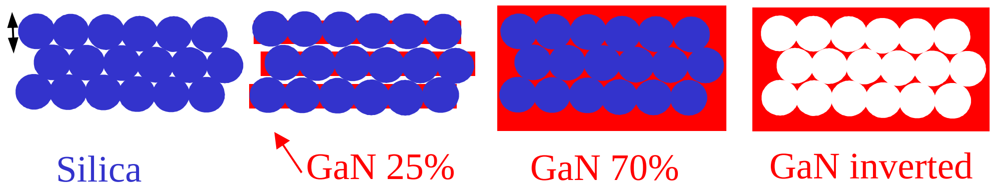

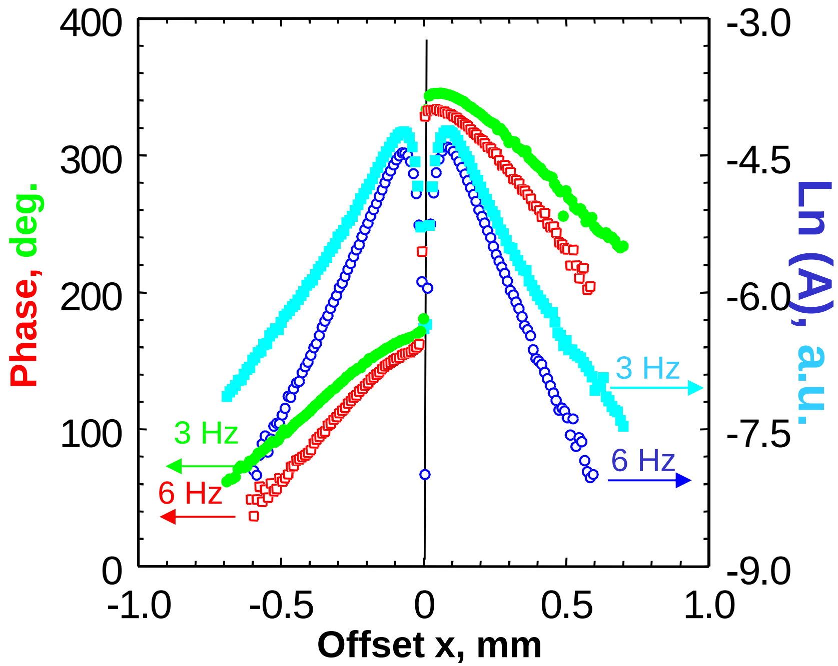

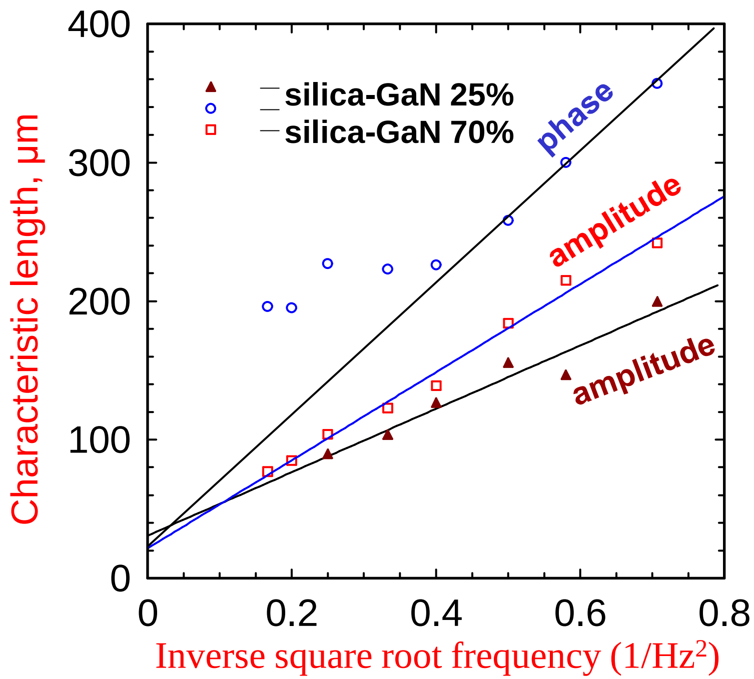

THERMAL WAVE REFLECTION AND REFRACTION

for plane waves

$$\begin{cases} \tilde{T}_1(x,z) = Ae^{-\beta_1[\sin(\theta_1)x+\cos(\theta_1)z]} + rAe^{-\beta_1[\sin(\theta_1')x-\cos(\theta_1')z]} \\ \tilde{T}_2(x,z) = tAe^{-\beta_2[\sin(\theta_2)x+\cos(\theta_2)z]} \end{cases}$$

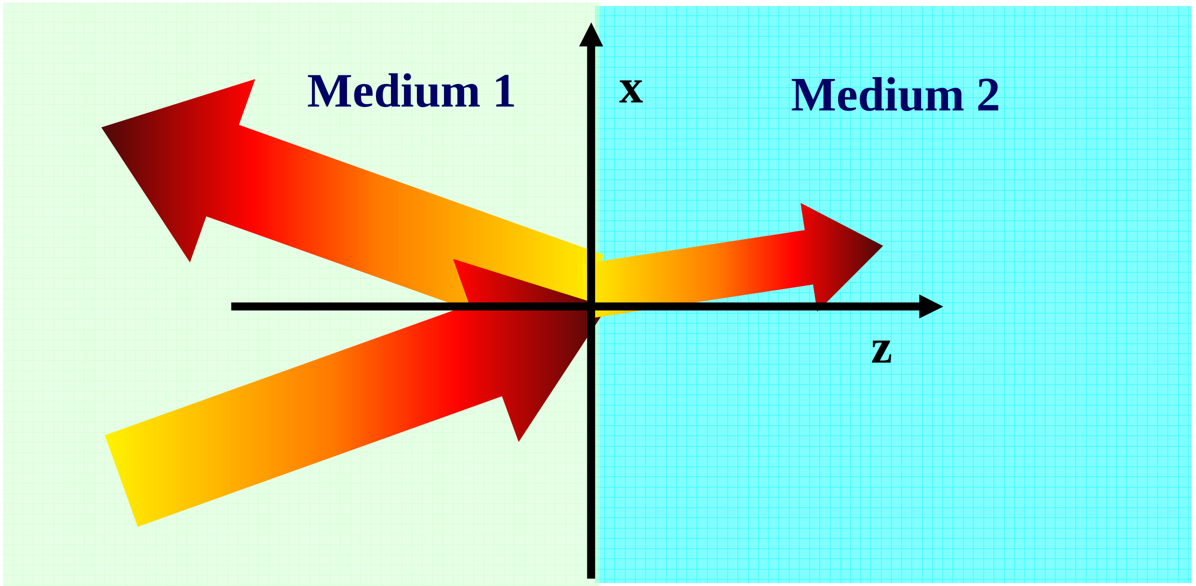

$$\begin{cases} \tilde{T}_1 = \tilde{T}_2 \\ k_1 \dfrac{\partial \tilde{T}_1}{\partial z} = k_2 \dfrac{\partial \tilde{T}_2}{\partial z} \end{cases}$$

Temperature must be conserved at z=0

Normal heat flux must be conserved at z=0

JOURNAL OF APPLIED PHYSICS VOLUME 85, NUMBER 7 1 APRIL 1999

Thermal wave reflection and refraction: Theoretical and experimental evidence

M. Bertolotti,[a] G. L. Liakhou,[b] R. Li Voti, S. Paoloni, and C. Sibilia
Istituto Nazionale Fisica della Materia (INFM) and Dipartimento di Energetica, Università di Roma "La Sapienza," Via Scarpa 16, 00161, Roma, Italy

(Received 7 July 1998; accepted for publication 23 December 1998)

This article describes and proves the basic phenomena which take place when thermal waves approach an interface between two media: the *reflection* and the *refraction*. In synthesis the Snell law for plane thermal waves is proved, both theoretically and experimentally, by means of the mirage technique. [S0021-8979(99)02307-5]

"Thermal Snell law"

$$\begin{cases} \theta_1' = \theta_1 \\ \dfrac{1}{\sqrt{D_1}} \sin(\theta_1) = \dfrac{1}{\sqrt{D_2}} \sin(\theta_2) \end{cases}$$

$$\theta_1 \le \theta_{\text{lim}} = \arcsin\left(\sqrt{D_1/D_2}\right)$$

Numerical simulation of the temperature field at the Invar-Air interface. The diffusivities are D_{Invar}=0.05 cm^2/s, D_{air}=0.2 cm^2/s. The incidence angle is θ_1=20°< θ_{lim} =30° and the refracted angle is consequently θ_2=43°.

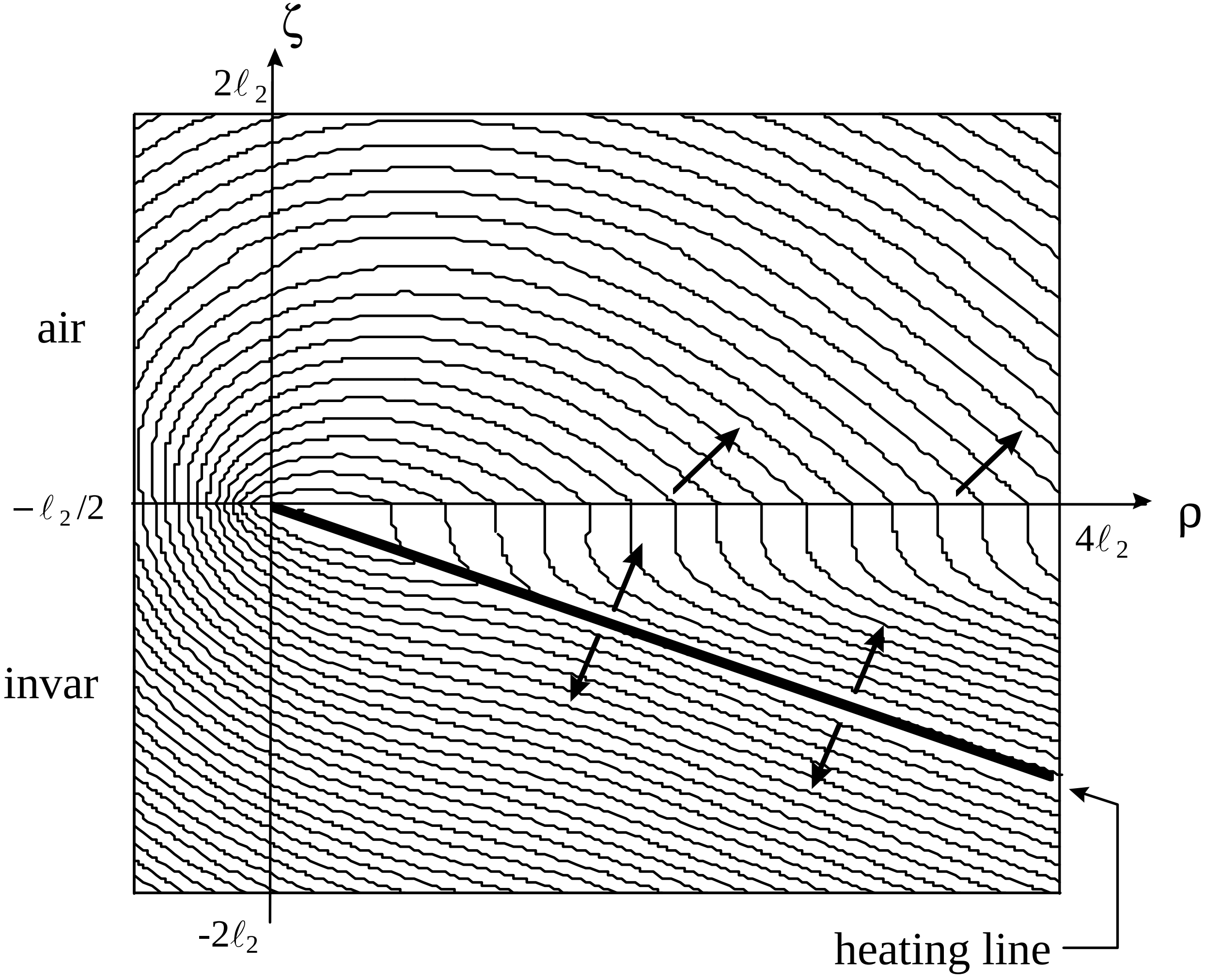

"Thermal Fresnel coefficients"

$$r = \frac{e_1 \cos(\theta_1) - e_2 \cos(\theta_2)}{e_1 \cos(\theta_1) + e_2 \cos(\theta_2)}$$

$$t = \frac{2 e_1 \cos(\theta_1)}{e_1 \cos(\theta_1) + e_2 \cos(\theta_2)}$$

What the thermal effusivity is?

$$e = k/\sqrt{D} = \sqrt{k\rho c}$$

THERMAL WAVE REFLECTION

experimental evidence

Experimental setup

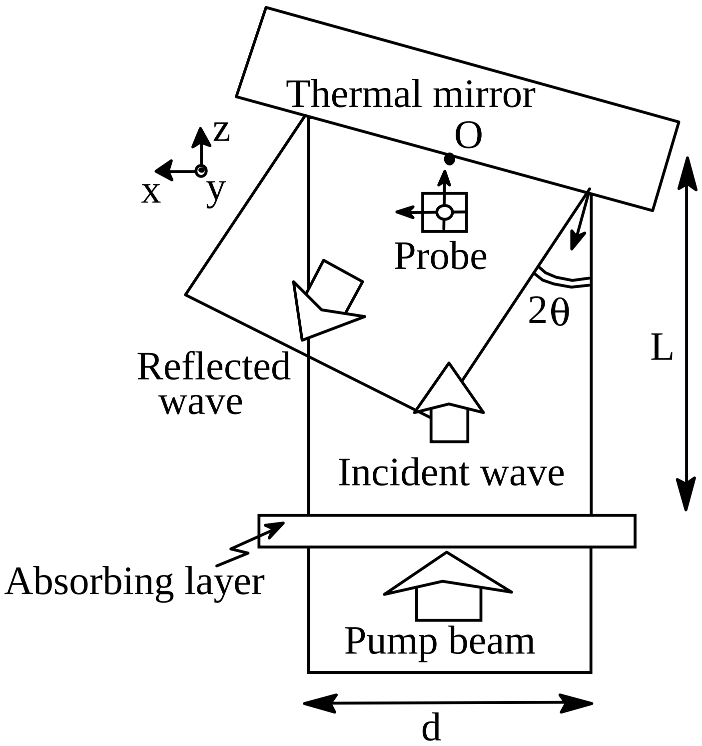

Temperature in air

$$\tilde{T}_{air}(x,z) = Ae^{-\beta_{air} z} + rAe^{\beta_{air}[\cos(2\theta)z - \sin(2\theta)x]}$$

Deflection in air

$$\Phi_x = \frac{1}{n}\left(\frac{dn}{dT}\right)\int_y \frac{\partial T_{air}}{\partial x} dy = \frac{1}{n}\left(\frac{dn}{dT}\right) L_{eff} \frac{\partial T_{air}}{\partial x}$$

$$\Phi_z = \frac{1}{n}\left(\frac{dn}{dT}\right)\int_y \frac{\partial T_{air}}{\partial z} dy = \frac{1}{n}\left(\frac{dn}{dT}\right) L_{eff} \frac{\partial T_{air}}{\partial z}$$

Factor independent on the angle

$$C = -\frac{1}{n}\left(\frac{dn}{dT}\right) L_{eff}\, \beta_{air} A$$

Final expression for the deflection

$$\tilde{\Phi}_x = C \left[r\sin(2\theta) e^{\beta_{air}[\cos(2\theta)z - \sin(2\theta)x]} \right] \cong C \left[r\sin(2\theta) \right]$$

$$\tilde{\Phi}_z = C \left[e^{-\beta_{air} z} - r\cos(2\theta) e^{\beta_{air}[\cos(2\theta)z - \sin(2\theta)x]} \right] \cong C \left[1 - r\cos(2\theta) \right]$$

THERMAL WAVE REFLECTION
experimental evidence

$$\tilde{\Phi}_x = C \left| r sin(2\theta) e^{\beta_{air}[\cos(2\theta)z - sin(2\theta)x]} \right| \cong C \left[r sin(2\theta) \right]$$

$$\tilde{\Phi}_z = C \left[e^{-\beta_{air} z} - r\cos(2\theta) e^{\beta_{air}[\cos(2\theta)z - sin(2\theta)x]} \right] \cong C \left[1 - r\cos(2\theta) \right]$$

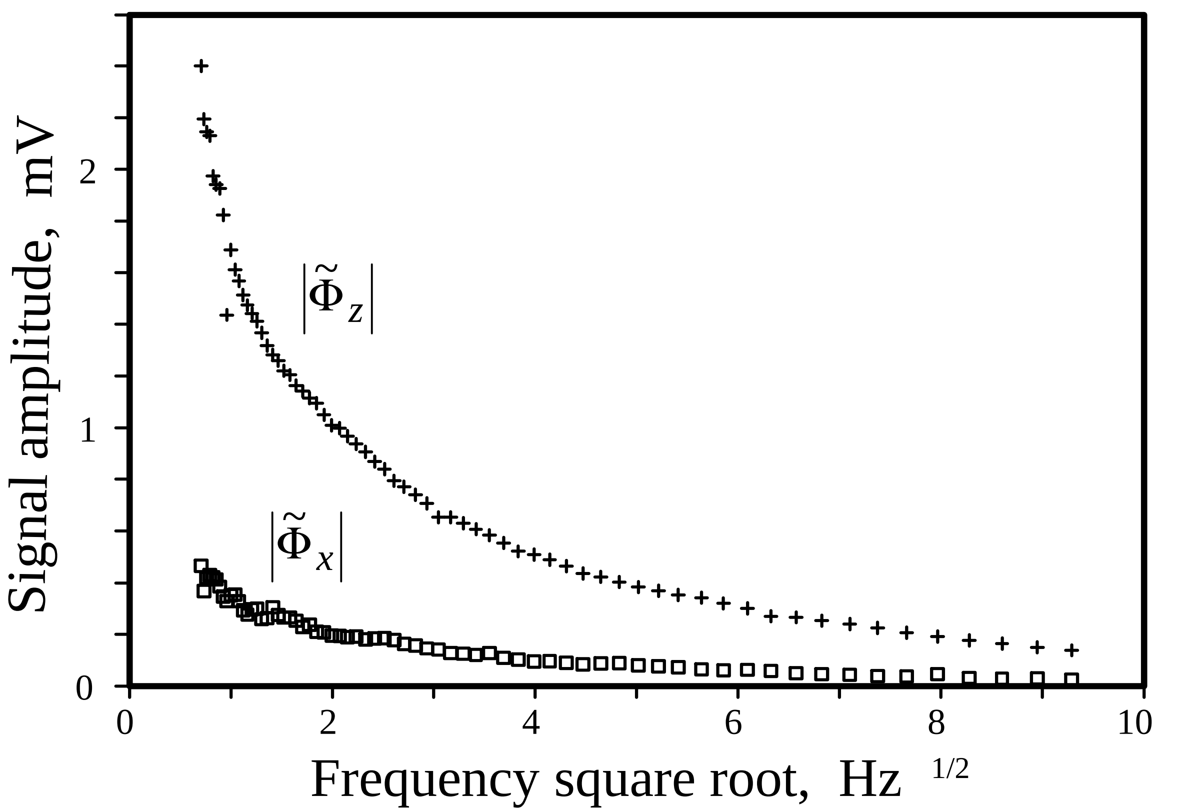

THERMAL WAVE REFLECTION

experimental evidence

Deflection ratio

$$R = \frac{\tilde{\Phi}_x}{\tilde{\Phi}_z} = \frac{r sin(2\theta)}{1 - r\cos(2\theta)} \cong \frac{-sin(2\theta)}{1+\cos(2\theta)} = -tg(\theta)$$

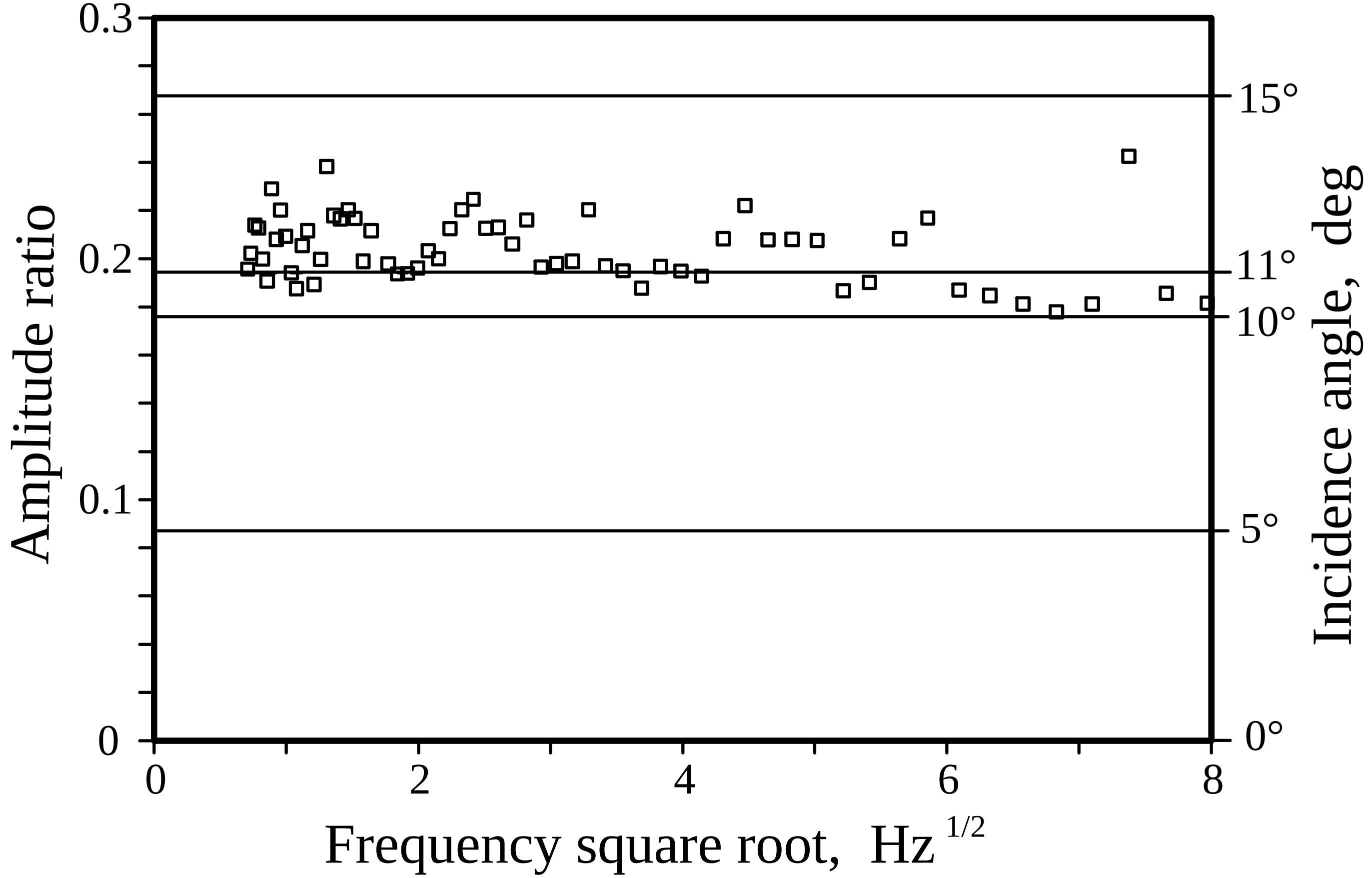

THERMAL WAVE REFRACTION

experimental evidence

Experimental setup

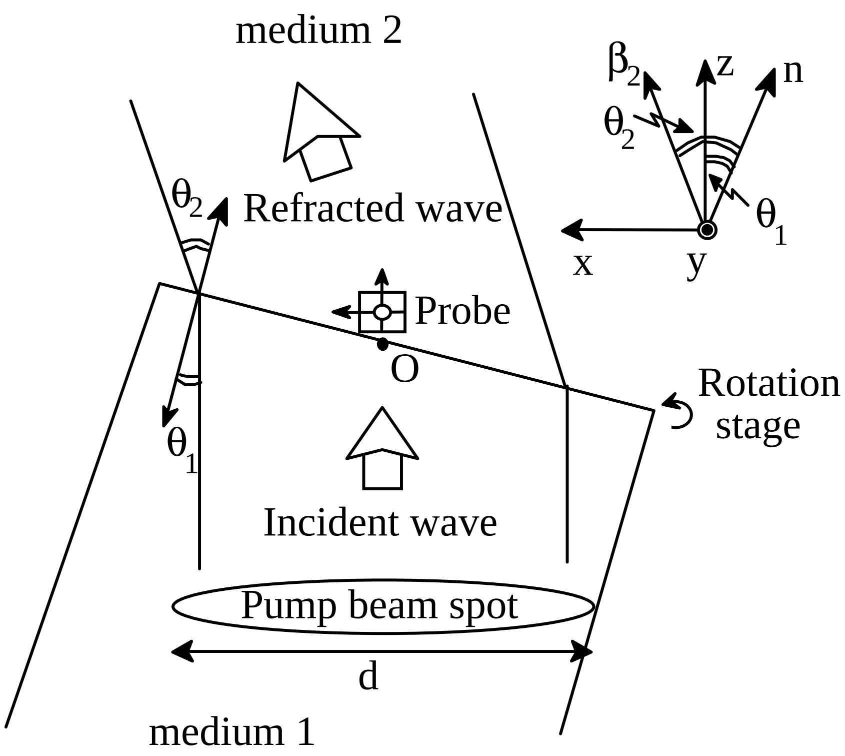

Refracted thermal wave (in air)

$$\tilde{T}_2(x,z) = tAe^{-\vec{\beta}_2\vec{r}} = tAe^{-\beta_2[\sin(\theta_2-\theta_1)x+\cos(\theta_2-\theta_1)z]}$$

Deflection in the second medium (air)

$$\tilde{\Phi}_x = C\left[t \quad \sin(\theta_2-\theta_1) \quad e^{-\beta_2[\sin(\theta_2-\theta_1)x+\cos(\theta_2-\theta_1)z]}\right]$$

$$\tilde{\Phi}_z = C\left[t \quad \cos(\theta_2-\theta_1) \quad e^{-\beta_2[\sin(\theta_2-\theta_1)x+\cos(\theta_2-\theta_1)z]}\right]$$

Deflection ratio

$$R = \frac{\tilde{\Phi}_x}{\tilde{\Phi}_z} = tg(\theta_2-\theta_1)$$

THERMAL WAVE REFRACTION

experimental evidence

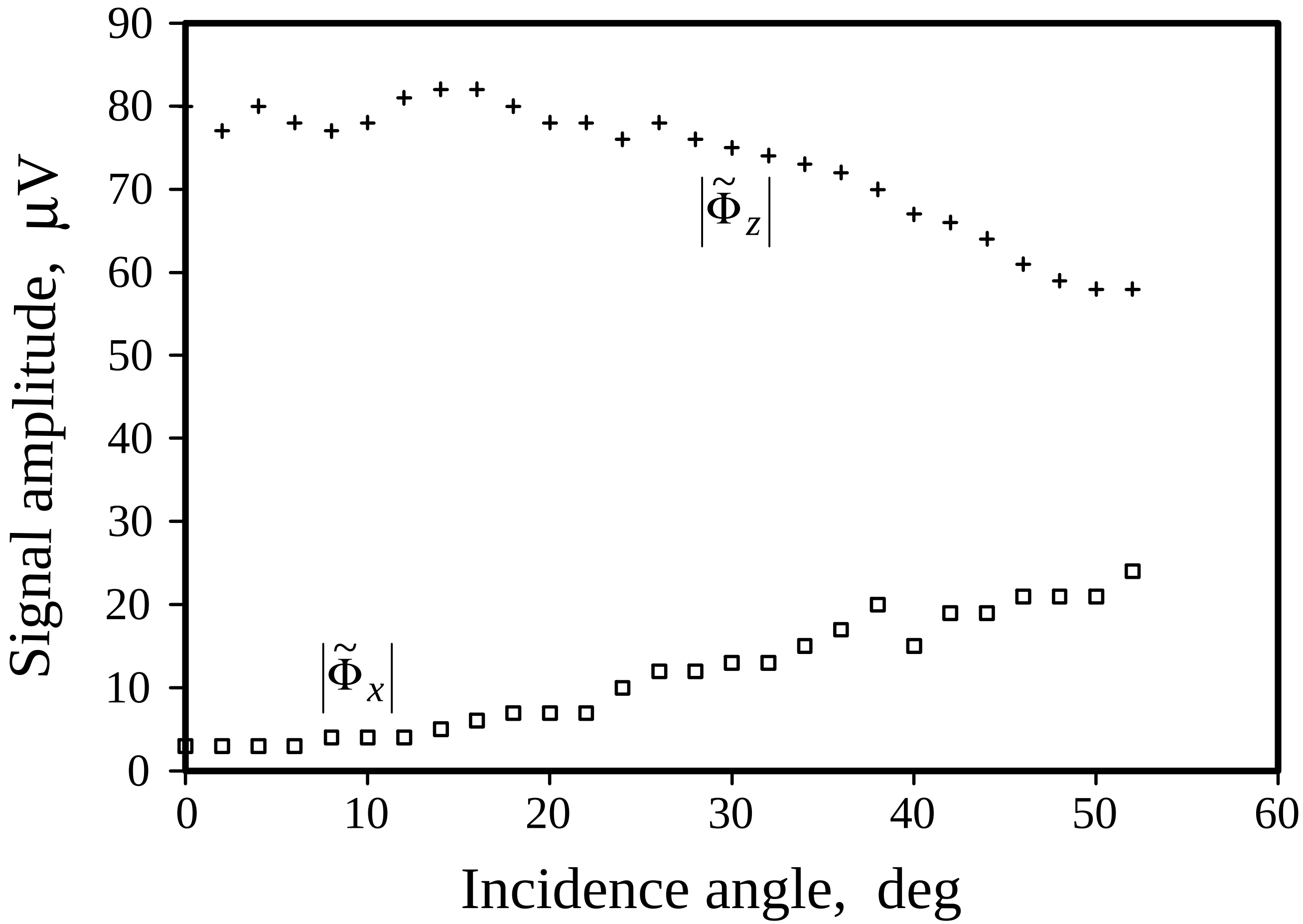

ANOMALOUS THERMAL REFRACTED FIELD

What happens when the Snell law is not valid? $\theta_1 > \theta_{\lim} = arcsin\left(\sqrt{D_1/D_2}\right)$

$$\tilde{T}_{2\pm}(\rho,\zeta) = Be^{-\frac{(1+j)}{\ell_1}sin(\theta_1)\rho \pm \frac{(1-j)}{\ell_2}\zeta\sqrt{\frac{D_2}{D_1}sin^2(\theta_1)-1}}$$

Temperature field at the Invar- Air interface. The incidence angle is $\theta_1 = 70° > \theta_{lim}$.

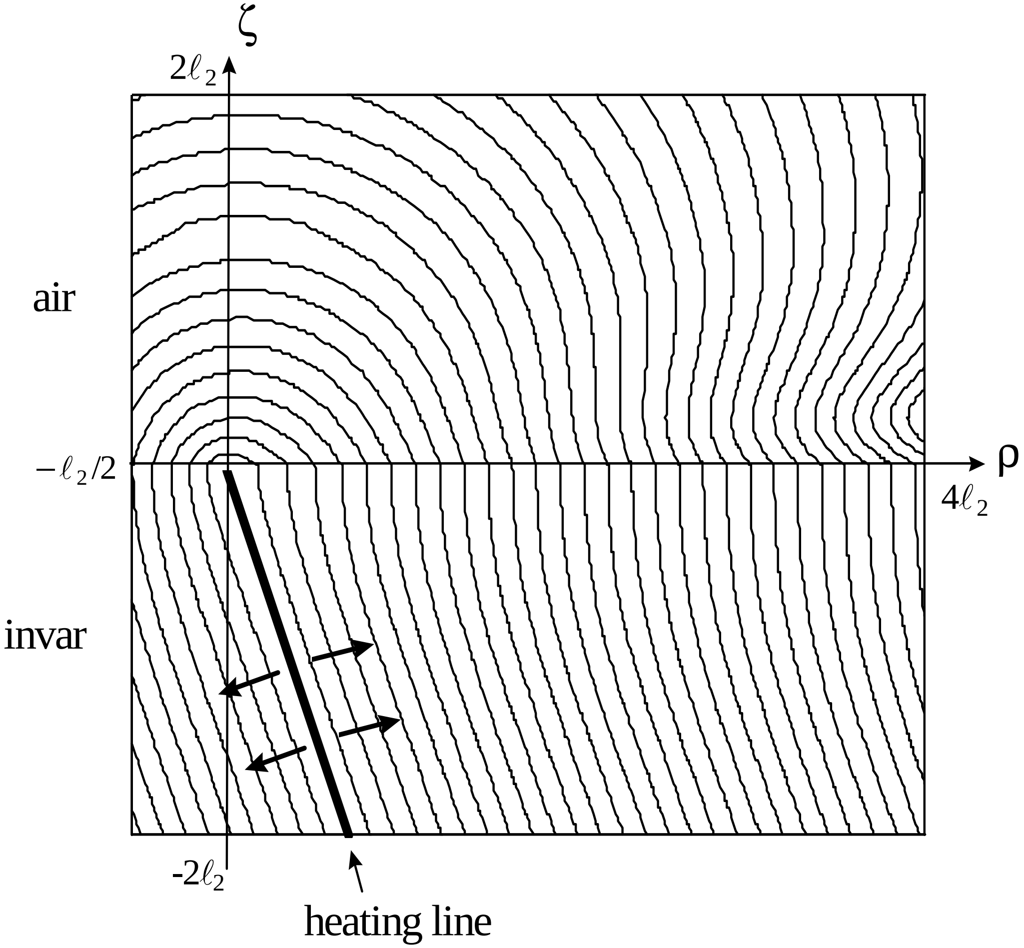

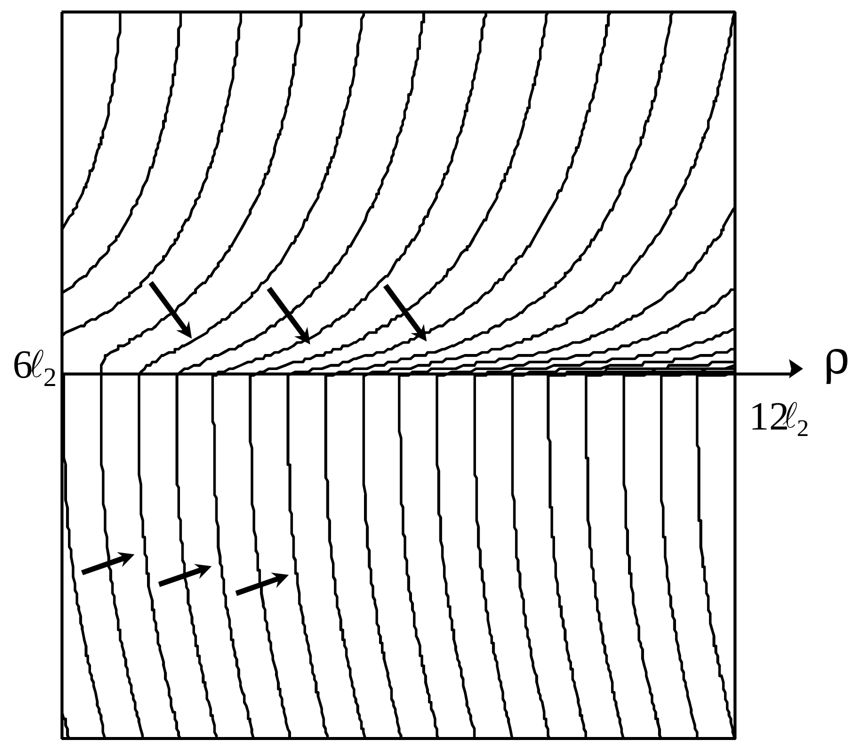

THERMAL WAVE REFRACTION

experimental evidence

$$R = \frac{\tilde{\Phi}_x}{\tilde{\Phi}_z} = tg(\theta_2 - \theta_1) \quad \Rightarrow \quad \theta_2 = \theta_1 + \mathrm{arctg}[R(\theta_1)]$$

Linear scale in θ

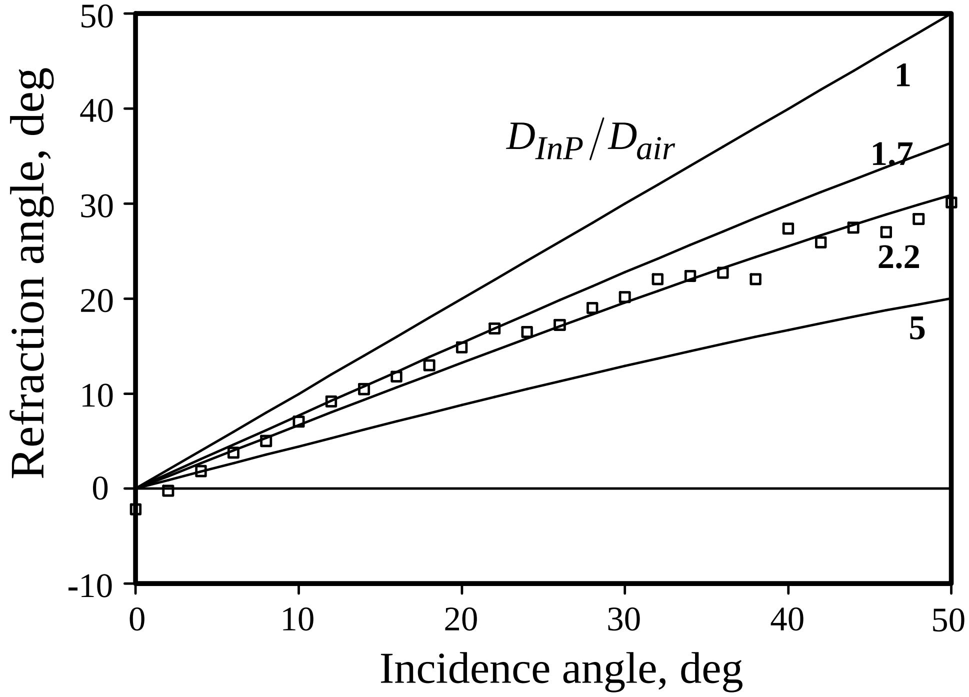

Linear scale in $\sin(\theta)$

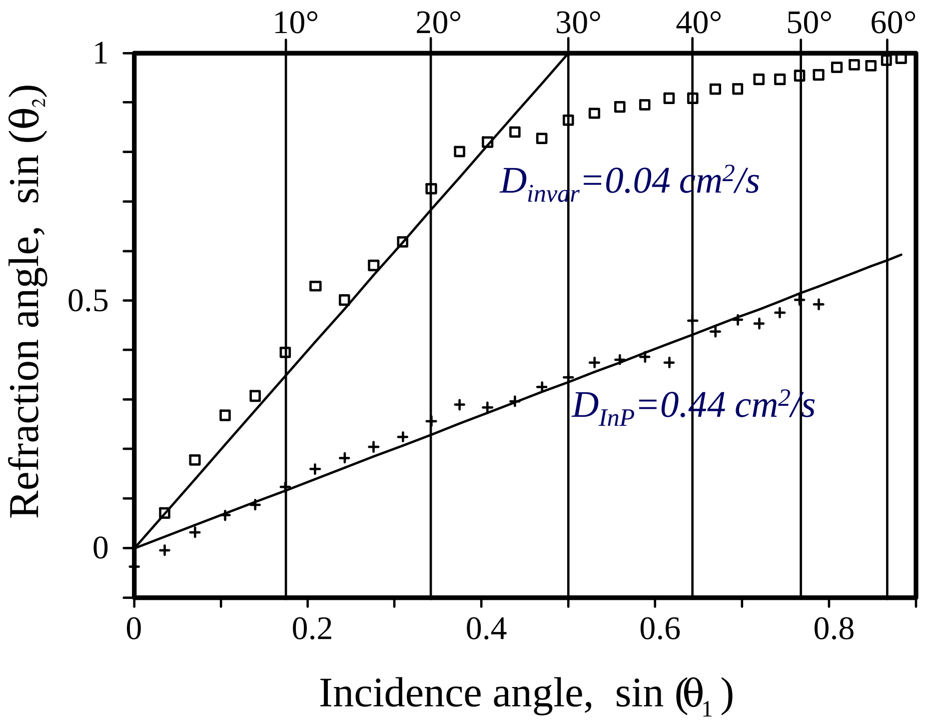

Snell law

$$\frac{1}{\sqrt{D_1}} \sin(\theta_1) = \frac{1}{\sqrt{D_2}} \sin(\theta_2)$$

THERMAL WAVE INTERFEROMETRY

BASIC PRINCIPLE

To generate plane thermal waves of a given frequency at the front surface of the sample by heating it periodically with a pump laser beam.

The waves propagate inside the structure and, if they approach a buried layer with different thermal properties, they are partially reflected giving rise, together with the incident waves, to an interference effect at the front surface.

APPLICATIONS

Nondestructive evaluation of the thermophysical properties and the thickness of layered samples

DETECTION

Photoacoustic

Radiometry

Photothermal Deflection techniques

THERMAL WAVE INTERFEROMETRY

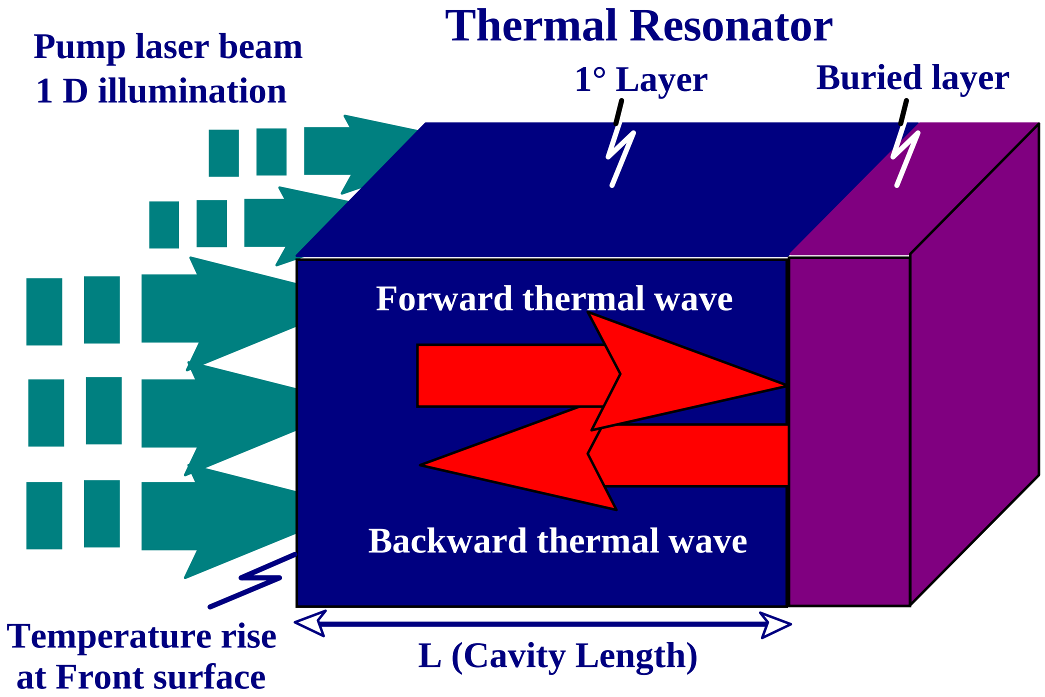

INTERNAL TEMPERATURE RISE

$$T(z) = Ae^{-\beta z} + Be^{\beta z}$$

MATERIAL/BULK INTERFACE

$$R = \frac{e_m - e_{bulk}}{e_m + e_{bulk}}$$

$$R = \frac{reflected \quad wave}{incidence \quad wave} = \frac{Be^{\beta L}}{Ae^{-\beta L}}$$

$$B = R \cdot A \cdot e^{-2\beta \cdot L}$$

$$A = \frac{I}{k\beta} \frac{1}{\left(1 - \mathrm{Re}^{-2\beta \cdot L}\right)}$$

BOUNDARY CONDITIONS AT THE SURFACE (z=0)

$$T(0) = A + B$$ *Temperature*

$$I = -k\frac{dT}{dz} = k\beta A\left(1 - e^{-2\beta \cdot L}\right)$$ *heat flux*
I; Power intensity

THERMAL WAVE INTERFEROMETRY

TEMPERATURE RISE AT THE SURFACE

$$T_{air}(o) = \frac{I}{k\beta}\left(\frac{1 + R\, e^{-2(1+j)L\sqrt{\pi f/D}}}{1 - \mathrm{R}e^{-2(1+j)L\sqrt{\pi f/D}}}\right) \qquad R = \frac{e_m - e_{bulk}}{e_m + e_{bulk}}$$

PHASE SIGNAL

$$\varphi\left(\sqrt{f}\right) = -arc\tan\left(\frac{2R\sin\left(2L\sqrt{\pi f/D}\right)e^{-2L\sqrt{\pi f/D}}}{1 - R^2 e^{-4L\sqrt{\pi f/D}}}\right)$$

amplitude

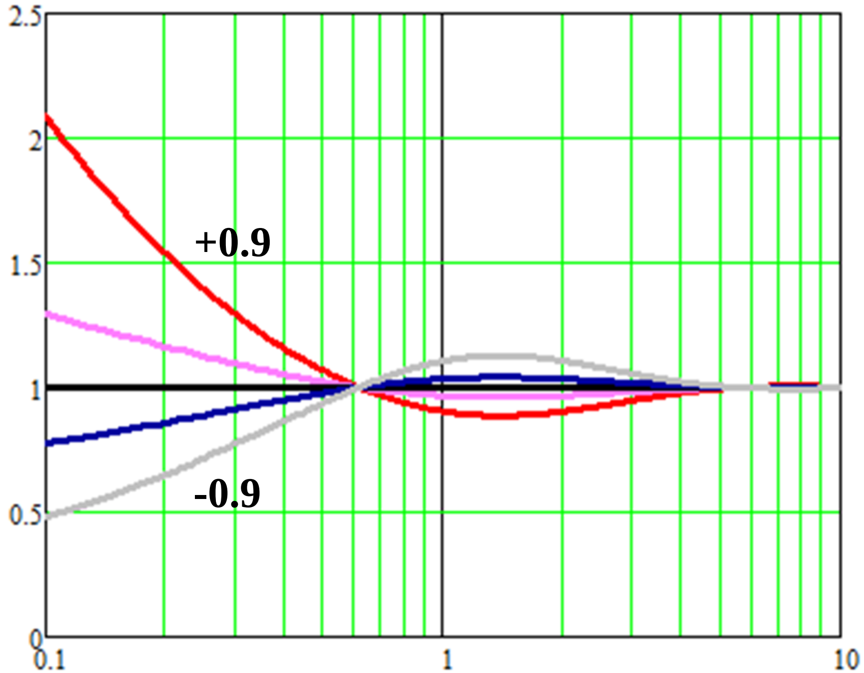

$\left(L\sqrt{\pi f/D}\right)^2$

phase

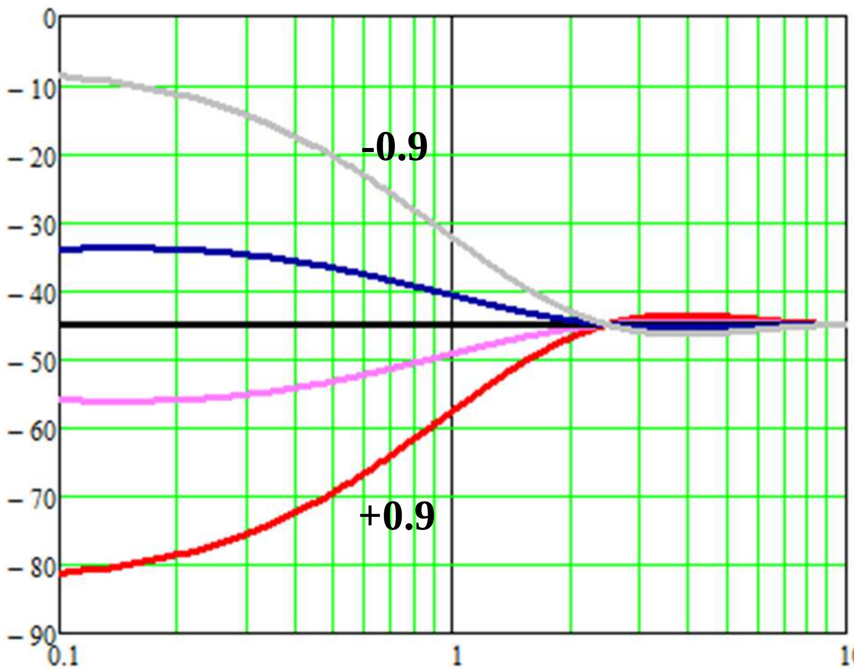

$\left(L\sqrt{\pi f/D}\right)^2$

THERMAL WAVE INTERFEROMETRY

TEMPERATURE RISE AT THE SURFACE

$$T_{air}(o) = \frac{I}{k\beta}\left(\frac{1+R\,e^{-2(1+j)L\sqrt{\pi f/D}}}{1-\mathrm{Re}^{-2(1+j)L\sqrt{\pi f/D}}}\right)$$

PHASE SIGNAL

$$\varphi\left(\sqrt{f}\right) = -arc\tan\left(\frac{2R\sin\left(2L\sqrt{\pi f/D}\right)e^{-2L\sqrt{\pi f/D}}}{1-R^2 e^{-4L\sqrt{\pi f/D}}}\right)$$

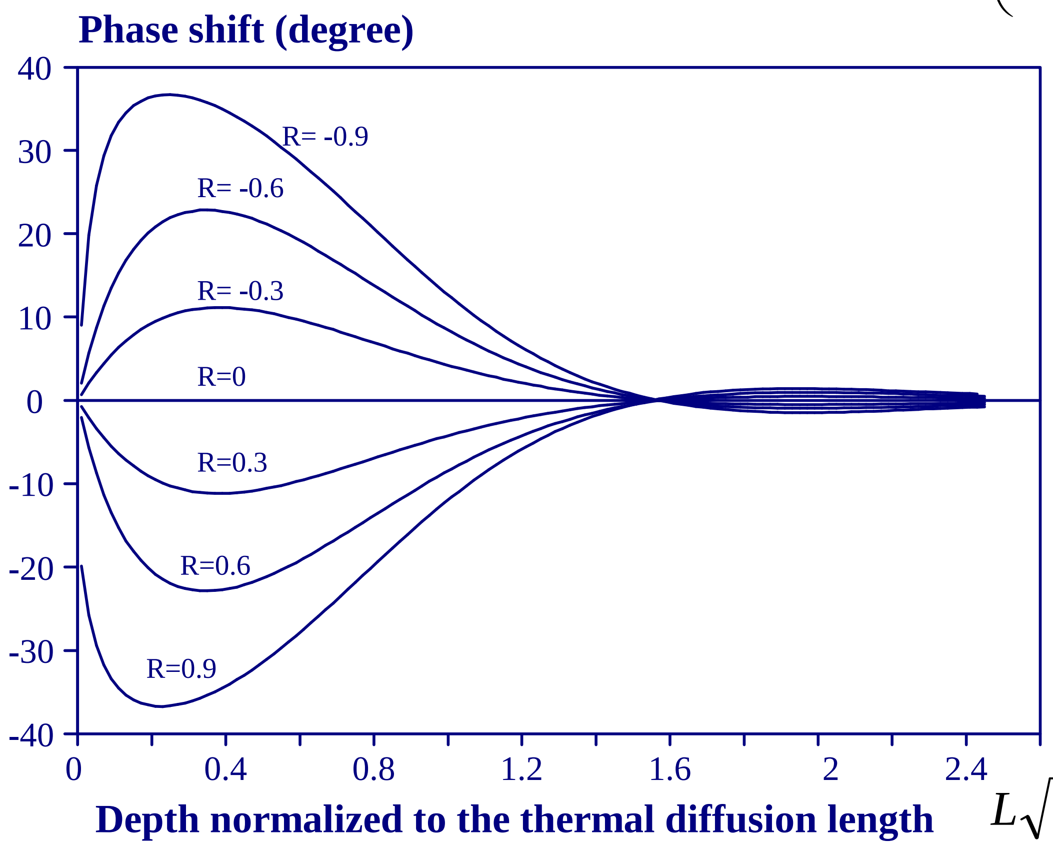

$L\sqrt{\pi f/D}$

Note that the interference effect (oscillation) is seen when the cavity length is of the same order of the thermal diffusion length of the resonator and when the coefficient R is large enough.

The maximum oscillation is of 45° degrees and is obtained in case of perfect reflection from the buried layer with R=±1

THERMAL WAVE INTERFEROMETRY

Diffusivity measurement by Mirage

$$\hat{T}_{surf} = \frac{I}{(e_c + e_{air})\sqrt{j\omega}} \cdot \left[\frac{1 + R_2 \exp[-2(1+j)L/\ell_c]}{1 - R_1 R_2 \exp[-2(1+j)L/\ell_c]} \right] \qquad R_1 = \frac{e_c - e_{air}}{e_c + e_{air}} \approx 1 \qquad R_2 = \frac{e_c - e_b}{e_c + e_b}$$

$$\Delta\varphi = \varphi - \varphi_{ref} = -arc\tan\left(\frac{2R_2 \cdot sin(2L/\ell_c) \cdot e^{-2L/\ell_c}}{1 - R_2^2 \cdot e^{-4L/\ell_c}} \right)$$

Inox L=200μm

D=0.04, 0.046 or 0.06 cm²/s

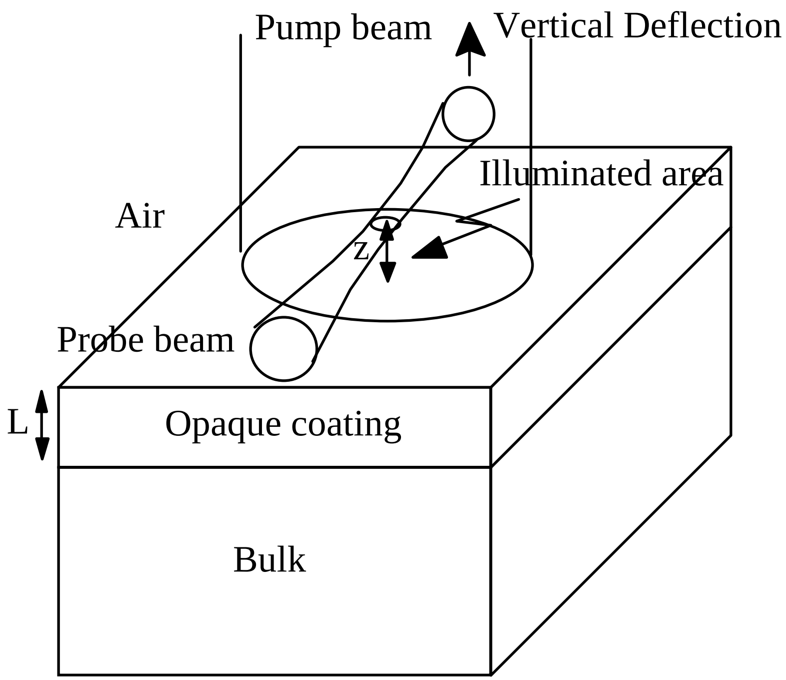

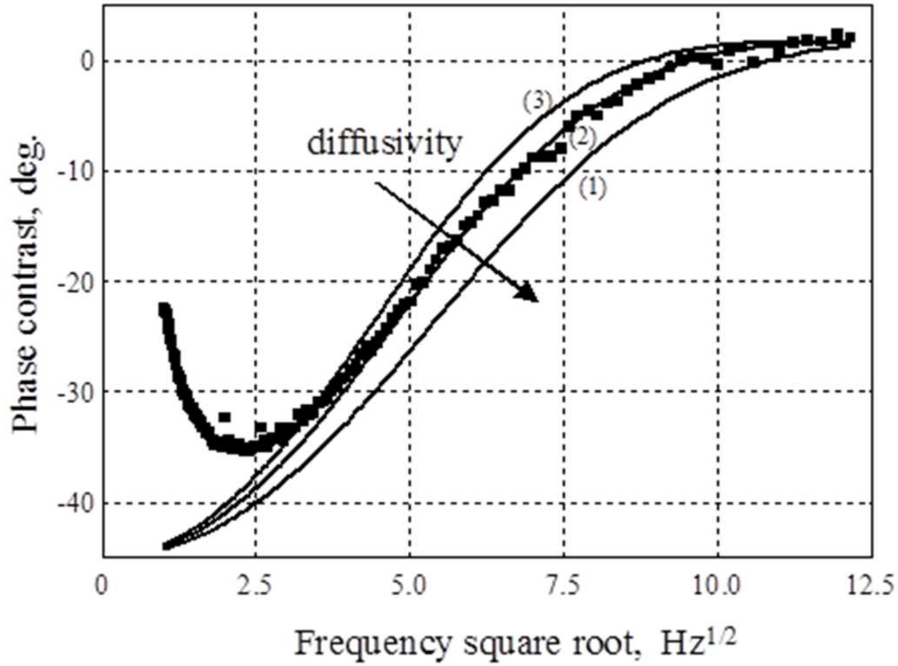

THERMAL WAVE INTERFEROMETRY

Diffusivity measurement by Mirage

$$\hat{T}_{surf} = \frac{I}{(e_c + e_{air})\sqrt{j\omega}} \cdot \left[\frac{1 + R_2 \exp[-2(1+j)L/\ell_c]}{1 - R_1 R_2 \exp[-2(1+j)L/\ell_c]} \right] \qquad R_1 = \frac{e_c - e_{air}}{e_c + e_{air}} \approx 1 \qquad R_2 = \frac{e_c - e_b}{e_c + e_b}$$

$$\Delta\varphi = \varphi - \varphi_{ref} = -arc\tan\left(\frac{2R_2 \cdot sin(2L/\ell_c) \cdot e^{-2L/\ell_c}}{1 - R_2^2 \cdot e^{-4L/\ell_c}} \right)$$

Inox L=200µm

D=0.046 cm²/s

Spot size = 1mm, 2.3mm, 5mm

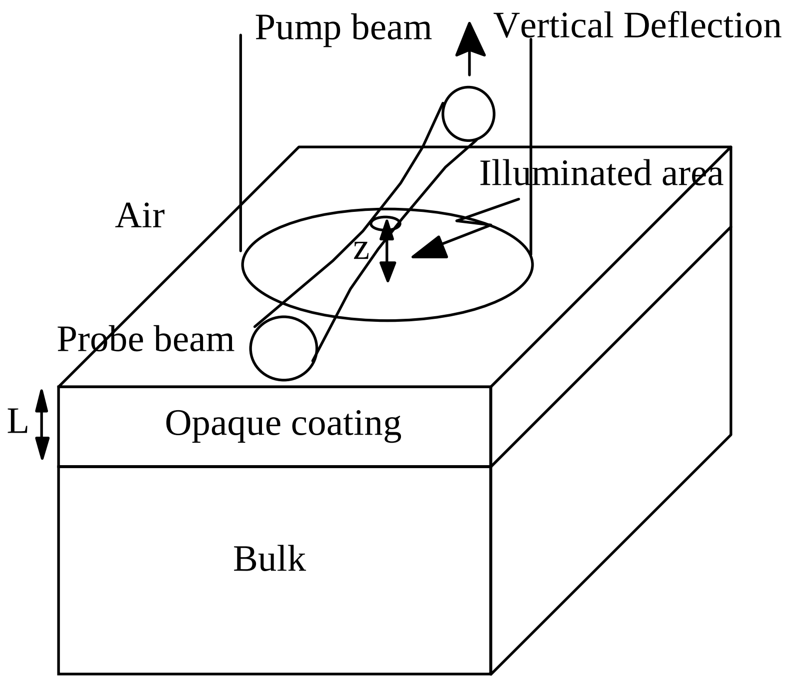

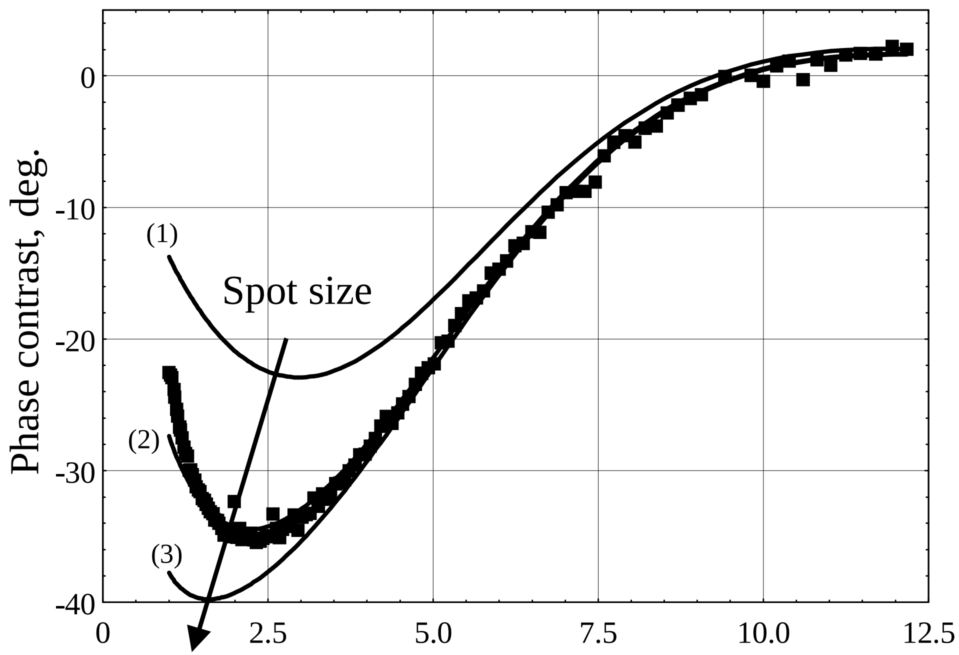

THERMAL WAVE INTERFEROMETRY

Diffusivity measurement by Mirage

$$\hat{T}_{surf} = \frac{I}{(e_c + e_{air})\sqrt{j\omega}} \cdot \left[\frac{1 + R_2 \exp[-2(1+j)L/\ell_c]}{1 - R_1 R_2 \exp[-2(1+j)L/\ell_c]}\right] \qquad R_1 = \frac{e_c - e_{air}}{e_c + e_{air}} \approx 1 \qquad R_2 = \frac{e_c - e_b}{e_c + e_b}$$

$$\Delta\varphi = \varphi - \varphi_{ref} = -arc\tan\left(\frac{2R_2 \cdot sin(2L/\ell_c) \cdot e^{-2L/\ell_c}}{1 - R_2^2 \cdot e^{-4L/\ell_c}}\right)$$

Inox L=200μm

D=0.046 cm²/s

Spot size = 2.3 mm

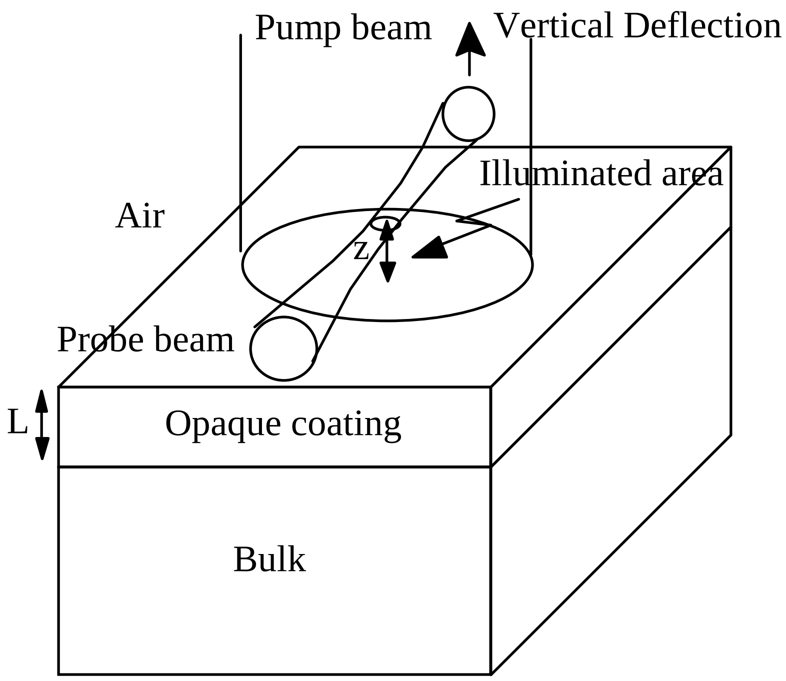

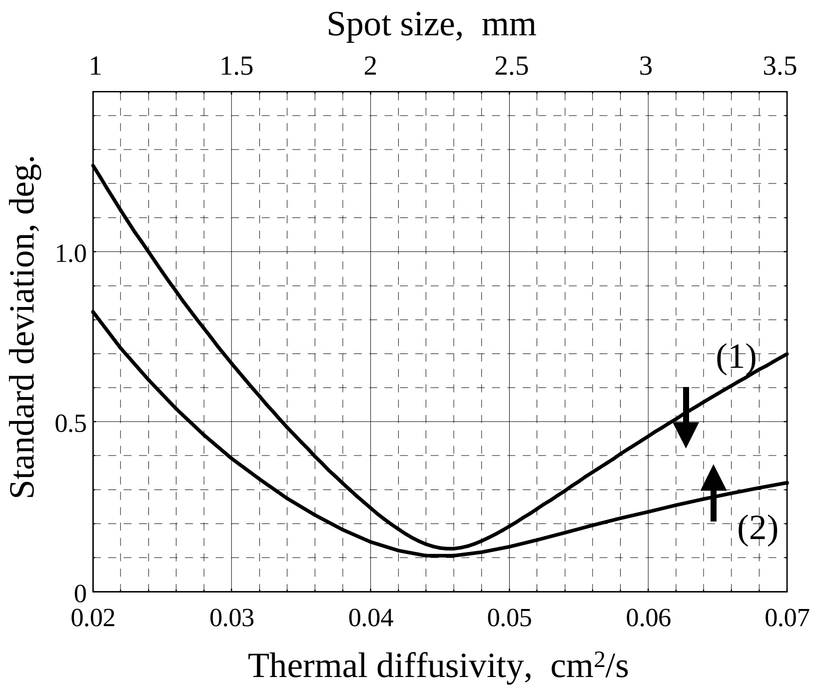

THERMAL WAVE INTERFEROMETRY

Diffusivity measurement by Mirage – Reflectivity

$$\Gamma_{surf}(f) = \frac{\sqrt{f}\cdot\hat{T}_{surf}(f) - \lim\limits_{p\to\infty}\sqrt{p}\cdot\hat{T}_{surf}(p)}{\sqrt{f}\cdot\hat{T}_{surf}(f) + \lim\limits_{p\to\infty}\sqrt{p}\cdot\hat{T}_{surf}(p)} = R_2\cdot\exp\left[-2(1+j)\frac{L\sqrt{\pi f}}{\sqrt{D_c}}\right] \Rightarrow$$

$$R_2 = \frac{e_c - e_b}{e_c + e_b}$$

$$\Rightarrow \begin{cases} \ln(|\Gamma_{surf}|) = -2L\sqrt{\pi f}/\sqrt{D_c} + \ln[R_2] \\ \arg(\Gamma_{surf}) = -2L\sqrt{\pi f}/\sqrt{D_c} \end{cases}$$

Inox L=200μm

D=0.046 cm^2/s

Spot size = 2.3 mm

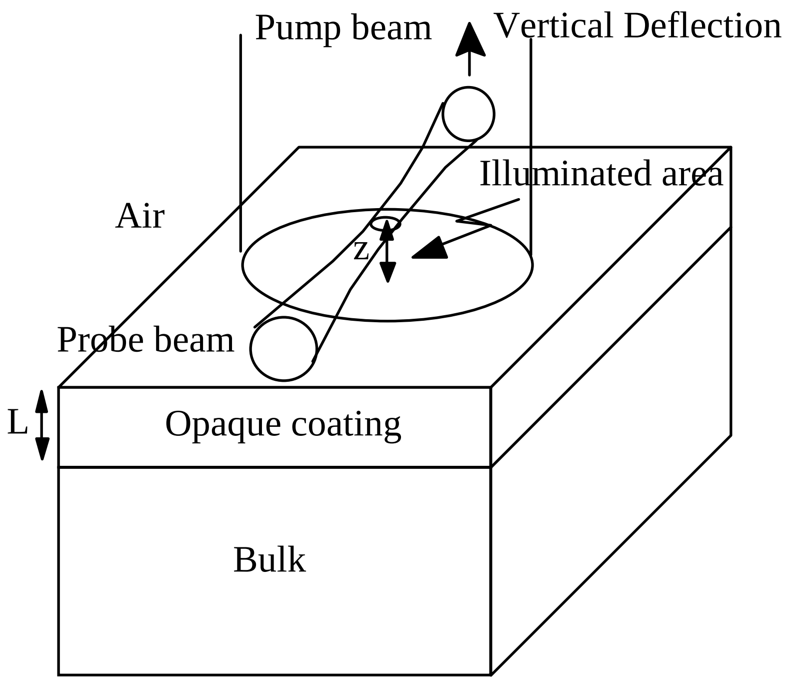

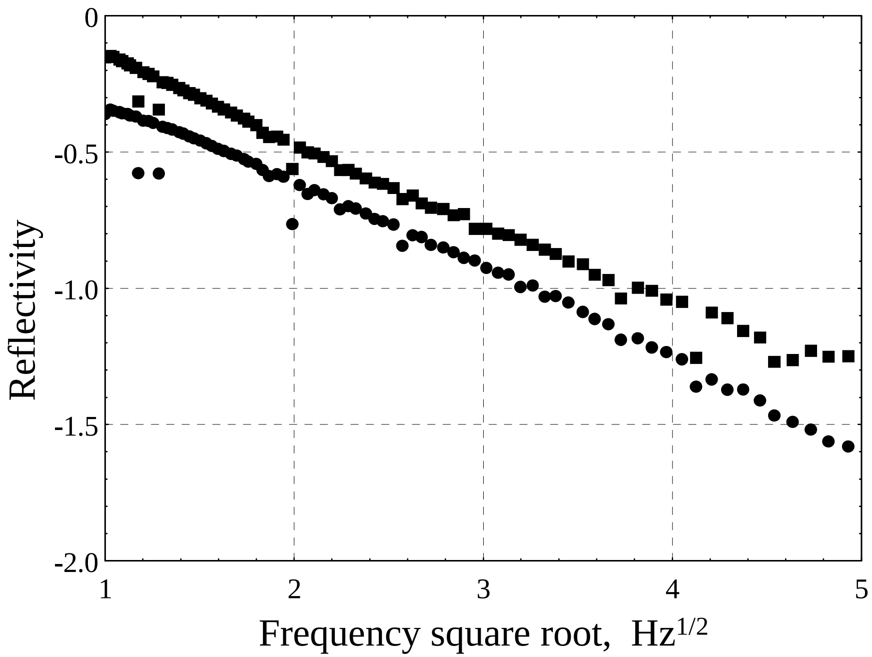

Main applications

- *Thermal diffusivity and effusivity measurements*
- *Absorption spectroscopy*
- *Effusivity and optical absorption depth profiling*
- *Measurement of the attenuation in optical waveguides*
- *Evaluation of the thickness of thin layers*
- *Trace gas analysis*
- *Evaluation of the photoelastic constants*

IR PDS device for trace gas analysis

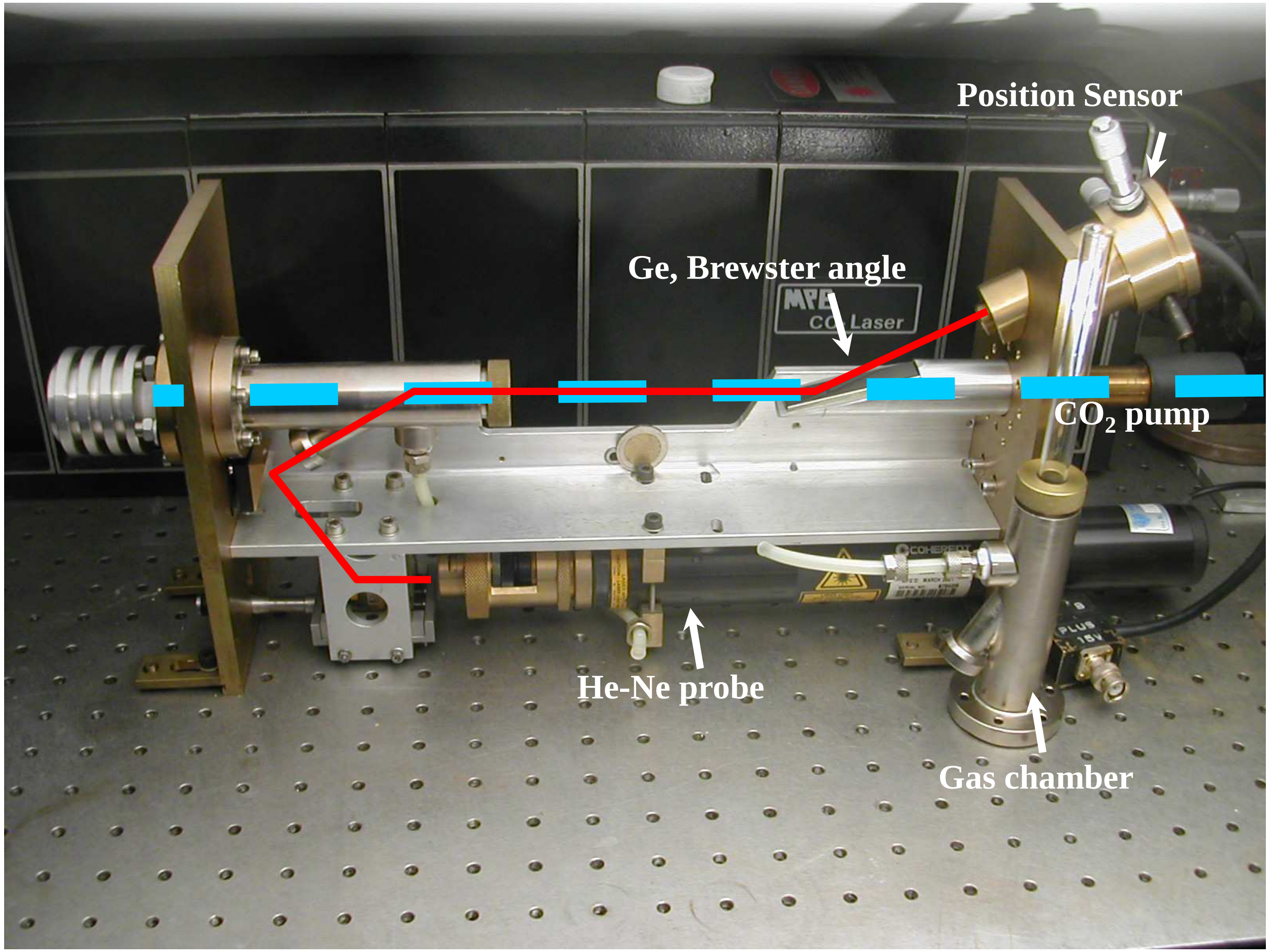

Università degli Studi di Roma "La Sapienza" - Dipartimento di Energetica - Via A Scarpa 14 - 00161 - Roma
Per informazioni Prof. M.Bertolotti Tel. 06.49916542 - Email: mario.bertolotti@uniroma1.it

Trace Gas Analysis – Infrared Photothermal Deflection Spectroscopy

Collinear configuration

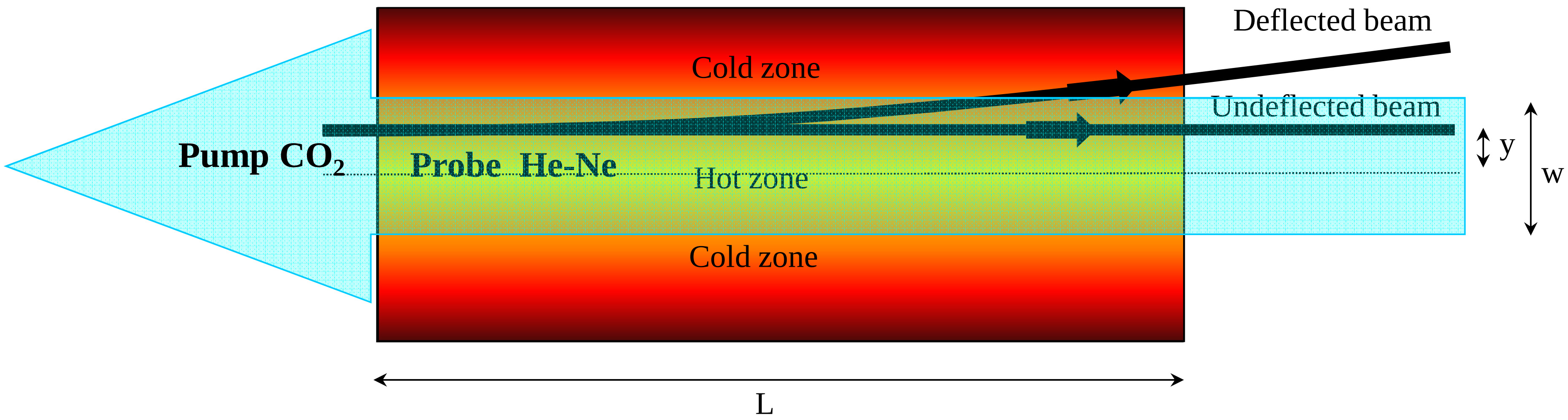

Photothermal deflection angle

$$\vec{\Phi}(y) = -2\left(\frac{1}{n}\frac{dn}{dT}\right)\frac{P\left(1-e^{-\alpha L}\right)}{\omega\rho c\pi^2 w^2}\left(\frac{y}{w}\right)\cdot e^{-(y/w)^2} \cong A\alpha L$$

Experimental results – Test on CO_2

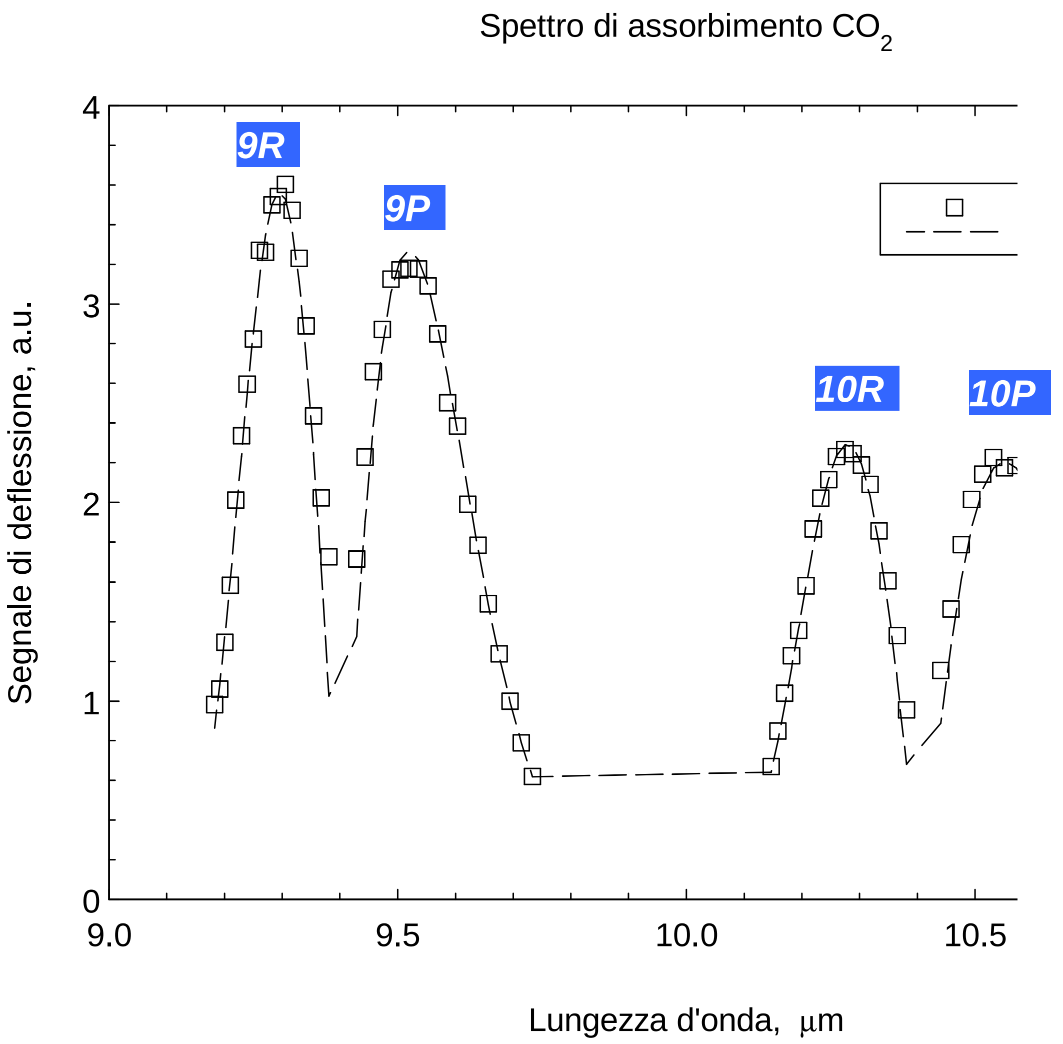

Experimental Results – Test on C_2H_4

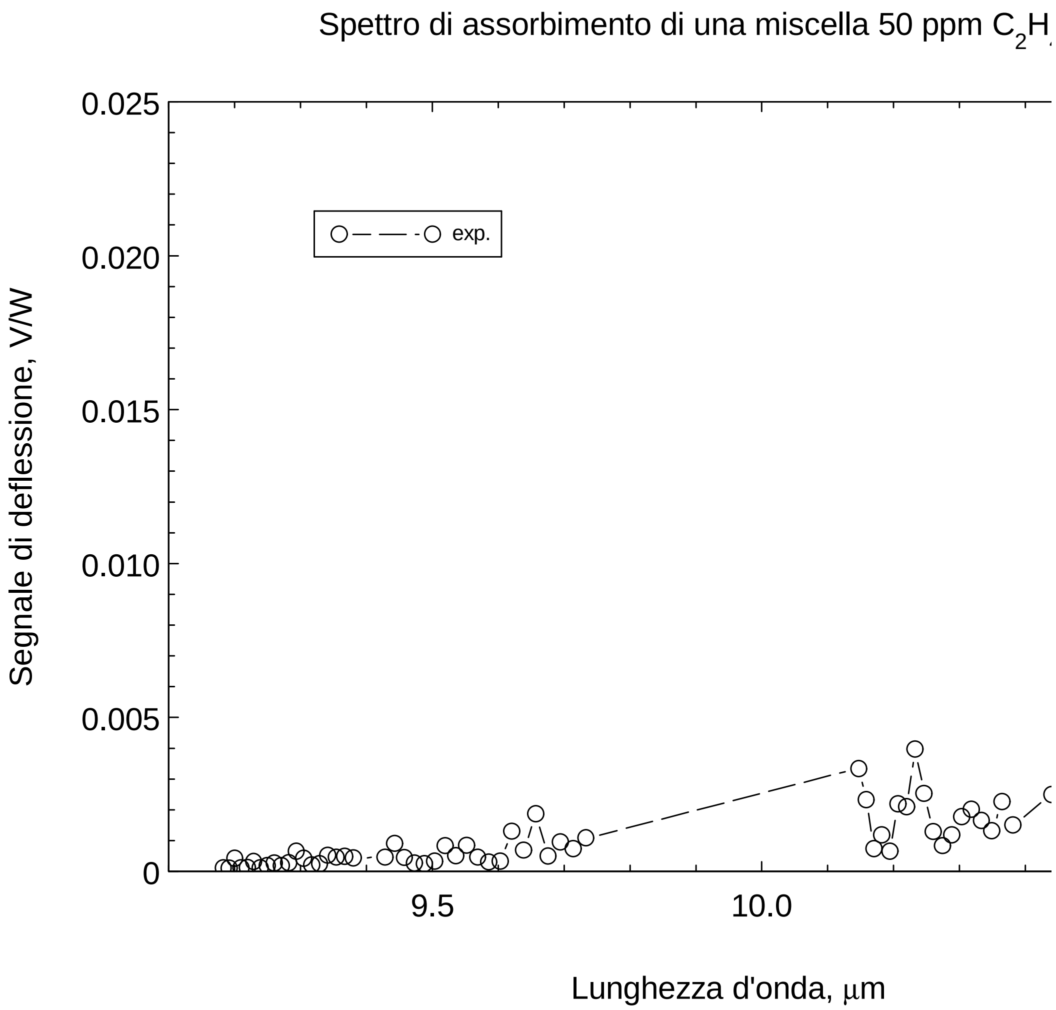

10P(14) di C_2H_4

Experimental results on carbossimetilcellulosa

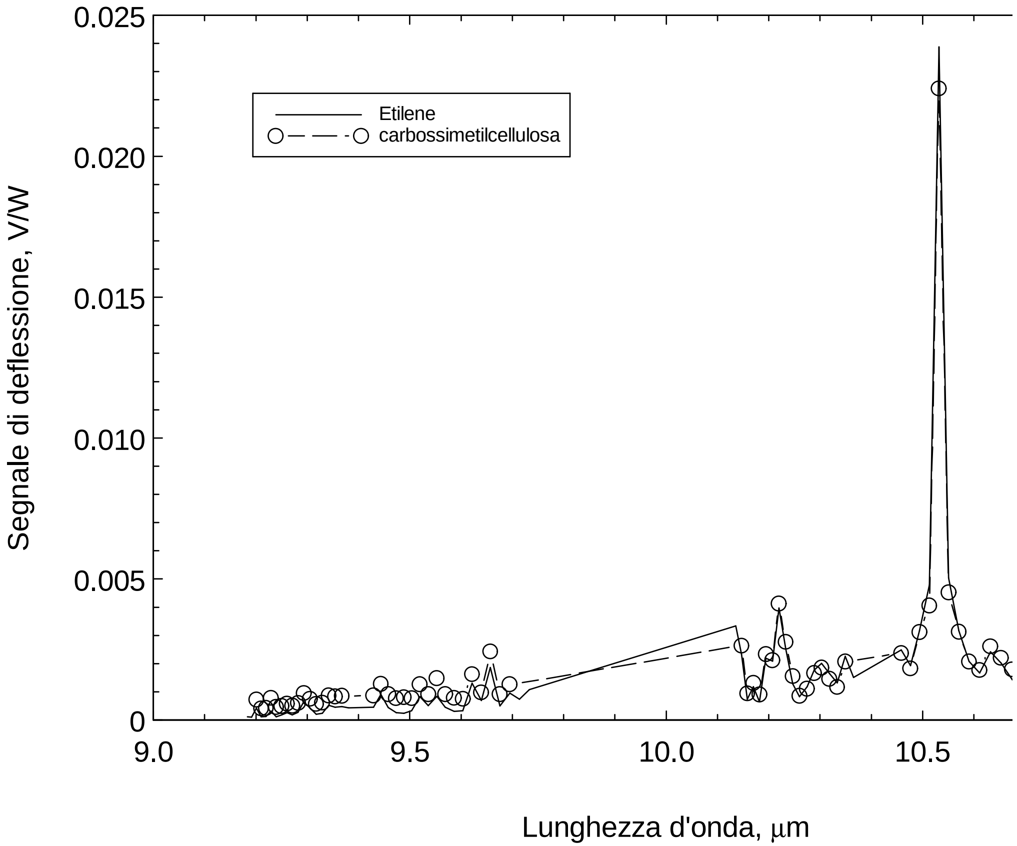

Carbossimetilcellulosa	
Temperature of the treatment	Concentration of the emitted ethylene
450°C	7.07 ppm
480°C	46.8 ppm

PLANE THERMAL WAVE RESONATOR

Experimental setup

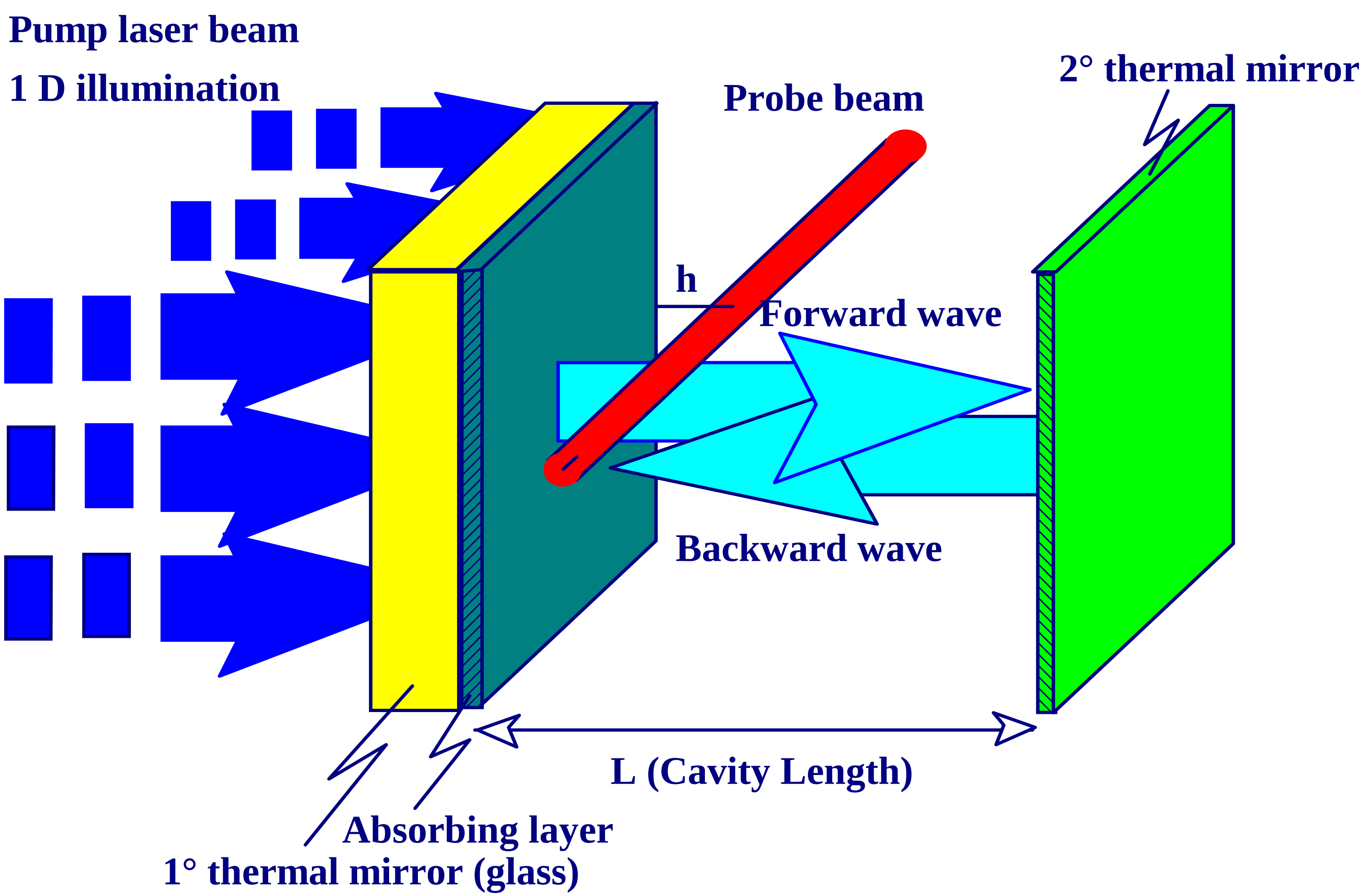

THERMAL WAVE RESONATOR

Experimental evidence in air

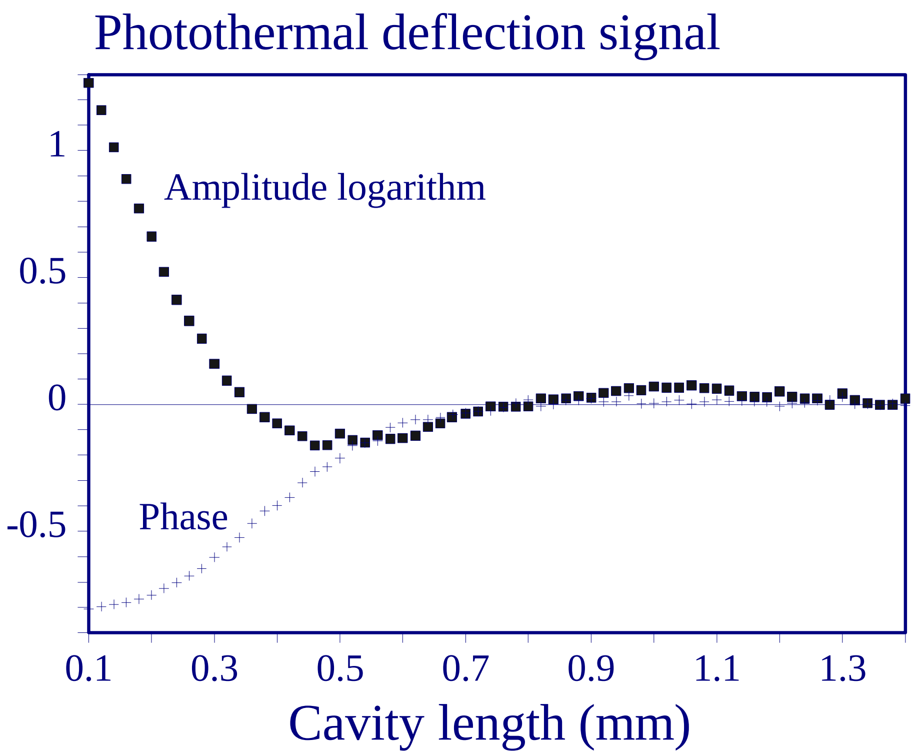

frequency 36 Hz

CONCLUSIONS

- **PHOTOTHERMAL TECHNIQUES**
- **PRINCIPLE OF PHOTOTHERMAL DEFLECTION**
- **THE HEAT DIFFUSION**
- **MEASUREMENT OF THERMAL DIFFUSIVITY**
- **OTHER APPLICATIONS**